

## INFORMATION TO USERS

This manuscript has been reproduced from the microfilm master. UMI films the text directly from the original or copy submitted. Thus, some thesis and dissertation copies are in typewriter face, while others may be from any type of computer printer.

**The quality of this reproduction is dependent upon the quality of the copy submitted.** Broken or indistinct print, colored or poor quality illustrations and photographs, print bleedthrough, substandard margins, and improper alignment can adversely affect reproduction.

In the unlikely event that the author did not send UMI a complete manuscript and there are missing pages, these will be noted. Also, if unauthorized copyright material had to be removed, a note will indicate the deletion.

Oversize materials (e.g., maps, drawings, charts) are reproduced by sectioning the original, beginning at the upper left-hand corner and continuing from left to right in equal sections with small overlaps.

Photographs included in the original manuscript have been reproduced xerographically in this copy. Higher quality 6" x 9" black and white photographic prints are available for any photographs or illustrations appearing in this copy for an additional charge. Contact UMI directly to order.

ProQuest Information and Learning  
300 North Zeeb Road, Ann Arbor, MI 48106-1346 USA  
800-521-0600

UMI<sup>®</sup>



# Hamiltonian methods for some geophysical vortex dynamics models

by

M. I. Jamaloodeen

---

A Dissertation Presented to the  
FACULTY OF THE GRADUATE SCHOOL  
UNIVERSITY OF SOUTHERN CALIFORNIA

In Partial Fulfillment of the  
Requirements for the Degree  
DOCTOR OF PHILOSOPHY  
(Applied Mathematics)

August 2000

Copyright 2000

M. I. Jamaloodeen

UMI Number: 3018091

Copyright 2000 by  
Jamaloodeen, Mohamed Iqbal

All rights reserved.

UMI<sup>®</sup>

---

UMI Microform 3018091

Copyright 2001 by Bell & Howell Information and Learning Company.  
All rights reserved. This microform edition is protected against  
unauthorized copying under Title 17, United States Code.

---

Bell & Howell Information and Learning Company  
300 North Zeeb Road  
P.O. Box 1346  
Ann Arbor, MI 48106-1346


UNIVERSITY OF SOUTHERN CALIFORNIA  
THE GRADUATE SCHOOL  
UNIVERSITY PARK  
LOS ANGELES, CALIFORNIA 90007

*This dissertation, written by*

MOHAMED I. JAMALDOOPEEN

*under the direction of his..... Dissertation  
Committee, and approved by all its members,  
has been presented to and accepted by The  
Graduate School, in partial fulfillment of re-  
quirements for the degree of*

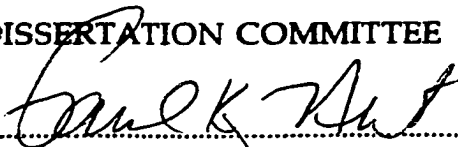
**DOCTOR OF PHILOSOPHY**



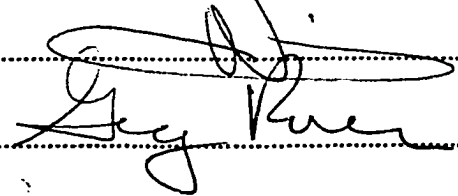
.....  
Dean of Graduate Studies

Date July 13, 2000.....

**DISSERTATION COMMITTEE**



.....  
Chairperson



(Re)Discovering Fundamentalism in the Cultural Margins:  
Calvary Chapel Congregations as Sites of Cultural Resistance  
and Religious Transformation

This dissertation examines the changing face of the Calvary Chapel movement, a religious “awakening” that began among the hippies of the 1960s and has continued to appeal to a new generation of “alternative” youth involved in various subcultures. The focus of the study is four Calvary Chapel congregations in the Southern California area, in which I conducted participant observation and in-depth interviews for four years. I conclude that these churches are sites of symbolic resistance and transformation, similar to the Gramscian model, where resistance is mounted against the hegemonic religious and cultural establishment.

Such protest and resistance is accomplished through the charismatic leadership of the pastors, which enters a ripe social context and leads those in the cultural margins into a transformative religious faith. These transformed individuals are then empowered to live purposeful lives in the name of something higher than themselves. This empowerment by the churches is manifested through a conservative, straightforward ideology; charismatic worship that transcends the mundane; close-knit and intimate community; flexible organization and loose operational structure; and acceptance and appropriation of certain cultural forms, while rejecting and replacing the cultural content. Indeed, these churches consider themselves to be in the center of a cosmic battle waged on various fronts, with the churches providing specific locations for spiritual, as well as cultural, resistance. Moreover, it is in this tension with the culture about them that these churches exhibit certain sectarian qualities. However, they defy the previous definitions of “sect” and “cult,” challenging the current classifications of religious movements,

and appear to be a new type of religious form. Thus, these churches have (re)discovered (as this type of protest has been present throughout the history of Christianity in various forms) a fundamentalist strain of Protestantism in the most unlikely places—that of the cultural margins.

## **Dedication**

...to my parents, my wife Kathija, my family and my friends



## Acknowledgements

I am grateful to Dr. Paul Newton for making my Ph.D experience a rewarding and challenging one. I have learnt much under his supervision and I appreciate his constant encouragement and inspiration.

I am thankful to Dr. Chunming Wang for his encouragement and continuing support throughout my graduate career at the University of Southern California.

My special thanks to Dr. Ronald Bruck who assisted me with some *Mathematica* queries, and Dr. Taufiqar Khan for helping with some *MATLAB* coding issues.

I would like to recognize all the mathematics teachers throughout my young career, and who have, in some way or other, allowed me to reach this far. Most notable amongst these, at USC, has been Dr. Igor Kukavica.

Finally, I must acknowledge the University of Southern California, for the financial and academic opportunities I have received over the last five years. I am particularly indebted to all the staff and faculty of the USC Department of Mathematics.

M.I.J.

Los Angeles, California

July 2000

# Contents

<b>Dedication</b>	<b>ii</b>
<b>Acknowledgements</b>	<b>iii</b>
<b>List Of Figures</b>	<b>v</b>
<b>1 Introduction</b>	<b>1</b>
1.1 Outline . . . . .	1
1.2 The Two-layer Model . . . . .	2
1.3 Derivation of the relative equations. . . . .	9
1.4 Literature review . . . . .	10
<b>2 Symmetries and conservation laws for the two-layer model</b>	<b>15</b>
2.1 Outline . . . . .	15
2.2 Infinite-dimensional Hamiltonian Formalism . . . . .	15
2.2.1 The infinite-dimensional Poisson bracket . . . . .	17
2.2.2 Conservation laws . . . . .	21
2.2.3 The Casimir invariants . . . . .	22
2.3 Hamiltonian formalism for point vortices . . . . .	24
2.3.1 Point symmetries . . . . .	24
2.3.2 Discrete symmetries . . . . .	27
<b>3 Equilibrium solutions for the 2-layer quasi-geostrophic model</b>	<b>29</b>
3.1 Location of fixed equilibria . . . . .	29
3.2 Location of relative equilibria . . . . .	33
3.2.1 Relative equilibria and the energy-momentum mapping . . . . .	44
3.3 Trilinear formulation and location of equilibria in the trilinear plane . . . . .	45
<b>4 Vortex collapse and vortex alignment for the 3-vortex quasi-geostrophic model</b>	<b>51</b>
4.1 Vortex collapse in the two-layer model . . . . .	51
4.2 Vortex alignment in the two-layer model . . . . .	56

<b>5</b>	<b>Numerical investigation of integrable 2-layer quasi-geostrophic vortex dynamics</b>	<b>62</b>
5.1	On streamline patterns for rotating two vortex configurations . . . . .	62
5.1.1	Two rotating vortices in the same layer . . . . .	63
5.1.2	Two rotating vortices in different layers . . . . .	63
5.2	Numerical simulation of integrable four-vortex dynamics . . . . .	65
5.2.1	On integrable four-vortex coaxial configurations . . . . .	65
5.2.2	Numerical simulation of collinear four-vortex configurations . .	70
5.2.2.1	Example 1: coupling and scattering . . . . .	70
5.2.2.2	Example 2: periodic and quasiperiodic behavior . . .	71
5.2.2.3	Example 3: From (quasi-)periodic to scattering behavior . . . . .	73
<b>6</b>	<b>On the motion of point vortices on the sphere</b>	<b>77</b>
6.1	Equations of motion and geometrical formulation . . . . .	77
6.2	On the collapse of three vortices on the sphere . . . . .	78
6.3	Further solutions of integrable point vortex dynamics on the sphere .	89
6.3.1	Non-great-circle four-vortex relative equilibria . . . . .	89
6.3.2	Explicit integration of three-vortex configurations on the sphere	89
6.3.2.1	Example 1 . . . . .	89
6.3.2.2	Example 2 . . . . .	93
6.3.3	Remarks on integrable four-vortex problems on the sphere . .	96
<b>7</b>	<b>On the collapse of two vortices in a circular (planar) domain</b>	<b>100</b>
7.1	Derivation of the Hamiltonian for the $N$ -vortex system in a circular domain . . . . .	100
7.2	Proof that two vortices in a circular domain cannot collide . . . . .	102
	<b>Reference List</b>	<b>105</b>

# List Of Figures

1.1	The quasi-geostrophic two-layer model. . . . .	3
3.1	Typical graphs of the functions (a) $f, g, h$ ; (b) $\frac{f(l)}{l}, \frac{g(l)}{l}, \frac{h(l)}{l}$ . ( $l > 0$ )	34
3.2	Graph of the function $x^2 K_2(x)$ . . . . .	38
3.3	Families of relative equilibria for different Rossby radii of deformation, $\lambda$ . ( $s$ is one length of the isosceles triangle, and $t(s)$ the other, (a) $t$ against $s$ , (b) The ratio $\frac{t}{s}$ against $s$ . ( $\lambda = 0.5, 1, 2, 3$ , with $\lambda = 0.5$ , the bottom curve and $\lambda = 3$ the topmost curve.) . . . . .	40
3.4	The trilinear plane and physical region: three vortices in the same layer with $\Gamma_1 = \Gamma_2 = \Gamma_3 = 1$ . The arrows indicate the positive directions of $b_i$ . (Negative values are possible and correspond to vortices not restricted to being positive.) . . . . .	47
4.1	Phase diagram for $C_1 = 0$ : (a) $\Gamma_1 = \Gamma_2 = 1, \Gamma_3 = 0.5$ , for three vortices in the same layer, using the two-layer model, showing non-self-similar collapsing configurations. . . . .	54
4.2	Typical graphs of the functions, $F(l)$ and $G(l)$ . The function $H(l)$ is qualitatively similar to $F(l)$ , and is not shown. In plotting $F(l)$ , one may take $\lambda_1 > \lambda_2$ , without loss of generality . . . . .	57
4.3	Phase curves of vortex alignment. $C_1 = 0$ ; $\Gamma_1 = 0.25, \Gamma_2 = -\Gamma_3 = 1$ . . . . .	60
5.1	Streamline patterns: two rotating vortices in the same layer, (a) $\frac{d}{\lambda} = 2$ , (b) $\frac{d}{\lambda} = 4$ , (c) $\frac{d}{\lambda} = 4.082$ , (d) $\frac{d}{\lambda} = 8$ . . . . .	64
5.2	Streamline patterns ( $\psi_1$ ): two rotating vortices in different layers, (a) $\frac{d}{\lambda} = 2$ , (b) $\frac{d}{\lambda} = 4$ , (c) $\frac{d}{\lambda} = 5$ , (d) $\frac{d}{\lambda} = 5.128$ , (e) $\frac{d}{\lambda} = 8$ . . . . .	66
5.3	Integrable 4 vortex configurations, showing initial positions of vortices. (a) Two coaxial vortex pairs 12 and 34; (b) two collinear vortex pairs. . . . .	67
5.4	Numerical integration of collinear vortices showing a scattering of vortices. (a) Strongly symmetric configuration (b) Weakly symmetric configuration. Initial positions are:(a)Top layer (1,2) and (-1,-2) and bottom layer (1,-2), and (-1,2), and for (b)Vortices in top layer at (1,2), and (1,-2) with image vortices at (-1,-2), and (-1,2) respectively. . . . .	71

5.5	Numerical integration of scattering for $b = b^* = 0.6$ for a strongly symmetric system . . . . .	72
5.6	Strongly symmetric simulation for Example 2: $x = 4$ . (Image vortices not shown) . . . . .	72
5.7	Strongly symmetric simulation for Example 2: $x^* = 1.03$ . (Image vortices not shown) . . . . .	73
5.8	Strongly symmetric simulation for Example 2: $x = 0.5$ . (Image vortices not shown) . . . . .	73
5.9	Weakly symmetric simulation for Example 2: $x=4$ . (Image vortices not shown) . . . . .	74
5.10	Weakly symmetric simulation for Example 2: $x^* = 3.48$ . (Image vortices not shown) . . . . .	74
5.11	Strongly symmetric simulation for Example 3: quasiperiodic behavior, $x = 3$ . (Image vortices not shown) . . . . .	75
5.12	Strongly symmetric simulation for Example 3: scattering. (a) $x = x^* = 2.1$ , (b) $x = 1 < x^*$ . . . . .	75
5.13	Weakly symmetric simulation for Example 3: quasiperiodic behavior, $x = 4$ . (Image vortices not shown) . . . . .	75
5.14	Weakly symmetric simulation for Example 3: scattering. (a) $x = x^* = 3$ , (b) $x = 2 < x^*$ . . . . .	76
6.1	Phase diagram for $C_1 = 0$ : (a) $\Gamma_1 = \Gamma_2 = -\Gamma_3 = 1$ ( $h > 0$ ), phase curves are open and do not pass through the origin; (b) $\Gamma_1 = \Gamma_2 = 1$ $\Gamma_3 = -\frac{1}{4}$ ( $h < 0$ ) phase curves are closed through the origin but are intercepted by $V = 0$ before reaching it. . . . .	84
6.2	Four-vortex collapsing systems on the plane. . . . .	86
6.3	Non-great-circle 4-vortex relative equilibria. (a) $l_{12} = l_{13} = l_{14} = l_{23} = l_{24}$ where $\Gamma_1$ is at $(0, 0, 1)$ , $\Gamma_2$ is at $(0, -1, 0)$ and $\Gamma_3$ and $\Gamma_4$ are at $(-1, 0, 0)$ and $(1, 0, 0)$ , (b) A tetrahedral configuration. . . . .	90
6.4	Phase curves for $\Gamma_1 = \Gamma_2 = \Gamma_3 = 1$ and $C_1 = 3R^2$ , showing a family of periodic solutions ( $\mu < \tilde{\mu}$ ), a saddle connection, where the phase plane and the physical region boundary $V = 0$ are tangential ( $\mu = \tilde{\mu}$ ), which we explicitly integrate, and a family of solutions where the physical region boundary is reached, ( $\mu > \tilde{\mu}$ ) transversally. . . . .	91
6.5	Co-axial four-vortex configurations on the sphere . . . . .	98
7.1	Method of Images . . . . .	101

# Chapter 1

## Introduction

### 1.1 Outline

In this thesis we study, through the use of Hamiltonian methods, some vortex dynamics problems, with particular emphasis on the two-layer geostrophic model.

We begin, in this chapter, by describing the geostrophic equations of the two-layer model. We compute the streamfunctions and Hamiltonian for  $N$  point vortices using these equations. We conclude our introduction to the two-layer model by describing, in detail the two-vortex problem and its solution, due to Gryanik [26], and present our first result which is a derivation of the relative equations of three point vortices. We end the first chapter by providing a review of some of the literature on vortex dynamics, mentioning, in particular, work that has been done on the sphere, on the plane, on domains with boundaries, and non-integrable problems as well as a summary of the work that has been done for two-layer geostrophic (baroclinic) vortex dynamics. In Chapter 2 we formulate the geostrophic two-layer model as an infinite dimensional Hamiltonian system. Analogously, the point (singular) vortex model is written as a finite dimensional Hamiltonian system. In this framework, we obtain, by virtue of symmetries, the conservation laws and invariants of the respective systems. In the point vortex case it is shown that the three-vortex problem is integrable. We also present other integrable four-vortex systems for the two-layer model. In Chapter 3 we locate and characterize all the equilibrium solutions, for the three-vortex two-layer problem, including both fixed and relative equilibria. We are also able to locate the relative equilibria in the trilinear plane. We continue our discussion of the two-layer model in Chapter 4 by describing some aspects of the finite-time

collision problem as well as the alignment process for three vortices in the two-layer problem. In our main results we show that for the three-vortex problem, two-vortices in the same layer cannot collide in finite time if the third vortex is in the other layer. We also demonstrate that the two-layer model admits non-self-similar collapse for three vortices in the same layer. We end that chapter by explicitly constructing vortex alignment solutions for the three-vortex problem. We conclude our study of the two-layer model in Chapter 5, which is a numerical study of integrable two-layer vortex dynamics. We present some numerical work on streamlines, integrable four-vortex dynamics and a brief study of particle advection.

Chapter 6 contains some results on point vortex dynamics on the sphere. In our first result we show that the only finite-time collapsing solutions for three vortices on the sphere (or on the plane) are self-similar ones. This allows us to conclude that the only self-similar solutions for the three-vortex problem on the sphere are either equilibrium solutions or self-similar collisions. We also obtain a negative result on the collapse of certain symmetrical paralleloid configurations of four vortices on the sphere. We conclude Chapter 6 by presenting new solutions. Included amongst these are relative equilibrium solutions of four vortices that are not great-circle equilibria. Other solutions include two explicit quadratures of three vortex-configurations where the orbits asymptotically approach equilibria. We end Chapter 6 with a result on new integrable four-vortex systems possessing coaxial symmetry.

We conclude with Chapter 7, in which we study vortex dynamics in a circular (planar) domain. We show that two vortices in a circular domain cannot collide (self similarly or otherwise) in a finite time.

## 1.2 The Two-layer Model

The evolution equations for the  $f$ -plane 2-layer quasi geostrophic potential vortex model are:

$$\begin{aligned}\frac{\partial \omega_i}{\partial t} + [\omega_i, \psi_i] &= 0, & i = 1, 2, \\ \omega_1 &= \Delta \psi_1 + \epsilon_1(\psi_2 - \psi_1), \\ \omega_2 &= \Delta \psi_2 - \epsilon_2(\psi_2 - \alpha \psi_1),\end{aligned}\tag{1.1}$$

where  $[,]$  is the Jacobian given by  $[a, b] := a_x b_y - a_y b_x$ ,  $\omega_i$  the geostrophic potential vorticity in the  $i$ -th layer  $\psi_i$  the corresponding streamfunction,  $\rho_i$  the respective fluid densities ( $\rho_1 < \rho_2$ ),  $H_i$  the thicknesses of each layer,  $l$  the Coriolis parameter and  $g$  the constant of gravitational acceleration. The thicknesses of the layers  $H_i$  are assumed to be much smaller than the horizontal scale  $L$  of the system so that the fluid is always in hydrostatic equilibrium, as shown in Fig. 1.1. A free upper

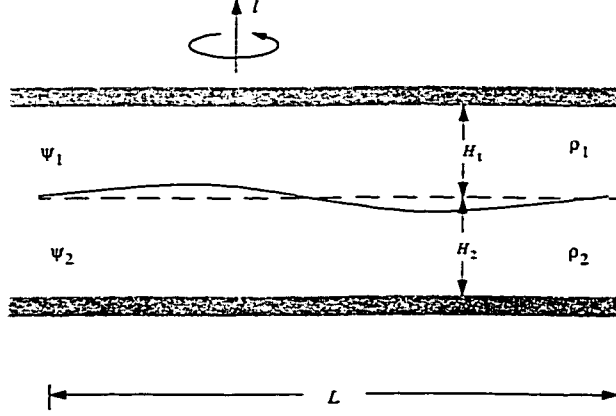


Figure 1.1: The quasi-geostrophic two-layer model.

boundary is assumed and the lower boundary is solid. Observe that the first of these equations are evolution equations that describe the evolution of the vorticity field. The second set of equations are Poisson-like equations with the vorticity on the left hand side. These are nonlinearly coupled to the evolution equations. A nice derivation of these equations can be found in [54].

We can write the two equations for the vector potentials  $\psi_i$ , in operator form,

$$\begin{aligned}\mathcal{L}\psi &= \omega, \\ \mathcal{L} &:= \Delta + M, \\ M &= \begin{pmatrix} -\epsilon_1 & \epsilon_1 \\ \alpha\epsilon_2 & -\epsilon_2 \end{pmatrix},\end{aligned}\tag{1.2}$$



$$\alpha = \frac{\rho_1}{\rho_2}, \quad \epsilon_1 = \frac{l^2 \rho_2}{(\rho_2 - \rho_1)gH_1}, \quad \epsilon_2 = \frac{l^2 \rho_2}{(\rho_2 - \rho_1)gH_2}.$$

By introducing new dependent variables we may diagonalize the system of equations (1.1):

$$\begin{aligned} T\tilde{\psi} &:= \psi, \\ \mathcal{L}T\tilde{\psi} &:= \omega, \\ T^{-1}\mathcal{L}T\tilde{\psi} &:= T^{-1}\omega, \end{aligned}$$

so that

$$(\Delta + D)\tilde{\psi} = T^{-1}\omega, \quad (1.3)$$

where

$$D = \begin{pmatrix} -\lambda_1^2 & 0 \\ 0 & -\lambda_2^2 \end{pmatrix}, \quad T = \begin{pmatrix} \frac{H_1 - H_2 - \sqrt{d}}{2\alpha H_1} & \frac{H_1 - H_2 + \sqrt{d}}{2\alpha H_1} \\ 1 & 1 \end{pmatrix}.$$

It can be shown that  $\lambda_{1,2}^2 = \frac{H_1 + H_2 \pm \sqrt{d}}{H_1 H_2 (1 - \alpha)}$  and  $d = (H_2 - H_1)^2 + 4\alpha H_1 H_2$ . Thus by a change of variables the streamfunctions  $\tilde{\psi}$  can be computed by solving a pair of reduced wave equations given by:

$$\begin{pmatrix} (\Delta - \lambda_1^2)\tilde{\psi}_1 \\ (\Delta - \lambda_2^2)\tilde{\psi}_2 \end{pmatrix} = T^{-1}\omega. \quad (1.4)$$

By standard techniques, one can write the solution of the reduced wave equation in terms of the Green's function for the reduced wave operator

$$\psi_i = \int G(x - z)\omega_i(z)dz, \quad i = 1, 2.$$

The velocity profiles in turn are obtained from the equations (1.12). In the singular or point geostrophic vortex model we consider a vortex distribution of the form:

$$\omega_i = \sum_{k=1}^{N_i} \Gamma_k^i \delta(x - x_k^i) \delta(y - y_k^i) \quad i = 1, 2. \quad (1.5)$$

where the superscript  $i$  denotes the layer, the subscript  $k$  indexes the vortices in that layer and  $N_i$  is the number of vortices in that layer. The  $\Gamma_k^i$  are the strengths of the vortices. The solution of (1.4) with the point vortex allocation (1.5) can be expressed by the Green function for the reduced wave equation  $\frac{1}{2\pi}K_0(\lambda_i r)$ , where  $K_0(x)$  is the modified zero-order Bessel function of the first kind. In the sequel  $|r - r_a| := [(x - x_a)^2 + (y - y_a)^2]^{1/2}$ . Consider first a single vortex in the upper layer labeled by its vortex strength  $\Gamma_i^1$ ,

$$\omega = \begin{pmatrix} \Gamma_i^1 \delta(x - x_i^1) \delta(y - y_i^1) \\ 0 \end{pmatrix},$$

so that

$$T^{-1}\omega = \frac{\alpha H_1}{\sqrt{d}} \begin{pmatrix} -\Gamma_i^1 \delta(x - x_i^1) \delta(y - y_i^1) \\ \Gamma_i^1 \delta(x - x_i^1) \delta(y - y_i^1) \end{pmatrix} = \begin{pmatrix} (\Delta - \lambda_1^2) \tilde{\psi}_1 \\ (\Delta - \lambda_2^2) \tilde{\psi}_2 \end{pmatrix},$$

or, upon solving for  $\tilde{\psi}$ , using the Green function and recalling that  $\psi = T\tilde{\psi}$ , we get

$$\tilde{\psi} = \frac{\alpha H_1 \Gamma_i^1}{2\pi \sqrt{d}} \begin{pmatrix} -K_0(\lambda_1 |r - r_i^1|) \\ K_0(\lambda_2 |r - r_i^1|) \end{pmatrix}.$$

We finally obtain the contribution to the streamfunctions due to the vortex  $\Gamma_i^1$  as:

$$\psi_1 = \frac{\Gamma_i^1}{4\pi} \left[ \left( \frac{H_2 - H_1}{\sqrt{d}} + 1 \right) K_0(\lambda_1 |r - r_i^1|) + \left( \frac{H_1 - H_2}{\sqrt{d}} + 1 \right) K_0(\lambda_2 |r - r_i^1|) \right], \quad (1.6)$$

$$\psi_2 = \frac{\alpha H_1 \Gamma_i^1}{2\pi \sqrt{d}} [K_0(\lambda_2 |r - r_i^1|) - K_0(\lambda_1 |r - r_i^1|)]. \quad (1.7)$$

We follow the same procedure for a single vortex in the lower layer labeled  $\Gamma_j^2$  to obtain the contribution of this vortex to the stream functions:

$$\psi_1 = \frac{\Gamma_j^2 H_2}{2\pi \sqrt{d}} [-K_0(\lambda_1 |r - r_j^2|) + K_0(\lambda_2 |r - r_j^2|)], \quad (1.8)$$

$$\psi_2 = \frac{\Gamma_j^2}{2\pi} [A_- K_0(\lambda_1 |r - r_j^2|) + A_+ K_0(\lambda_2 |r - r_j^2|)], \quad (1.9)$$

where

$$A_- := \frac{H_1 - H_2 + \sqrt{d}}{2\sqrt{d}}, \quad A_+ := \frac{H_2 - H_1 + \sqrt{d}}{2\sqrt{d}}.$$

By linear superposition, the stream functions in the two layers due to an ensemble of point vortices with  $N_1$  of strength  $\Gamma_i^1$  in layer 1 and  $N_2$  of strength  $\Gamma_j^2$  in layer 2 is given by <sup>1</sup>

$$\psi_1 = \frac{1}{2\pi} \sum_{i=1}^{N_1} \Gamma_i^1 [A_+ K_0(\lambda_1 |r - r_i^1|) + A_- K_0(\lambda_2 |r - r_i^1|)] + \quad (1.10)$$

$$\sum_{j=1}^{N_2} \Gamma_j^2 \frac{H_2}{\sqrt{d}} [K_0(\lambda_2 |r - r_j^2|) - K_0(\lambda_1 |r - r_j^2|)],$$

$$\psi_2 = \frac{1}{2\pi} \sum_{i=1}^{N_1} \Gamma_i^1 \frac{\alpha H_1}{\sqrt{d}} [K_0(\lambda_2 |r - r_i^1|) - K_0(\lambda_1 |r - r_i^1|)] + \quad (1.11)$$

$$\sum_{j=1}^{N_2} \Gamma_j^2 [A_- K_0(\lambda_1 |r - r_j^2|) - A_+ K_0(\lambda_2 |r - r_j^2|)].$$

Now the dynamics of the point vortices can be obtained by differentiating the stream-functions as follows:

$$\dot{x}_k^i = -\frac{\partial \psi_i}{\partial y} \Big|_{r=r_i}, \quad \dot{y}_k^i = \frac{\partial \psi_i}{\partial x} \Big|_{r=r_i} \quad i = 1, 2, \quad (1.12)$$

where  $i$  denotes the layer and  $k$  indexes a vortex in that layer. To this end we use the recurrence relation,  $K_0'(x) = -K_1(x)$ , for the zero and first order modified Bessel functions, to obtain the equations for a vortex  $k$  in the first layer:

$$\dot{x}_k^1 = -\frac{1}{2\pi} \sum_{i=1}^{N_1} \Gamma_i^1 \frac{(y_k^1 - y_i^1)}{|r_k^1 - r_i^1|} g(|r_k^1 - r_i^1|) - \frac{1}{2\pi} \sum_{j=1}^{N_2} \Gamma_j^2 \frac{H_2}{\sqrt{d}} \frac{(y_k^1 - y_j^2)}{|r_k^1 - r_j^2|} f(|r_k^1 - r_j^2|), \quad (1.13)$$

$$\dot{y}_k^1 = \frac{1}{2\pi} \sum_{i=1}^{N_1} \Gamma_i^1 \frac{(x_k^1 - x_i^1)}{|r_k^1 - r_i^1|} g(|r_k^1 - r_i^1|) + \frac{1}{2\pi} \sum_{j=1}^{N_2} \Gamma_j^2 \frac{H_2}{\sqrt{d}} \frac{(x_k^1 - x_j^2)}{|r_k^1 - r_j^2|} f(|r_k^1 - r_j^2|). \quad (1.14)$$

---

<sup>1</sup>Note that there is a disagreement with the computations in Gryanik [26].

Here and throughout the ' on the summation means omission of the singular term  $i = k$ . A similar set of formulae hold for the dynamical equations of a vortex  $m$  in the second layer:

$$\begin{aligned} \dot{x}_m^2 &= -\frac{1}{2\pi} \sum_{i=1}^{N_1} \Gamma_i^1 \frac{\alpha H_1}{\sqrt{d}} \frac{(y_m^2 - y_i^1)}{|r_m^2 - r_i^1|} f(|r_m^2 - r_i^1|) \\ &\quad - \frac{1}{2\pi} \sum_{j=1}^{N_2} \Gamma_j^2 \frac{(y_m^2 - y_j^2)}{|r_m^2 - r_j^2|} h(|r_m^2 - r_j^2|) \end{aligned} \quad (1.15)$$

$$\begin{aligned} \dot{y}_m^2 &= -\frac{1}{2\pi} \sum_{i=1}^{N_1} \Gamma_i^1 \frac{\alpha H_1}{\sqrt{d}} \frac{(x_m^2 - x_i^1)}{|r_m^2 - r_i^1|} f(|r_m^2 - r_i^1|) \\ &\quad - \frac{1}{2\pi} \sum_{j=1}^{N_2} \Gamma_j^2 \frac{(x_m^2 - x_j^2)}{|r_m^2 - r_j^2|} h(|r_m^2 - r_j^2|) \end{aligned} \quad (1.16)$$

where for  $l > 0$  and  $\lambda_1 > \lambda_2$

$$\begin{aligned} h(l) &:= -[A_- \lambda_1 K_1(\lambda_1 l) + A_+ \lambda_2 K_1(\lambda_2 l)], \\ f(l) &:= \lambda_1 K_1(\lambda_1 l) - \lambda_2 K_1(\lambda_2 l), \\ g(l) &:= -[A_+ \lambda_1 K_1(\lambda_1 l) + A_- \lambda_2 K_1(\lambda_2 l)]. \end{aligned} \quad (1.17)$$

Extensive use will be made of these functions (1.17) in much of what follows. Similarly, we will also make use of the functions appearing in the streamfunctions and the Hamiltonian. These are defined as follows,

$$\begin{aligned} G(l) &:= A_+ K_0(\lambda_1 l) + A_- K_0(\lambda_2 l), \\ H(l) &:= A_- K_0(\lambda_1 l) + A_+ K_0(\lambda_2 l), \\ F(l) &:= K_0(\lambda_2 l) - K_0(\lambda_1 l). \end{aligned} \quad (1.18)$$

We now mention that there are other simpler two-layer models, that are often used in the geophysical community. One that we will often consider shares many of the features of the full two-layer model of (1.1). The evolution equations are the same, but the equations for the potential vorticity are

$$\omega_i = \Delta \psi_i + (-1)^i \lambda^{-2} (\psi_1 - \psi_2) \quad i = 1, 2. \quad (1.19)$$

There is just one parameter  $\lambda$  to consider here, which can be interpreted as the rigidity of the interface separating the two-layers. The Green's functions corresponding to this system is a little different and the functions corresponding to  $f, g, h$ , and  $F, G, H$ , take the form

$$\begin{aligned}\tilde{f}(l) &:= \frac{1}{l} - \frac{1}{\lambda} K_1 \left( \frac{l}{\lambda} \right), \\ \tilde{g}(l) &:= \frac{1}{l} + \frac{1}{\lambda} K_1 \left( \frac{l}{\lambda} \right), \\ \tilde{F}(l) &:= \ln(l) - \frac{1}{\lambda} K_0 \left( \frac{l}{\lambda} \right), \\ \tilde{G}(l) &:= \ln(l) + \frac{1}{\lambda} K_0 \left( \frac{l}{\lambda} \right).\end{aligned}$$

The two-vortex problem has been studied by Gryanik [26]. It is shown that as a consequence of the conservation of energy the two vortices either rotate about their common center of vorticity or if their center of vorticity is at infinity the pair translates uniformly. The center of vorticity, given in general by

$$(X, Y) = \frac{\sum_{i=1}^2 \rho_i H_i \sum_{j=1}^{N_i} \Gamma_j^i \mathbf{x}_j^i}{\sum_{i=1}^2 \rho_i H_i \sum_{j=1}^{N_i} \Gamma_j^i},$$

is invariant in view of the conservation of linear momentum and is located at  $X = \frac{\Gamma_1 x_1 + \Gamma_2 x_2}{\Gamma_1 + \Gamma_2}$  and  $Y = \frac{\Gamma_1 y_1 + \Gamma_2 y_2}{\Gamma_1 + \Gamma_2}$  for two vortices in the same layer. For two vortices in the top layer, for which  $\Gamma_1 + \Gamma_2 \neq 0$ , with the initial distance between them  $r(t) = r(0) = a$  the periodic orbit is given by  $x = a \cos \omega t$  and  $y = a \sin \omega t$  where  $x$  and  $y$  are relative coordinates,  $x = x_1 - x_2$  and  $y = y_1 - y_2$ . The angular frequency is given by

$$\Omega = \left| \frac{\Gamma_1 + \Gamma_2}{2\pi a} g(a) \right|.$$

If  $\Gamma_1 + \Gamma_2 = 0$  then the speed of translation is

$$v = \left| \Gamma_1 \frac{g(a)}{2\pi} \right|.$$

Similar formulae hold for two vortices in the bottom layer with  $h(a)$  replacing  $g(a)$ . For two vortices in different layers,  $\Gamma_1, \Gamma_2$  in the top and bottom layers respectively, say, the center of vorticity is

$$(X, Y) = \left( \frac{\rho_1 H_1 \Gamma_1 x_1 + \rho_2 H_2 \Gamma_2 x_2}{\rho_1 H_1 \Gamma_1 + \rho_2 H_2 \Gamma_2}, \frac{\rho_1 H_1 \Gamma_1 y_1 + \rho_2 H_2 \Gamma_2 y_2}{\rho_1 H_1 \Gamma_1 + \rho_2 H_2 \Gamma_2} \right)$$

For  $\rho_1 H_1 \Gamma_1 + \rho_2 H_2 \Gamma_2 \neq 0$  the vortices rotate about the center of vorticity with angular frequency:

$$\Omega = \left| \frac{(\Gamma_1 \alpha H_1 + \Gamma_2 H_2) f(a)}{2\pi a \sqrt{d}} \right|,$$

while if  $\rho_1 H_1 \Gamma_1 + \rho_2 H_2 \Gamma_2 = 0$  the vortices translate with speed:

$$v = \left| \frac{\Gamma_2 H_2}{2\pi \sqrt{d}} f(a) \right|.$$

In all cases the center of vorticity is invariant. These invariants will be described thoroughly in Chapter 2.

### 1.3 Derivation of the relative equations.

In this section we derive the relative equations for the two-layer three vortex problem. These equations are readily generalized to the  $N$ -vortex case. For the purpose of illustration, we focus on the case of three vortices in the upper layer, with strengths  $\Gamma_i$ , at positions  $(x_i, y_i)$ ,  $i = 1, 2, 3$ . We have shown that

$$\begin{aligned} 2\pi \dot{x}_1 &= -\Gamma_2 \frac{y_1 - y_2}{r_{12}} g(r_{12}) - \Gamma_3 \frac{y_1 - y_3}{r_{13}} g(r_{13}), \\ 2\pi \dot{y}_1 &= \Gamma_2 \frac{x_1 - x_2}{r_{12}} g(r_{12}) + \Gamma_3 \frac{x_1 - x_3}{r_{13}} g(r_{13}), \\ 2\pi \dot{x}_2 &= -\Gamma_1 \frac{y_2 - y_1}{r_{12}} g(r_{12}) - \Gamma_3 \frac{y_2 - y_3}{r_{23}} g(r_{23}), \\ 2\pi \dot{y}_2 &= \Gamma_1 \frac{x_2 - x_1}{r_{12}} g(r_{12}) + \Gamma_3 \frac{x_2 - x_3}{r_{23}} g(r_{23}). \end{aligned}$$

Subtracting these equations we obtain,

$$2\pi(\dot{x}_1 - \dot{x}_2) = (-\Gamma_2 - \Gamma_1) \frac{y_1 - y_2}{r_{12}} g(r_{12}) - \Gamma_3 \frac{y_1 - y_3}{r_{13}} g(r_{13}) + \Gamma_3 \frac{y_2 - y_3}{r_{23}} g(r_{23}),$$

$$2\pi(\dot{y}_1 - \dot{y}_2) = (\Gamma_2 + \Gamma_1) \frac{x_1 - x_2}{r_{12}} g(r_{12}) + \Gamma_3 \frac{x_1 - x_3}{r_{13}} g(r_{13}) - \Gamma_3 \frac{x_2 - x_3}{r_{23}} g(r_{23}).$$

Now,

$$\begin{aligned} \frac{1}{2} \frac{dr_{12}^2}{dt} &= (x_1 - x_2)(\dot{x}_1 - \dot{x}_2) + (y_1 - y_2)(\dot{y}_1 - \dot{y}_2) \\ &= (-\Gamma_2 - \Gamma_1) \frac{(x_1 - x_2)(y_1 - y_2)}{r_{12}} g(r_{12}) - \Gamma_3 \frac{(x_1 - x_2)(y_1 - y_3)}{r_{13}} g(r_{13}) \\ &\quad + \Gamma_3 \frac{(x_1 - x_2)(y_2 - y_3)}{r_{23}} g(r_{23}) \\ &\quad + (\Gamma_2 + \Gamma_1) \frac{(y_1 - y_2)(x_1 - x_2)}{r_{12}} g(r_{12}) + \Gamma_3 \frac{(y_1 - y_2)(x_1 - x_3)}{r_{13}} g(r_{13}) \\ &\quad - \Gamma_3 \frac{(y_1 - y_2)(x_2 - x_3)}{r_{23}} g(r_{23}) \\ &= \frac{\Gamma_3 g(r_{13})}{r_{13}} [(x_1 - x_3)(y_1 - y_2) - (x_1 - x_2)(y_1 - y_3)] \\ &\quad + \frac{\Gamma_3 g(r_{23})}{r_{23}} [-(x_2 - x_3)(y_1 - y_2) + (x_1 - x_2)(y_2 - y_3)]. \end{aligned}$$

In the last equation the terms in the square parentheses are  $\pm 2A_{123}$ , where  $A_{123}$  is the area of the triangle enclosed by the three vortices  $\Gamma_i$ ,  $i = 1, 2, 3$ , respectively. We conclude that

$$\frac{1}{2} \frac{dr_{12}^2}{dt} = \frac{\Gamma_3 \sigma A_{123}}{2\pi} \left[ \frac{g(r_{13})}{r_{13}} - \frac{g(r_{23})}{r_{23}} \right], \quad (1.20)$$

where  $\sigma$  is the orientation of the triangle, 1 for a cyclic permutation of 1, 2, 3 and -1 otherwise. Similar equations are obtained for  $r_{13}$  and  $r_{23}$  as well as for various allocation of vortices in different layers. One can generalize these relative equations for  $N$  point vortices, however the notation becomes too cumbersome if one is to consider general permutations of  $N$  vortices between the two layers. The relevant equations will be cited where these are needed.

## 1.4 Literature review

There is by now a vast literature on the  $N$ -body problem. The Hamiltonian framework of these mechanical systems can be found in the books by [5, 6, 24]. An

excellent review article is that by Deift [14]. Literature on the  $N$ -vortex problem, is extensive and can be found in many papers, many of which are referenced in the upcoming book by Newton [46]. The geostrophic vortex models are described in many geophysics texts including [51, 54]. There is also a body of review papers on the Hamiltonian description of geostrophic fluid dynamics [45, 55]. There has been some work done on two-layer point vortex dynamics. These include the works of Young, and Hogg and Stommel [57, 29, 30], and, which have been primarily numerical investigations. More analytic results can be found in the work of Gryanik [26] and Zabusky and McWilliams [44]. Some experimental work has been done by Griffiths and Hopfinger [25]. There is also a growing literature on baroclinic vortex patches [18, 52, 53]. Since our work can be seen as an extension of [26], we describe the results obtained there. Gryanik systematically derives the equations of motion for point vortices in the two-layer (baroclinic) model using the evolution equations of potential vorticity. The uncoupling of the streamfunctions by the diagonalization technique, described in Section 1.2 is due to him. He is also credited with formulating the dynamical equations for two-layer point vortices as a Hamiltonian system. He also derives the motion integrals by appealing to Noether's theorem. Although mention is made of integrable four-vortex problems, these are not explicitly presented. The two-vortex problem is integrated by virtue of the integral invariants. We extend these results by studying the *three-vortex* problem and begin by deriving the relative equations and finding the equilibrium solutions. In addition the collapse and alignment processes can occur only with a minimum of three vortices, since the distance between two vortices is always invariant. Our work on these aspects of two-layer point-vortex dynamics is therefore new, as is our application of the trilinear plane reduction techniques in studying qualitative features of three-vortex two-layer point-vortex dynamics.

In addition, Gryanik also studies point vortices in a flow with the simplest regular current, namely constant potential vorticity. Again, the study is restricted to the case of two vortices. The work also contains a study of non-conservative effects, and contains ideas which have not been fully exploited. We have not pursued either of these directions in our study.

Our numerical work in Chapter 5 is in the spirit of [57]. In that work Young studies various interactions between two and four baroclinic point vortices. The



study focuses on the qualitative changes in behavior which occur as the size of the Rossby deformation radius is varied. He also investigates the transport of passive fluid by a translating baroclinic pair. He found that a pair of vortices in the top layer transports no lower layer fluid if the distance between the vortices is less than 1.72 deformation radii. Our study is very similar; whereas he studied coaxial four-vortex configurations, we show that collinear four-vortex configurations are also integrable, and study the various interactions of these four-vortex systems, by demonstrating the various types of motions including direct scattering, exchange scattering, and (quasi-) periodic behavior. We extend his study of the advection problem for translating vortex pairs to rotating vortex pairs.

We compare many of our results, for both the geostrophic two-layer model as well as the model on the sphere, with analogous results on the plane. There is a vast body of literature for point vortex dynamics on the plane. Our work is compared with some of the results obtained by Aref [2] and Synge [56]. The work of Aref, is the first systematic study of three vortices of arbitrary strengths on the plane, and so extends the work of Novikov [47]. Aref's work contains a thorough qualitative analysis of the three-vortex problem. Using trilinear plane techniques the regimes of motion are classified according to the signs of the arithmetic, geometric, and harmonic means of the three vortex strengths. For the special case where the vortex strengths take the values  $(+\Gamma, +\Gamma, -\Gamma)$ , the motion has an interpretation in terms of the scattering of a neutral pair by a single vortex. Quantitative details, including explicit integration in terms of elliptic integrals, are presented for this special case. A systematic study of the finite-time collapse process is also studied. He obtains necessary and sufficient conditions for three vortices to collide in finite time. He also provides a method for explicitly constructing initial conditions which lead to finite-time collapse of the three vortices.

We study the collapse process for the two-layer model as well as the sphere. On the plane explicit collapsing solutions can be found in the works of Aref [2] and Kimura [35]. Four- and five-vortex collapsing solutions have been obtained by Novikov [49]. On the sphere vortex collision has been studied extensively, for the three-vortex problem, by Kidambi and Newton [31, 33]. In Chapter 4 we investigate the alignment process for point vortices in the two-layer model. Work in this area has been done for vortex patches. It has been studied in detail by Polvani [52].

Numerical simulations have also been performed by McWilliams [43]. A general discussion of the mechanism of vortex alignment can be found in the article by Salmon [53]. There is also an extensive literature on equilibria of vortex dynamics. Our work for the two-layer model follows, fairly closely, that of Synge [56]. The papers by Lewis and Ratiu [38] and Marsden and Pekarsky [42], contain ideas that may apply to relative equilibria for the two-layer model.

Nonintegrable vortex dynamics have been studied in the work of Ziglin [58], Aref [3, 4] and Novikov [48]. Detailed presentations can be found in [11, 12, 13].

Our primary reference for our work on the sphere is [31]. In their study, Kidambi and Newton, present a thorough analysis of the three-vortex problem on the sphere, in the spirit of Aref's work on the plane [2]. Instead of using spherical coordinates, they use cartesian coordinates. They present the Poisson-bracket formalism and prove that the three-vortex problem on the sphere is integrable, as well as describe integrable four-vortex systems. In our work we present new integrable four-vortex configurations. In addition to obtaining all the motion integrals, they use the invariance of the center of vorticity vector  $\mathbf{c}$ , to geometrically classify the motions into five distinct families. They then fully characterize all fixed and relative equilibria on the sphere. They show that for fixed equilibria the vortices must lie on great circles. The relative equilibria are classified as either degenerate,  $\mathbf{c} = 0$ , or non-degenerate otherwise. For each type the shape of the vortex triangle is described and the frequency of rotation is computed. As in the planar problem the trilinear plane is introduced to study the motion in the phase plane. All equilibrium solutions are located in the trilinear phase plane, and more complex relative dynamics are also characterized in terms of these coordinates. As on the plane, they state necessary and sufficient conditions for self-similar collapse of three vortices, computing the collapse times and vortex trajectories on the route to collapse. The collapse formulas on the plane and on the sphere are also compared asymptotically. In our work we show that the only (finite-time) collapse of three-vortices on the sphere (or on the plane) is self-similar. We show that the only self-similar solutions of the three-vortex problem on the sphere (or on the plane) are equilibria or self-similar collapsing solutions. We then study the collapse of a four-vortex problem on the sphere. Our work also includes four-vortex relative equilibria that are not trivial great-circle (geodesic)

configurations. We present the explicit integration of special three-vortex solutions, analogous to a periodic one computed in [31].

Systematic derivations for the equations of motion for point vortices on the sphere can be found in [7, 34]. The paper [8] contains a study of the motion of three identical point vortices on the sphere and generalizes the planar results of [47]. Papers that address the effects of rotation include [9, 16, 22, 37, 15]. The recent and ongoing work of Lim [39] uses symplectic reduction and symmetry techniques for the general  $N$ -body problem on the sphere, with applications to vortex dynamics. The work of Hally [28] and Kirwan [36] contains interesting and general ideas that have not been fully exploited. There are several papers, including [10, 17], that address the importance of vortex triples and their emergence in physical systems.

In Chapter 7 we study the collision process for two vortices in a circular domain. Flucher and Gustafsson have studied the collapse for a more general class of domains in [19]. Other references for vortex dynamics in regions with boundaries include [40], where the existence of the Kirchhoff-Routh function was established. Other explicit solutions and proofs of non-integrability for specific domains can be found in [11, 21]. Recently Kidambi and Newton have worked on the problem of vortex dynamics on the sphere with solid boundaries [32].

## Chapter 2

# Symmetries and conservation laws for the two-layer model

## 2.1 Outline

It is well known that many of the equations of geophysical fluid dynamics have Hamiltonian formulations. In this chapter we present the Hamiltonian formalism for the two-layer quasi-geostrophic equations. Our presentation is in the spirit of the review papers [45, 55]. We first present the infinite-dimensional Hamiltonian formalism, by introducing the Poisson bracket and then showing that it is well-defined. We then derive conservation laws for the infinite-dimensional Hamiltonian system by invoking Noether's theorem. Likewise, we present the analogous Hamiltonian formalism, for the discrete (point-vortex) geophysical model. In the point-vortex case, we obtain the integral invariants and show that for the three-vortex problem (in the unbounded plane) there are sufficiently many integrals in involution to make the problem integrable. We also present some symmetrical four-vortex problems that are integrable. We conclude with a description of the discrete symmetries present in the equations for point vortices.

## 2.2 Infinite-dimensional Hamiltonian Formalism

As in the 2D Euler equations the energy of the system (1.1) is given by

$$\int_D |v|^2 d\mathbf{x} .$$

Integrating by parts and substituting for  $v$  by  $\omega_i$  and  $\psi_i$ ,

$$\mathcal{H}(\omega) = -\frac{1}{2} \int (\rho_1 H_1 \psi_1 \omega_1 + \rho_2 H_2 \psi_2 \omega_2) dx dy. \quad (2.1)$$

For simplicity we assume that  $\psi_i \rightarrow 0$  as  $r \rightarrow \infty$ . Substituting into (2.1) the equations for  $\omega_i$  from (1.1), and integrating by parts, we obtain:

$$\begin{aligned} \mathcal{H} &= -\frac{1}{2} \int (\rho_1 H_1 \psi_1 [\Delta \psi_1 + \frac{l^2 \rho_2}{g H_1 (\rho_2 - \rho_1)} (\psi_2 - \psi_1)] \\ &\quad + \rho_2 H_2 \psi_2 [\Delta \psi_2 - \frac{l^2}{g H_2} (\frac{\rho_2}{\rho_2 - \rho_1} \psi_1 - \frac{\rho_1}{\rho_2 - \rho_1} \psi_2)]) dx dy \\ &= \frac{1}{2} \int \{ \rho_1 H_1 \psi_1 |\nabla \psi_1|^2 + \rho_2 H_2 \psi_2 |\nabla \psi_2|^2 \\ &\quad + \frac{l^2}{g} \left[ \frac{\rho_2 \rho_1}{\rho_2 - \rho_1} \psi_1 (\psi_1 - \psi_2) + \rho_2 \psi_2 (\frac{\rho_2}{\rho_2 - \rho_1} \psi_2 - \frac{\rho_1}{\rho_2 \rho_1} \psi_1) \right] \} dx dy. \end{aligned}$$

Rearranging yields:

$$\begin{aligned} \mathcal{H} &= \frac{1}{2} \int \{ \rho_1 H_1 \psi_1 |\nabla \psi_1|^2 + \rho_2 H_2 \psi_2 |\nabla \psi_2|^2 \\ &\quad + \frac{l^2}{g} \left[ \rho_1 \psi_1^2 + \frac{\rho_2^2}{\rho_2 - \rho_1} (\psi_2 - \frac{\rho_1}{\rho_2} \psi_1)^2 \right] \} dx dy. \end{aligned}$$

Introduce the standard inner product  $(\cdot, \cdot)$  for  $F, G : \mathbf{R}^2 \mapsto \mathbf{R}^2$ :

$$(F, G) = \int_{\mathbf{R}} F \cdot G dx dy.$$

where  $F, G \in L^2(\mathbf{R}^2)^2$ . We work in the function space:

$$\mathcal{A} = \{F \in L^2(\mathbf{R}^2)^2 | F \rightarrow 0, \text{ as } r \rightarrow \infty\}.$$

Using this and the definition of  $\mathcal{H}(\omega)$  in (2.1), one can show that the vorticity formulation and integration by parts leads to the following variational derivatives:

$$\frac{\delta \mathcal{H}}{\delta \omega_1} = -\rho_1 H_1 \psi_1, \quad \frac{\delta \mathcal{H}}{\delta \omega_2} = -\rho_2 H_2 \psi_2.$$

Recall that the variational derivative of a functional  $\mathcal{F}$  with respect to  $u$  is given by

$$\delta\mathcal{F} = \mathcal{F}(u + \delta u) - \mathcal{F}(u) = \left(\frac{\delta\mathcal{F}}{\delta u}, \delta u\right) + O(\delta u^2),$$

for admissible but otherwise arbitrary variations. More details can be found in the article of Shepherd [55] or in Olver [50] (Sec 4.1). Note that a functional derivative is itself a function (possibly nonlocal) of  $u$ .

### 2.2.1 The infinite-dimensional Poisson bracket

Introduce the Poisson bracket between two functionals, for a linear operator  $J$  acting on functions belonging to  $\mathcal{A}$ ,

$$[\mathcal{F}, \mathcal{G}] := \left(\frac{\delta\mathcal{F}}{\delta\omega}, J\frac{\delta\mathcal{G}}{\delta\omega}\right). \quad (2.2)$$

**Definition 2.1**  *$J$  will be called Hamiltonian if its Poisson bracket satisfies the conditions of*

(i) *Skew-symmetry*

$$[\mathcal{P}, \mathcal{L}] = -[\mathcal{L}, \mathcal{P}],$$

(ii) *and the Jacobi-identity,*

$$[[\mathcal{P}, \mathcal{L}], \mathcal{R}] + [[\mathcal{R}, \mathcal{P}], \mathcal{L}] + [[\mathcal{L}, \mathcal{R}], \mathcal{P}] = 0.$$

*for all functionals  $\mathcal{P}$ ,  $\mathcal{L}$  and  $\mathcal{R}$  for which (2.2) is well-defined.*

To verify these we use the language of functional multi-vectors and the exposition in Olver [50] (Chapter 7.1). We shall make use of the following theorem [50].

**Theorem 2.2** *Let  $\mathcal{D}$  be a skew-adjoint  $q \times q$  matrix differential operator and  $\Theta = \frac{1}{2} \int \{\theta \wedge \mathcal{D}\theta\} dx$ , the corresponding functional bi-vector, then  $\mathcal{D}$  is Hamiltonian if and only if*

$$pr \nabla_{\mathcal{D}\theta}(\Theta) = 0. \quad (2.3)$$

Here  $pr \mathbf{v}_{\mathcal{D}\theta}(\Theta)$  is the action of the prolongation of the “vector field”  $\mathbf{v}_{\mathcal{D}\theta}$ , on the functional bi-vector  $\Theta$  and is given by (2.4) for the particular case of the two-layer model. In addition, for the two-layer model,

$$\mathcal{D} = J = \begin{pmatrix} -\frac{[\omega_1, \cdot]}{\rho_1 H_1} & -\frac{[\omega_2, \cdot]}{\rho_2 H_2} \end{pmatrix},$$

$$J_{ii} = -\frac{[(\omega_i)_x D_y - (\omega_i)_y D_x]}{\rho_i H_i} = \frac{(\omega_i)_y D_x - (\omega_i)_x D_y}{\rho_i H_i}, \quad i = 1, 2,$$

where, following the notation of Chapter 1,  $[a, b] := a_x b_y - a_y b_x$ . The adjoint of  $J_{11}$  is

$$\begin{aligned} J_{11}^* &= \frac{1}{\rho_1 H_1} [(-D_x) \cdot (\omega_1)_y + (D_y) \cdot (\omega_1)_x] \\ &= \frac{1}{\rho_1 H_1} [-(\omega_1)_{xy} - (\omega_1)_y D_x + (\omega_1)_{xy} + (\omega_1)_x D_y] \\ &= \frac{1}{\rho_1 H_1} [(\omega_1)_x D_y - (\omega_1)_y D_x] = -J_{11}. \end{aligned}$$

Likewise  $J_{22}^* = -J_{22}$ , thereby verifying that  $J$  is skew-adjoint. We now apply the theorem to verify the Jacobi identity. To ease notation, let  $\omega^1$  and  $\omega^2$  denote the vorticity fields in layer 1 and layer 2 respectively. In this framework the functional bi-vector becomes:

$$\begin{aligned} \Theta &= \frac{1}{2} \int \theta \wedge \mathcal{D}\theta dx dy = \frac{1}{2} \int [\theta^1 \wedge \mathcal{D}_{11}\theta^1 + \theta^2 \wedge \mathcal{D}_{22}\theta^2] dx dy \\ &= \frac{1}{2\rho_1 H_1} \int [\omega_y^1 \theta^1 \wedge \theta_x^1 - \omega_x^1 \theta^1 \wedge \theta_y^1] dx dy + \frac{1}{2\rho_2 H_2} \int [\omega_y^2 \theta^2 \wedge \theta_x^2 - \omega_x^2 \theta^2 \wedge \theta_y^2] dx dy. \end{aligned}$$

Here, the prolongation of the “vector field”  $\mathbf{v}_{\mathcal{D}\theta}$  is given by

$$pr \mathbf{v}_{\mathcal{D}\theta} = \sum_I D_I (\mathcal{D}_{11}\theta^1) \frac{\partial}{\partial \omega_I^1} + D_I (\mathcal{D}_{22}\theta^2) \frac{\partial}{\partial \omega_I^2}, \quad (2.4)$$

where  $D_I$  is the total derivative given by the multi-index  $I$ .

In this framework, we can state the fundamental theorem of this chapter.

**Theorem 2.3** *The two-layer geostrophic vorticity equations, (1.1), form an infinite-dimensional Hamiltonian system.*

**Proof:** According to the Theorem 2.2 it remains to show that

$$pr \ v_{\mathcal{D}\theta}(\Theta) = 0.$$

The argument is a straightforward generalization of the one in Olver [50], (Example 7.10). Integrating by parts,

$$v_{\mathcal{D}\theta}(\Theta) = \frac{1}{2} \sum_{i=1}^2 \frac{1}{\rho_i H_i} \int \{ D_y [\omega_y^i \theta_x^i - \omega_x^i \theta_y^i] \wedge \theta^i \wedge \theta_x^i - D_x [\omega_y^i \theta_x^i - \omega_x^i \theta_y^i] \wedge \theta^i \wedge \theta_y^i \} dx dy.$$

Consider  $i = 1$ , and define:

$$\begin{aligned} A := \int & \{ [\omega_{yy}^1 \theta_x^1 + \omega_y^1 \theta_{xy}^1 - \omega_{xy}^1 \theta_y^1 - \omega_x^1 \theta_{yy}^1] \wedge \theta^1 \wedge \theta_x^1 \\ & - [\omega_{yx}^1 \theta_x^1 + \omega_y^1 \theta_{xx}^1 - \omega_{xx}^1 \theta_y^1 - \omega_x^1 \theta_{yx}^1] \wedge \theta^1 \wedge \theta_y^1 \} dx dy. \end{aligned}$$

But,

$$\omega_{yy}^1 \theta_x^1 \wedge \theta^1 \wedge \theta_x^1 = 0 = \omega_{xx}^1 \theta_y^1 \wedge \theta^1 \wedge \theta_y^1,$$

by the skew-linearity of the wedge-product, i.e:

$$\theta_x^1 \wedge \theta_x^1 = \theta_y^1 \wedge \theta_y^1 = 0.$$

Moreover,

$$-\omega_{xy}^1 \theta_y^1 \wedge \theta^1 \wedge \theta_x^1 = -\omega_{yx}^1 \theta_y^1 \wedge \theta^1 \wedge \theta_x^1 = -\omega_{yx}^1 \theta^1 \wedge \theta_x^1 \wedge \theta_x^1 = \omega_{yx}^1 \theta_x^1 \wedge \theta^1 \wedge \theta_y^1.$$

Hence the third and fourth terms cancel, giving

$$\begin{aligned} A := \int & \{ \omega_x^1 [\theta_{yx}^1 \wedge \theta^1 \wedge \theta_y^1 - \theta_{yy}^1 \wedge \theta^1 \wedge \theta_x^1] \\ & + \omega_y^1 [\theta_{xy}^1 \wedge \theta^1 \wedge \theta_x^1 - \theta_{xx}^1 \wedge \theta^1 \wedge \theta_y^1] \} dx dy. \end{aligned}$$



Integrating the second and fourth terms,

$$\begin{aligned} - \int \theta_{yy}^1 \wedge (\omega_x^1 \wedge \theta^1 \wedge \theta_x^1) dx dy &= \int \theta_y^1 \wedge [\omega_{xy}^1 \wedge \theta^1 \wedge \theta_x^1 + \omega_x^1 (\theta_y^1 \wedge \theta_x^1 + \theta^1 \wedge \theta_{xy}^1)] dx dy \\ &= \int [\omega_{xy}^1 \theta_y^1 \wedge \theta^1 \wedge \theta_x^1 + \omega_x^1 \theta_y^1 \wedge \theta^1 \wedge \theta_{xy}^1] dx dy, \end{aligned}$$

since  $\theta_y^1 \wedge \theta_y^1 = 0$ . Likewise,

$$- \int \theta_{xx}^1 \wedge (\omega_y^1 \wedge \theta^1 \wedge \theta_y^1) dx dy = \int [\omega_{xy}^1 \theta_x^1 \wedge \theta^1 \wedge \theta_y^1 + \omega_y^1 \theta_x^1 \wedge \theta^1 \wedge \theta_{xy}^1] dx dy.$$

Substituting these last two into  $A$ , and using the anti-commutative property of the wedge product gives, finally,

$$\begin{aligned} A &= \int \{ \omega_x^1 (\theta_{xy}^1 \wedge \theta^1 \wedge \theta_y^1 + \theta_y^1 \wedge \theta^1 \wedge \theta_{xy}^1) + \omega_{xy}^1 \theta_y^1 \wedge \theta^1 \wedge \theta_x^1 \\ &\quad + \omega_y^1 (\theta_{xy}^1 \wedge \theta^1 \wedge \theta_x^1 + \theta_x^1 \wedge \theta^1 \wedge \theta_{xy}^1) + \omega_{xy}^1 \theta_x^1 \wedge \theta^1 \wedge \theta_y^1 \} dx dy. \end{aligned}$$

This completes the proof, since  $i = 2$  is similar.  $\square$ .

Now that we have established that  $J$  is Hamiltonian, we express the Poisson bracket in a more familiar form:

$$\begin{aligned} [\mathcal{F}, \mathcal{G}] &= \left( \frac{\delta \mathcal{F}}{\delta \omega}, J \frac{\delta \mathcal{G}}{\delta \omega} \right) = \int \left( \frac{\delta \mathcal{F}}{\delta \omega_1}, \frac{\delta \mathcal{F}}{\delta \omega_2} \right) J \begin{pmatrix} \frac{\delta \mathcal{G}}{\delta \omega_1} \\ \frac{\delta \mathcal{G}}{\delta \omega_2} \end{pmatrix} dx dy \\ &= \int \left( \frac{\delta \mathcal{F}}{\delta \omega_1}, \frac{\delta \mathcal{F}}{\delta \omega_2} \right) \cdot \begin{pmatrix} -\frac{\partial(\omega_1, \frac{\delta \mathcal{G}}{\delta \omega_1})}{\frac{\rho_1 H_1}{\partial(\omega_2, \frac{\delta \mathcal{G}}{\delta \omega_2})}} \\ -\frac{\partial(\omega_2, \frac{\delta \mathcal{G}}{\delta \omega_2})}{\rho_2 H_2} \end{pmatrix} dx dy \\ &= \int \left[ \frac{1}{\rho_1 H_1} \omega_1 \partial \left( \frac{\delta \mathcal{F}}{\delta \omega_1}, \frac{\delta \mathcal{G}}{\delta \omega_1} \right) + \frac{1}{\rho_2 H_2} \omega_2 \partial \left( \frac{\delta \mathcal{F}}{\delta \omega_2}, \frac{\delta \mathcal{G}}{\delta \omega_2} \right) \right] dx dy, \end{aligned}$$

where the last follows after an integration by parts.

### 2.2.2 Conservation laws

In this section we present the conservation laws for the two-layer model in infinite-dimensional Hamiltonian form. First, recall that for any functional  $\mathcal{F}$ , the dynamics can be expressed by

$$\frac{d\mathcal{F}}{dt} = [\mathcal{F}, \mathcal{H}].$$

The invariants are summarized in the following proposition, and are derived essentially by appeal to Noether's theorem.

**Theorem 2.4** *The quasi-geostrophic two-layer model in the unbounded plane, has as integral motion invariants,  $\mathcal{H}$ , linear momentum  $\mathcal{M}_x$ , and,  $\mathcal{M}_y$ , and, angular momentum  $\mathcal{M}_\theta$ .*

**Proof:** The invariance of  $\mathcal{H}$  is immediate since  $\frac{d\mathcal{H}}{dt} = [\mathcal{H}, \mathcal{H}] = 0$ , by the skew-linearity of the Poisson bracket. Since  $\mathcal{H}$  and  $J$  have no explicit dependence on  $x$  or  $y$ ,  $\mathcal{H}$  is invariant with respect to spatial displacements. Applying Noether's theorem with respect to  $x$  we seek a function  $\mathcal{M}$  for which:

$$\begin{aligned} J \frac{\delta \mathcal{M}}{\delta \omega} &= -\omega_x, \text{ or} \\ (\omega_i)_x \left( \frac{\delta \mathcal{M}}{\delta \omega} \right)_y - (\omega_i)_y \left( \frac{\delta \mathcal{M}}{\delta \omega} \right)_x &= \rho_i H_i (\omega_i)_x. \end{aligned}$$

By inspection,

$$\frac{\delta \mathcal{M}}{\delta \omega_i} = \rho_i H_i y,$$

is a candidate, so that the linear momentum in the x-direction,

$$\mathcal{M}_x = \int [\rho_1 H_1 \omega_1 + \rho_2 H_2 \omega_2] y dx dy,$$

is an integral invariant and similarly so is the linear momentum in the y-direction,

$$\mathcal{M}_y = \int [\rho_1 H_1 \omega_1 + \rho_2 H_2 \omega_2] x dx dy.$$

We now consider rotational symmetry. In polar coordinates,  $x = r \cos \theta$ ,  $y = r \sin \theta$ , the Hamiltonian is expressed as:

$$\mathcal{H}(\omega) = \int [\rho_1 H_1 \psi_1 \omega_1 + \rho_2 H_2 \psi_2 \omega_2] r dr d\theta. \quad (2.5)$$

Using the chain-rule, we have, in polar coordinates,

$$[a, b] := a_x b_y - a_y b_x = \frac{1}{r} (a_r b_\theta - a_\theta b_r). \quad (2.6)$$

From (2.5) and (2.6) it is clear that  $\mathcal{H}$  and  $J$  do not depend explicitly on  $\theta$  so applying Noether's theorem, we seek a functional  $\mathcal{M}$  for which:

$$\begin{aligned} J \frac{\delta \mathcal{M}}{\delta \omega} &= -\omega_\theta, \text{ or} \\ (\omega_i)_r \left( \frac{\delta \mathcal{M}}{\delta \omega} \right)_\theta - (\omega_i)_\theta \left( \frac{\delta \mathcal{M}}{\delta \omega} \right)_r &= \rho_i H_i r (\omega_i)_\theta. \end{aligned}$$

By inspection,

$$\frac{\delta \mathcal{M}}{\delta \omega_i} = \rho_i H_i \frac{r^2}{2},$$

so that the angular momentum,

$$\mathcal{M}_\theta = \frac{1}{2} \int [\rho_1 H_1 \omega_1 + \rho_2 H_2 \omega_2] r^2 dx dy,$$

is also an integral invariant. □

We remark that these conservation laws are the natural generalizations of the planar or one-layer model. An alternative derivation of these invariants can be found in the article by Young [57].

### 2.2.3 The Casimir invariants

In addition to the conservation laws arising from the Hamiltonian symmetries, there are also “distinguished functionals,” arising from the degeneracies of the Poisson bracket itself. These Casimir invariants are solutions of

$$J \frac{\delta \mathcal{C}}{\delta \omega} = 0. \quad (2.7)$$

To see that  $\mathcal{C}$  indeed determines a conservation law observe that

$$\frac{d\mathcal{C}}{dt} = [\mathcal{C}, \mathcal{H}] = \left( \frac{\delta\mathcal{C}}{\delta\omega}, J \frac{\delta\mathcal{H}}{\delta\omega} \right) = - \left( J \frac{\delta\mathcal{C}}{\delta\omega}, \frac{\delta\mathcal{H}}{\delta\omega} \right).$$

Now the solutions of (2.7) are given by

$$[\omega_i, \frac{\delta\mathcal{C}}{\delta\omega_i}] = 0 \quad i = 1, 2,$$

which implies that

$$\frac{\delta\mathcal{C}}{\delta\omega_i} = \frac{\partial C(\omega_1, \omega_2)}{\partial\omega_i}, \quad (2.8)$$

for some sufficiently smooth function  $C(\omega_1, \omega_2)$ , of  $\omega = (\omega_1, \omega_2)$ , Necessary and sufficient conditions on  $C$  and  $\mathcal{C}$  for solutions of (2.8) are:

$$\mathcal{C}(\omega) = \int C(\omega_1, \omega_2) dx dy.$$

Observe, in particular, the following invariants which are conservation of cirulation and enstrophy respectively:

$$\begin{aligned} \mathcal{C}_1 &= \int (\rho_1 H_1 \omega_1 + \rho_2 H_2 \omega_2) dx dy, \\ \mathcal{C}_2 &= \int (\rho_1 H_1 \omega_1^2 + \rho_2 H_2 \omega_2^2) dx dy. \end{aligned}$$

Other conservation laws can be obtained from manipulation of the invariants  $\mathcal{H}$ ,  $\mathcal{M}_x$ ,  $\mathcal{M}_y$ ,  $\mathcal{M}_r$ ,  $\mathcal{C}_1$ ,  $\mathcal{C}_2$ . We mention two important ones in the following corollary.

**Corollary 2.5** *The center of vorticity*

$$\begin{aligned} X &:= \frac{\mathcal{M}_x}{\mathcal{C}_1} = \frac{\int x[\rho_1 H_1 \omega_1 + \rho_2 H_2 \omega_2] dx dy}{\int (\rho_1 H_1 \omega_1 + \rho_2 H_2 \omega_2) dx dy}, \\ Y &:= \frac{\mathcal{M}_y}{\mathcal{C}_1} = \frac{\int y[\rho_1 H_1 \omega_1 + \rho_2 H_2 \omega_2] dx dy}{\int (\rho_1 H_1 \omega_1 + \rho_2 H_2 \omega_2) dx dy}, \end{aligned}$$

*is invariant as is the vorticity distribution about its center of vorticity:*

$$D^2 := \frac{\int [(x - X)^2 + (y - Y)^2] (\rho_1 H_1 \omega_1 + \rho_2 H_2 \omega_2) dx dy}{\int (\rho_1 H_1 \omega_1 + \rho_2 H_2 \omega_2) dx dy}.$$

## 2.3 Hamiltonian formalism for point vortices

### 2.3.1 Point symmetries

We now present the Hamiltonian formalism for the point vortices introduced in Chapter 1. Using the formula for the energy (2.1) and the singular (point) vortices from Chapter 1, one obtains the following finite-dimensional Hamiltonian system:

$$\begin{aligned}
H &= \frac{1}{4\pi} \sum_{i,I,i \neq I}^{N_1} (\rho_1 H_1) \Gamma_i^1 \Gamma_I^1 [A_+ K_0(\lambda_1 l_{iI}) + A_- K_0(\lambda_2 l_{iI})] \\
&\quad + \frac{1}{4\pi} \sum_{j,J,j \neq J}^{N_2} (\rho_2 H_2) \Gamma_j^2 \Gamma_J^2 [A_+ K_0(\lambda_1 l_{iI}) + A_- K_0(\lambda_2 l_{iI})] \\
&\quad + \frac{1}{2\pi} \sum_{i,j}^{N_1, N_2} \frac{\rho_1 H_1 H_2}{\sqrt{d}} \Gamma_i^1 \Gamma_j^2 [K_0(\lambda_2 l_{ij}) - K_0(\lambda_1 l_{ij})] \\
&= \frac{1}{\pi} \sum_{i,I,i \neq I}^{N_1} (\rho_1 H_1) \Gamma_i^1 \Gamma_I^1 F(l_{iI}) + \frac{1}{4\pi} \sum_{j,J,j \neq J}^{N_2} (\rho_2 H_2) \Gamma_j^2 \Gamma_J^2 G(l_{jJ}) \\
&\quad + \frac{1}{4\pi} \sum_{i,j}^{N_1, N_2} \frac{\rho_1 H_1}{\sqrt{d}} \Gamma_i^1 \Gamma_J^2 H(l_{ij}), \tag{2.9}
\end{aligned}$$

where  $l_{k,m}$  denotes the distance between the vortices labeled  $k$  and  $m$ , and where all constants and functions were defined in Chapter 1. With this, the dynamical equations can be put in the following Hamiltonian form:

$$\dot{q}_k^i = \frac{\partial H}{\partial p_k^i}, \quad \dot{p}_k^i = -\frac{\partial H}{\partial q_k^i}, \tag{2.10}$$

$$q_k^i := x_k^i \quad p_k^i := \Gamma_k^i \rho_i H_i y_k^i \quad i = 1, 2 \text{ and } k = 1, \dots, N_i. \tag{2.11}$$

The Poisson bracket then becomes the canonical one:

$$[F, H] = \sum_{i=1}^2 \sum_{k=1}^{N_i} \left( \frac{\partial F}{\partial q_k^i} \frac{\partial H}{\partial p_k^i} - \frac{\partial F}{\partial p_k^i} \frac{\partial H}{\partial q_k^i} \right), \tag{2.12}$$

and the conservation of  $H$  is immediate. The other invariants are obtained by appealing to Noether's theorem, since the Hamiltonian (2.9) is seen to be invariant with respect to arbitrary spatial displacements as well as rotations. Alternatively,

and more tediously, they can be verified by substituting into the Poisson bracket (2.12). These invariants are linear and angular momentum,

$$\begin{aligned}\mathcal{M}_x &:= Q = \sum_{i=1}^2 \rho_i H_i \sum_{j=1}^{N_i} \Gamma_j^i x_j^i, \\ \mathcal{M}_y &:= P = \sum_{i=1}^2 \rho_i H_i \sum_{j=1}^{N_i} \Gamma_j^i y_j^i, \\ \mathcal{M}_r &:= I = \sum_{i=1}^2 \rho_i H_i \sum_{j=1}^{N_i} \Gamma_j^i l_j^{i^2},\end{aligned}$$

where

$$l_j^{i^2} = x_j^{i^2} + y_j^{i^2}.$$

Now, by the conservation of  $P$ ,  $Q$ , and  $I$ , it is clear that

$$[H, P] = [H, Q] = [H, I] = 0. \quad (2.13)$$

It is straightforward, if laborious, to compute that

$$[Q, I] = 2P, \quad [P, I] = 2Q.$$

Using the Leibnitz rule and these last two we obtain,

$$\begin{aligned}[P^2, I] &= -[I, P^2] = -[I, PP] = -2[I, P]P = -4QP, \\ [Q^2, I] &= -[I, Q^2] = -[I, QQ] = -2[I, Q]Q = 4QP.\end{aligned}$$

Hence we see that

$$[P^2 + Q^2, I] = 0. \quad (2.14)$$

These calculations allow us to conclude the following theorem.

**Theorem 2.6** *The three-vortex two-layer problem on the unbounded plane is integrable.*

**Proof:** The invariance of  $H$ ,  $I$ , and  $P^2 + Q^2$ , either by appeal to Noether's theorem or through the use of the Poisson bracket, has already been established. The calculations leading to (2.13) and (2.14) show that there are three analytic integrals in involution, namely  $H$ ,  $I$ , and  $P^2 + Q^2$ . For the three-vortex problem this is sufficient to conclude integrability.  $\square$

As in the one-layer model, since  $I$ ,  $P$ ,  $Q$  and  $\Gamma_i$  are all conserved quantities, so is the following:

$$\begin{aligned} \left[ \sum_{i=1}^2 \rho_i H_i \sum_{j=1}^{N_i} \Gamma_j^i \right] I - Q^2 - P^2 &= (\rho_1 H_1)^2 \sum_{i < j} \Gamma_i^1 \Gamma_j^1 l_{ij}^2 + (\rho_2 H_2)^2 \sum_{i < j} \Gamma_i^2 \Gamma_j^2 l_{ij}^2 \\ &+ \frac{\rho_1 \rho_2 H_1 H_2}{2} \sum_{i,j}^{N_1, N_2} \Gamma_i^1 \Gamma_j^2 l_{ij}^2. \end{aligned} \quad (2.15)$$

The invariance of the left-hand side is evident, the equality however is straightforward if tedious to verify. As in the one-layer case (or as on the sphere) we will make use of this invariant, in much of what follows, particularly in reducing the three-vortex problem through the use of the trilinear plane in Chapter 3. This will be achieved, for the three-vortex problem, by regarding this invariant as a parameter to characterize the dynamical regimes of motion. We remark, also, that the center of vorticity given by

$$(X, Y) = \frac{(Q, P)}{\sum_{i=1}^2 \rho_i H_i \sum_{j=1}^{N_i} \Gamma_j^i},$$

is invariant. This together with the invariants  $\mathcal{M}_x, \mathcal{M}_y, \mathcal{M}_r$  show that the distribution of the vorticity about its center of vorticity,

$$\frac{\sum_{i=1}^2 \sum_{j=1}^{N_i} [(x_j^i - X)^2 + (y_j^i - Y)^2]}{\sum_{i=1}^2 \rho_i H_i \sum_{j=1}^{N_i} \Gamma_j^i}, \quad (2.16)$$

is also invariant. We conclude by considering integrable four-vortex two-layer problems, and prove the following result.

**Theorem 2.7** *If  $P = Q = 0$  and*

$$\sum_{i=1}^2 \rho_i H_i \sum_{j=1}^{N_i} \Gamma_j^i = 0, \quad (2.17)$$

holds, then the four-vortex two-layer problem on the unbounded plane is integrable.

**Proof:** An easy computation shows that

$$[Q, P] = \sum_{i=1}^2 \rho_i H_i \left( \sum_{j=1}^{N_i} \Gamma_j^i \right), \quad (2.18)$$

and since

$$[Q, I] = 2P, \quad [P, I] = -2Q,$$

if we have  $P = Q = 0$ , then there are four integrals in involution, namely  $(H, P, Q, I)$ . But since  $P = Q = 0$  and (2.18) holds it is clearly necessary that (2.17) holds. We conclude that if  $P = Q = 0$  and (2.17) holds then the four-vortex two-layer problem is integrable.  $\square$

We remark that this is similar to the one-layer model on the plane, but differs from the situation on the sphere, for example, where the corresponding requirement, (2.17) is not necessary, as shown in [31]. This is also discussed in Chapter 6. Other integrable four-vortex configurations possessing other symmetries such as axial or collinear symmetry, are also discussed in Chapter 5.

### 2.3.2 Discrete symmetries

The dynamical equations of Chapter 1, or the equations (2.10-2.11), explicitly expanded, possess certain discrete symmetries. In particular, it is not difficult to prove the following result:

**Theorem 2.8** *If  $\Gamma_1, \Gamma_2, \dots, \Gamma_n; \mathbf{x}_1, \mathbf{x}_2, \dots, \mathbf{x}_n; t$  satisfy the equations of motion, then so do:*

- (a)  $-\Gamma_1, -\Gamma_2, \dots, -\Gamma_n; -\mathbf{x}_1, -\mathbf{x}_2, \dots, -\mathbf{x}_n; t,$
- (b)  $-\Gamma_1, -\Gamma_2, \dots, -\Gamma_n; \mathbf{x}_1, \mathbf{x}_2, \dots, \mathbf{x}_n; -t,$
- (c)  $\Gamma_1, \Gamma_2, \dots, \Gamma_n; -\mathbf{x}_1, -\mathbf{x}_2, \dots, -\mathbf{x}_n; -t.$



*In addition, for the case of two vortices in the same layer (labeled 1 and 2) and the third vortex (labeled 3) in the other, the equations of motion are invariant with respect to interchanging the indices 1 and 2.*

These symmetries mean that in the study of the three vortex problem, it will be sufficient to consider only the three cases (i)  $\Gamma_1, \Gamma_2, \Gamma_3 > 0$ , (ii)  $\Gamma_1, \Gamma_2 < 0, \Gamma_3 > 0$ , and (iii)  $\Gamma_1 > 0, \Gamma_2 < 0, \Gamma_3 > 0$ . Observe that the two-layer model gives rise to one more case than the planar model, where it suffices to consider only (i) and (ii). Naturally, for all three vortices in the same layer there are additional discrete symmetries, namely cyclically and anticyclically permuting the indices of the vortices, in which case, as in the planar model, one need only consider (i) and (ii).

Note also that the dynamical equations for the planar model are invariant with respect to the scale transformation [49]:

$$\mathbf{x} \mapsto \lambda \mathbf{x}' \quad t \mapsto \lambda^2 t'$$

The presence of the two length scales  $\lambda_{1,2}^{-1}$ , (the inner and outer Rossby radii of deformation), in the two layer model leads to a breakdown in this symmetry. It is conceivable that this may have implications for the existence of self-similar (homogenous) collapsing solutions in the two-layer model. See for instance some of the results in Chapter 4, in particular Fig. 4.1.

## Chapter 3

### Equilibrium solutions for the 2-layer quasi-geostrophic model

In this chapter we locate all the equilibria for the three-vortex two-layer problem. These are the simplest solutions of the dynamical equations, and are useful, for instance, in studying particle advection, due to the motion of these point vortices in relative equilibrium. They are also typically the solutions about which perturbations are made to study non-integrable vortex dynamics, as well as the reduced four-vortex problem. We define equilibria as vortex motions in which the inter-vortical distances stay fixed. Relative equilibria are the fixed points of the relative equations (1.20), and for which the vortices form rigid configurations either rotating about the center of vorticity, or rigidly translating. Fixed equilibria are the fixed points of the system (1.13-1.16). Our analysis, in this chapter, follows the methods used by Synge [56] and Aref [2]. To this end we will make extensive use of functions defined in (1.17) and (1.18) as well as some of their properties.

#### 3.1 Location of fixed equilibria

In our first result we locate all fixed three-vortex equilibria, where the vortices may be arbitrarily permuted between the two layers.

**Theorem 3.1 (Fixed equilibria)** *Necessary and sufficient conditions for fixed equilibria are:*

1. For three vortices in the top layer,

(a) The vortices are collinear with,

$$(\mathbf{x}_1 - \mathbf{x}_2) = \frac{\Gamma_3}{\Gamma_2} \frac{g(l_{13})}{l_{13}} \frac{l_{12}}{g(l_{12})} (\mathbf{x}_3 - \mathbf{x}_1), \text{ and,}$$

$$\left( \frac{\Gamma_2}{\Gamma_3} \right)^2 = \left( \frac{g(l_{13})}{g(l_{12})} \right)^2,$$

$$(b) \Gamma_1 \Gamma_2 g(l_{12}) l_{12} + \Gamma_1 \Gamma_3 g(l_{13}) l_{13} + \Gamma_3 \Gamma_2 g(l_{32}) l_{32} = 0.$$

2. For three vortices in the lower layer the above conditions hold with  $h(l)$  replacing  $g(l)$ .

3. For two vortices in the upper layer (labeled 1 and 2) and a third (labeled 3) in the bottom layer,

(a) The vortices are collinear with

$$(\mathbf{x}_1 - \mathbf{x}_2) = \frac{\Gamma_3}{\Gamma_2} \frac{H_2}{\sqrt{d}} \frac{f(l_{13})}{l_{13}} \frac{l_{12}}{g(l_{12})} (\mathbf{x}_3 - \mathbf{x}_1), \text{ and,}$$

$$\left( \frac{\Gamma_2}{\Gamma_3} \right)^2 = \left( \frac{H_2}{\sqrt{d}} \frac{f(l_{13})}{g(l_{12})} \right)^2,$$

$$(b) \Gamma_1 \Gamma_2 g(l_{12}) l_{12} + \Gamma_1 \Gamma_3 \frac{H_2}{\sqrt{d}} f(l_{13}) l_{13} + \Gamma_3 \Gamma_2 \frac{H_2}{\sqrt{d}} f(l_{32}) l_{32} = 0.$$

4. For 1 vortex in the upper layer (labeled 1) and two vortices in the lower layer (labeled 2 and 3),

(a) The vortices are collinear with

$$(\mathbf{x}_1 - \mathbf{x}_2) = \frac{\Gamma_3}{\Gamma_2} \frac{f(l_{13})}{l_{13}} \frac{l_{12}}{f(l_{12})} (\mathbf{x}_3 - \mathbf{x}_1), \text{ and,}$$

$$\left( \frac{\Gamma_2}{\Gamma_3} \right)^2 = \left( \frac{f(l_{13})}{f(l_{12})} \right)^2,$$

$$(b) \Gamma_1 \Gamma_2 \frac{H_2}{\sqrt{d}} f(l_{12}) l_{12} + \Gamma_1 \Gamma_3 \frac{H_2}{\sqrt{d}} f(l_{13}) l_{13} + \Gamma_3 \Gamma_2 h(l_{32}) l_{32} = 0.$$

**Proof.** We prove (3); the other statements have similar proofs. Using the Hamiltonian, obtain the following dynamical equations:

$$\dot{x}_1 = -\frac{1}{2\pi} \left[ \Gamma_2(y_1 - y_2) \frac{g(l_{12})}{l_{12}} + \frac{\Gamma_3 H_2}{\sqrt{d}} (y_1 - y_3) \frac{f(l_{13})}{l_{13}} \right], \quad (3.1)$$

$$\dot{y}_1 = \frac{1}{2\pi} \left[ \Gamma_2(x_1 - x_2) \frac{g(l_{12})}{l_{12}} + \frac{\Gamma_3 H_2}{\sqrt{d}} (x_1 - x_3) \frac{f(l_{13})}{l_{13}} \right], \quad (3.2)$$

$$\dot{x}_2 = -\frac{1}{2\pi} \left[ \Gamma_1(y_2 - y_1) \frac{g(l_{12})}{l_{12}} + \frac{\Gamma_3 H_2}{\sqrt{d}} (y_2 - y_3) \frac{f(l_{23})}{l_{23}} \right], \quad (3.3)$$

$$\dot{y}_2 = \frac{1}{2\pi} \left[ \Gamma_1(x_2 - x_1) \frac{g(l_{12})}{l_{12}} + \frac{\Gamma_3 H_2}{\sqrt{d}} (x_2 - x_3) \frac{f(l_{23})}{l_{23}} \right], \quad (3.4)$$

$$\dot{x}_3 = -\frac{\alpha H_1}{2\pi} \left[ \frac{\Gamma_1(y_3 - y_1) f(l_{13})}{\sqrt{d} l_{13}} + \frac{\Gamma_2(y_3 - y_2) f(l_{23})}{\sqrt{d} l_{23}} \right], \quad (3.5)$$

$$\dot{y}_3 = \frac{\alpha H_1}{2\pi} \left[ \frac{\Gamma_1(x_3 - x_1) f(l_{13})}{\sqrt{d} l_{13}} + \frac{\Gamma_2(x_3 - x_2) f(l_{23})}{\sqrt{d} l_{23}} \right]. \quad (3.6)$$

Setting  $\dot{x}_1 = \dot{y}_1 = 0$ , it is clear that

$$\Gamma_2(\mathbf{x}_1 - \mathbf{x}_2) \frac{g(l_{12})}{l_{12}} = \frac{\Gamma_3 H_2}{\sqrt{d}} \frac{f(l_{13})}{l_{13}} (\mathbf{x}_3 - \mathbf{x}_1),$$

so that the vortices are collinear. Taking dot products on the left with

$$\Gamma_2(\mathbf{x}_1 - \mathbf{x}_2) \frac{g(l_{12})}{l_{12}},$$

and on the right with,

$$\frac{\Gamma_3 H_2}{\sqrt{d}} \frac{f(l_{13})}{l_{13}} (\mathbf{x}_3 - \mathbf{x}_1),$$

yields,

$$\Gamma_2^2 l_{12}^2 \frac{g(l_{12})^2}{l_{12}^2} = \frac{\Gamma_3^2 H_2^2}{d} \frac{l_{13}^2}{l_{13}^2} f(l_{13})^2, \text{ or } \left( \frac{\Gamma_2}{\Gamma_3} \right)^2 = \left( \frac{H_2 f(l_{13})}{\sqrt{d} g(l_{12})} \right)^2.$$

We now establish (b) by taking “dot-products,” as follows (recall  $\dot{x}_i = \dot{y}_i = 0$ ):

$$-\dot{x}_1 \Gamma_1 y_1 + \dot{y}_1 \Gamma_1 x_1 - \dot{x}_2 \Gamma_2 y_2 + \dot{y}_2 \Gamma_2 x_2 - \dot{x}_3 \frac{\Gamma_3 y_3}{\alpha H_1} + \dot{y}_3 \frac{\Gamma_3 x_3}{\alpha H_1} = 0. \quad (3.7)$$

This establishes necessity, since

$$LHS = \Gamma_1 \Gamma_2 g(l_{12}) l_{12} + \Gamma_1 \Gamma_3 \frac{H_2}{\sqrt{d}} f(l_{13}) l_{13} + \Gamma_3 \Gamma_2 \frac{H_2}{\sqrt{d}} f(l_{32}) l_{32} = 0.$$

To establish sufficiency, begin by assuming:

$$(\mathbf{x}_1 - \mathbf{x}_2) = \frac{\Gamma_3 H_2 f(l_{13})}{\Gamma_2 \sqrt{d} l_{13}} \frac{l_{12}}{g(l_{12})} (\mathbf{x}_3 - \mathbf{x}_1), \quad (3.8)$$

$$\left(\frac{\Gamma_2}{\Gamma_3}\right)^2 = \left(\frac{H_2 f(l_{13})}{\sqrt{d} g(l_{12})}\right)^2, \text{ and,} \quad (3.9)$$

$$\Gamma_1 \Gamma_2 g(l_{12}) l_{12} + \Gamma_1 \Gamma_3 \frac{H_2}{\sqrt{d}} f(l_{13}) l_{13} + \Gamma_3 \Gamma_2 \frac{H_2}{\sqrt{d}} f(l_{32}) l_{32} = 0. \quad (3.10)$$

We show that this is a fixed equilibrium configuration. Substitute (3.8) into (3.1-3.2) to conclude that  $\dot{\mathbf{x}}_1 = \dot{\mathbf{y}}_i = 0$ . For (3.3-3.4) observe that it suffices to show that:

$$\Gamma_1 (\mathbf{x}_2 - \mathbf{x}_1) \frac{g(l_{12})}{l_{12}} = \frac{\Gamma_3 H_2}{\sqrt{d}} (\mathbf{x}_3 - \mathbf{x}_2) \frac{f(l_{23})}{l_{23}}. \quad (3.11)$$

Without loss of generality in (3.9) assume that

$$\Gamma_2 g(l_{12}) = \frac{\Gamma_3 H_2}{\sqrt{d}} f(l_{13}).$$

With this, (3.8), becomes

$$(\mathbf{x}_1 - \mathbf{x}_2) = \frac{l_{12}}{l_{13}} (\mathbf{x}_1 - \mathbf{x}_2), \text{ so that } (\mathbf{x}_3 - \mathbf{x}_2) = \left(1 + \frac{l_{13}}{l_{12}}\right) (\mathbf{x}_1 - \mathbf{x}_2)$$

and hence

$$l_{32}^2 = (l_{12} + l_{13})^2.$$

Taking  $l_{32} = l_{12} + l_{13}$ , and considering the right-hand side of (3.11),

$$\begin{aligned} RHS &= \frac{\Gamma_3 H_2}{\sqrt{d}} (\mathbf{x}_3 - \mathbf{x}_2) \frac{f(l_{23})}{l_{23}} = \frac{\Gamma_3 H_2}{\sqrt{d}} \frac{f(l_{23})}{l_{23}} \left(1 + \frac{l_{13}}{l_{12}}\right) (\mathbf{x}_1 - \mathbf{x}_2) \\ &= \frac{\Gamma_3 H_2}{l_{23} \sqrt{d}} f(l_{23}) l_{23} (\mathbf{x}_1 - \mathbf{x}_2) \left(\frac{l_{12} + l_{13}}{l_{12}}\right) = \frac{\Gamma_3 H_2}{\sqrt{d}} f(l_{23}) l_{12} (\mathbf{x}_1 - \mathbf{x}_2). \end{aligned}$$

Next use (3.10) and recall from (3.9) that,  $\Gamma_2 g(l_{12}) = \frac{\Gamma_3 H_2 f(l_{13})}{\sqrt{d}}$ , so that (3.10) becomes

$$\Gamma_1 \Gamma_2 g(l_{12}) l_{12} + \Gamma_1 \Gamma_2 g(l_{12}) l_{13} + \Gamma_2 \Gamma_3 \frac{H_2}{\sqrt{d}} f(l_{23}) l_{23} = 0.$$

Hence  $\Gamma_1 g(l_{12}) = -\frac{\Gamma_3 H_2}{\sqrt{d}} f(l_{23})$ , because  $l_{12} + l_{13} = l_{23}$ , so that the RHS of (3.11) becomes

$$RHS = \Gamma_1 \frac{g(l_{12})}{l_{12}} (\mathbf{x}_2 - \mathbf{x}_1) = LHS,$$

leading us to conclude that  $\dot{x}_2 = \dot{y}_2 = 0$ . Similarly we can show that  $\dot{x}_3 = \dot{y}_3 = 0$ .  $\square$

**Remark:** Notice that the conditions (b) involve the distances  $l_{ij}$  between the vortices. This is different from the one-layer case [56] where the criterion is simply  $\sum_{i < j} \Gamma_i \Gamma_j = 0$  and is independent of the vortex positions  $\mathbf{x}_i$ . The two-layer model is similar in this regard to the situation on the sphere, where the condition is [31]

$$\sum \Gamma_i (\Gamma_j + \Gamma_k) \mathbf{x}_i = 0, \quad i \neq j \neq k,$$

and which clearly depends on the initial positions,  $\mathbf{x}_i$ .

## 3.2 Location of relative equilibria

We now locate the relative equilibria for the three-vortex problem for the two-layer model. These equilibria are determined by the functions  $h(l)$ ,  $f(l)$  and  $g(l)$  defined in Chapter 1, (1.17). Typical graphs of these functions as well as the functions  $\frac{f(l)}{l}$ ,  $\frac{g(l)}{l}$ , and  $\frac{h(l)}{l}$  are shown in Fig. 3.1. Observe that while  $h(l)$  and  $g(l)$  are monotonic,  $f(l)$  is not. Notice however that all of the functions  $\frac{f(l)}{l}$ ,  $\frac{g(l)}{l}$  and  $\frac{h(l)}{l}$ , do appear to be monotonically decreasing. We will show that this property will be critical, particularly in locating relative equilibria for vortices in different layers. We begin by considering three vortices in the same layer, the upper layer say, for which the relative equations are:

$$\frac{dl_{12}^2}{dt} = \frac{2\sigma A \Gamma_3}{\pi} \left[ \frac{g(l_{13})}{l_{13}} - \frac{g(l_{23})}{l_{23}} \right],$$

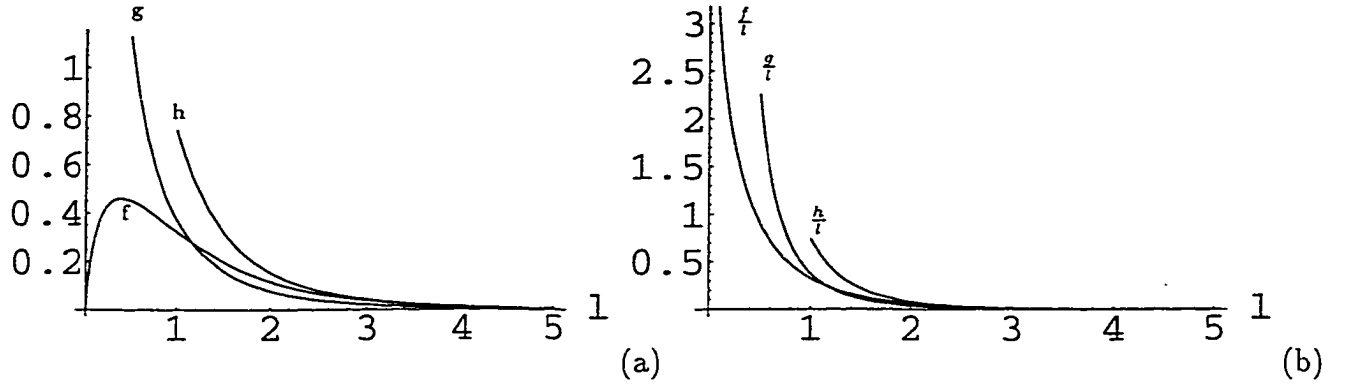


Figure 3.1: Typical graphs of the functions (a)  $f, g, h$ ; (b)  $\frac{f(l)}{l}, \frac{g(l)}{l}, \frac{h(l)}{l}$ . ( $l > 0$ )

$$\begin{aligned} \frac{dl_{23}^2}{dt} &= \frac{2\sigma A\Gamma_1}{\pi} \left[ \frac{g(l_{12})}{l_{12}} - \frac{g(l_{13})}{l_{13}} \right], \\ \frac{dl_{13}^2}{dt} &= \frac{2\sigma A\Gamma_2}{\pi} \left[ \frac{g(l_{23})}{l_{23}} - \frac{g(l_{12})}{l_{12}} \right], \end{aligned} \quad (3.12)$$

where  $\sigma$  is the orientation of the triangle formed by the three vortices and  $A(t)$  is the area enclosed by it. As mentioned in Chapter 1, the equations for three vortices in the lower layer are similar with  $g(l)$  replacing  $h(l)$ . Now the relative equilibria are the fixed points of the vector field (3.12). These occur where either  $A(t) = 0$  or terms of the form  $\left[ \frac{g(l_{23})}{l_{23}} - \frac{g(l_{12})}{l_{12}} \right] = 0$ . Now since  $K_1(l)$  is decreasing so is the linear combination given by  $-g(l)$ , (or  $-h(l)$ ). We conclude that since  $\frac{1}{l}$  is decreasing so is  $-\frac{g(l)}{l}$  (or  $-\frac{h(l)}{l}$ ). We can now locate all relative equilibria given by the equations, (3.12) and summarize this result in the following theorem:

**Theorem 3.2 (Location of relative equilibria: vortices in the same layer)** *For the two-layer model the only relative equilibria, for which all three vortices are in the same layer are:*

1. *Equilateral triangle configurations, and*
2. *Collinear states for which necessary and sufficient conditions are given by  $A(0) = \dot{A}(0) = 0$ .*

Assuming that  $\sum \Gamma_i \neq 0$ , we compute that the vortices rotate about the center of vorticity with rotation frequency

$$\Omega = \frac{g(s)}{2\pi s} (\Gamma_1 + \Gamma_2 + \Gamma_3),$$

for three vortices in the upper layer and,

$$\Omega = \frac{h(s)}{2\pi s} (\Gamma_1 + \Gamma_2 + \Gamma_3),$$

for three vortices in the lower layer. In either case if  $\sum \Gamma_i = 0$ , the center of vorticity is at infinity and the triangles move parallel to themselves with speeds

$$\begin{aligned} v &= \left[ \frac{1}{2} (\Gamma_1^2 + \Gamma_2^2 + \Gamma_3^2) \right]^{\frac{1}{2}} \frac{g(s)}{2\pi}, \\ v &= \left[ \frac{1}{2} (\Gamma_1^2 + \Gamma_2^2 + \Gamma_3^2) \right]^{\frac{1}{2}} \frac{h(s)}{2\pi}, \end{aligned}$$

respectively. By repeated differentiation and induction we can show that collinear configurations,  $A \equiv 0$  can form relative equilibria if and only if  $A(0) = \dot{A}(0) = 0$ . By Heron's formula for the area of a triangle this becomes, upon using the relative equations (3.12),

$$A(0) = [r(r - l_{23})(r - l_{31})(r - l_{12})]^{\frac{1}{2}} = 0, \quad (3.13)$$

$$\begin{aligned} \dot{A}(0) &= \frac{(r - l_{23})(r - l_{13})(r - l_{12})}{4\pi l_{12}l_{13}l_{23}} \sum \Gamma_i [l_{13}g(l_{12}) - l_{12}g(l_{13})] \\ &\quad + \frac{r}{4\pi l_{12}l_{13}l_{23}} \sum \{ -\Gamma_1 [l_{12}g(l_{13}) + l_{13}g(l_{12})] + \Gamma_1 [l_{12}g(l_{13}) + l_{13}g(l_{12})] \\ &\quad + \Gamma_1 [l_{12}g(l_{13}) + l_{13}g(l_{12})] \} (r - l_{31})(r - l_{12}), \end{aligned} \quad (3.14)$$

where

$$r = \frac{1}{2}(l_{12} + l_{13} + l_{23}).$$

In the last equation, (for  $\dot{A}(0) = 0$ ), both summations are over cyclic permutations of the indices, 1, 2, 3. Again, for three vortices in the lower layer, the same formula hold with  $g(l)$ , replaced by  $h(l)$ .



There is a similar analysis for vortices lying in different layers. We will need to use properties of the modified Bessel functions  $K_\nu(x)$ . These can be found in Abramowitz and Stegun [1]. To locate these equilibria we make use, in particular, of the following lemma.

**Lemma 3.3** *Let  $f(l) := \lambda_1 K_1(\lambda_1 l) - \lambda_2 K_1(\lambda_2 l)$  where  $l > 0$ , and  $\lambda_1 > \lambda_2 > 0$ , and where  $K_1(l)$  is the modified first-order Bessel function, then  $\frac{f(l)}{l}$  is a monotonic function*

**Proof.** We begin by defining the function  $\phi(x)$ ,

$$\phi(x) = \frac{f(x)}{x} = \frac{\lambda_1 K_1(\lambda_1 x) - \lambda_2 K_1(\lambda_2 x)}{x}, \text{ for } \lambda_1 > \lambda_2 > 0, \text{ and, } x > 0.$$

Differentiating, gives,

$$\phi'(x) = \frac{f'(x)x - f(x)}{x^2}.$$

We show that the numerator,  $f'(x)x - f(x)$ , is of one sign where,

$$f'(x) = \lambda_1^2 K_1'(\lambda_1 x) - \lambda_2^2 K_1'(\lambda_2 x).$$

We do this by making use of the following recurrence relation for modified Bessel functions [1]:

$$L_\nu'(z) = L_{\nu+1}(z) = \frac{\nu}{z} L_\nu(z), \quad (3.15)$$

where

$$L_\nu(z) := e^{\nu\pi i} K_\nu(z).$$

Thus, for instance,  $-K_1'(z) = K_2(z) - \frac{1}{z}K_1(z)$ , from which we may obtain

$$f'(x) = \lambda_1^2 \left[ \frac{1}{\lambda_1 x} K_1(\lambda_1 x) \right] - \lambda_2^2 \left[ \frac{1}{\lambda_2 x} K_1(\lambda_2 x) \right],$$

so that,

$$f'(x)x - f(x) = \lambda_1 K_1(\lambda_1 x) - \lambda_1^2 x K_2(\lambda_1 x) - \lambda_2 K_1(\lambda_2 x)$$

$$\begin{aligned}
& +\lambda_2^2 K_2(\lambda_2 x) \\
& -\lambda_1 K_1(\lambda_1 x) + \lambda_2 K_1(\lambda_2 x) \\
& = \lambda_2^2 x K_2(\lambda_2 x) - \lambda_2^2 x K_2(\lambda_2 x) \\
& = \frac{1}{x} \left[ (\lambda_2 x)^2 K_2(\lambda_1 x) - (\lambda_1 x)^2 K_2(\lambda_2 x) \right].
\end{aligned}$$

Since  $\lambda_1 > \lambda_2$ , and  $x > 0$ , this is clearly of one sign, since  $x^2 K_2(x)$  is a monotonically decreasing function, as shown in Figure 3.2. To rigorously prove this we begin by defining  $g(x) := x^2 K_2(x)$ . Then,

$$\begin{aligned}
g'(x) &= 2x K_2(x) + x^2 K_2'(x) \\
&= 2x \left[ \frac{2}{x} K_1(x) + K_0(x) \right] + x^2 \left[ -K_1(x) - \frac{2}{x} K_2(x) \right] \\
&= 2x \left[ \frac{2}{x} K_1(x) + K_0(x) \right] + x^2 \left[ -K_1(x) - \frac{2}{x} \left( \frac{2}{x} K_1(x) + K_0(x) \right) \right] \\
&= 4K_1(x) + 2x K_0(x) - x^2 K_1(x) - 4K_1(x) - 2x K_0(x) \\
&= -x^2 K_1(x),
\end{aligned}$$

where we have made repeated use of the recurrence relation (3.15).  $\square$

We mention that Lemma 3.3 is used in an essential way to locate all relative equilibria for three vortices lying in different layers. However it does not apply to the simplified model given by (1.19) and used for example in [57]. There the interaction terms for point vortices is a little different. A Hamiltonian formulation of that model leads to the Hamiltonian

$$\begin{aligned}
H &= -\frac{\pi}{4} \left\{ 2\Gamma_1 \Gamma_2 \left[ \ln(l_{12}) - K_0 \left( \frac{l_{12}}{\lambda} \right) \right] + 2\Gamma_1 \Gamma_3 \left[ \ln(l_{13}) - K_0 \left( \frac{l_{13}}{\lambda} \right) \right] \right. \\
&\quad \left. + 2\Gamma_3 \Gamma_2 \left[ \ln(l_{32}) - K_0 \left( \frac{l_{32}}{\lambda} \right) \right] \right\}, \tag{3.16}
\end{aligned}$$

where vortices 1 and 2 are in the upper layer, and vortex 3 is in the lower. The relative equations take the form

$$\frac{dl_{12}^2}{dt} = \Gamma_3 \sigma A [\tilde{g}(l_{23}) - \tilde{g}(l_{13})],$$

where,

$$\tilde{g}(l) := \frac{1}{l^2} - \frac{1}{\lambda l} K_1 \left( \frac{l}{\lambda} \right), \quad l, \lambda > 0.$$

Similar dynamical equations are obtained for  $l_{23}^2$ , and  $l_{13}^2$ , with terms that also involve the function  $\tilde{f}(l)$ ,

$$\tilde{f}(l) := \frac{1}{l^2} + \frac{1}{\lambda l} K_1 \left( \frac{l}{\lambda} \right), \quad l, \lambda > 0.$$

It is clear that  $\tilde{f}(l)$  is monotonic. As for  $\tilde{g}(l)$ , we use the recurrence relation  $-K_1'(z) = K_2(z) - \frac{1}{z} K_1(z)$ . Differentiating, yields,

$$\begin{aligned} \tilde{g}'(l) &= -\frac{2}{l^3} + \frac{1}{\lambda l^2} K_1 \left( \frac{l}{\lambda} \right) - \frac{1}{\lambda^2 l} K_1' \left( \frac{l}{\lambda} \right) \\ &= -\frac{2}{l^3} + \frac{1}{\lambda l^2} K_1 \left( \frac{l}{\lambda} \right) + \frac{1}{\lambda^2 l} \left\{ K_2(z) - \frac{\lambda}{l} K_1 \left( \frac{l}{\lambda} \right) \right\} \\ &= \frac{1}{l^3} \left[ -2 + \left( \frac{l}{\lambda} \right)^2 K_2 \left( \frac{l}{\lambda} \right) \right]. \end{aligned}$$

We now use the fact that  $x^2 K_2(x)$  is monotonically decreasing and bounded by 2 since (see Fig. 3.2),

$$\sup_{x>0} x^2 K_2(x) = \lim_{x \rightarrow 0+} x^2 K_2(x) = 2.$$

Conclude that  $\tilde{g}'(l)$  is negative, so that  $\tilde{g}(l)$  is a monotonically decreasing function. The preceding analysis shows that all of the qualitative conclusions arising due to Lemma 3.3 for the full two-layer model, apply to the simplified two-layer model given by (1.19).

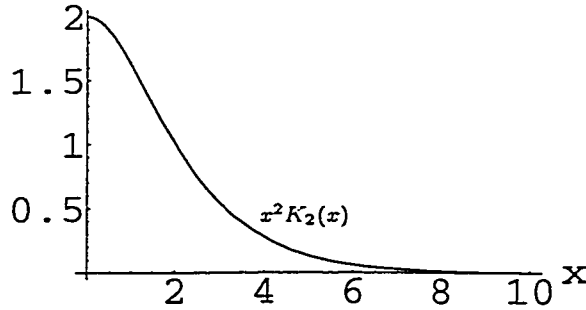


Figure 3.2: Graph of the function  $x^2 K_2(x)$ .

We begin by considering (for the full two-layer model), two vortices in the upper layer (labeled 1 and 2), and a third vortex (labeled 3) in the lower layer (Case I). The relative dynamical equations in this case are :

$$\begin{aligned}\frac{dl_{12}^2}{dt} &= \frac{H_2}{\sqrt{d}} \frac{2\sigma A \Gamma_3}{\pi} \left[ \frac{f(l_{13})}{l_{13}} - \frac{f(l_{23})}{l_{23}} \right], \\ \frac{dl_{23}^2}{dt} &= \frac{2\sigma A \Gamma_1}{\pi} \left[ \frac{g(l_{13})}{l_{12}} - \frac{\alpha H_1}{\sqrt{d}} \frac{f(l_{13})}{l_{13}} \right], \\ \frac{dl_{13}^2}{dt} &= \frac{2\sigma A \Gamma_2}{\pi} \left[ \frac{\alpha H_1}{\sqrt{d}} \frac{f(l_{23})}{l_{23}} - \frac{g(l_{12})}{l_{12}} \right].\end{aligned}\tag{3.17}$$

In order to locate the relative equilibria we see that finding the zeros of the first equation in (3.17) gives,

$$\frac{f(l_{13})}{l_{13}} = \frac{f(l_{23})}{l_{23}}.$$

The monotonicity of the function  $\frac{f(l)}{l}$  implies that this can occur only when  $l_{13} = l_{23} := s$ . We now use the second and third equations to obtain that  $l_{12}$  is given by the solution of

$$\frac{g(l_{12})}{l_{12}} = \frac{\alpha H_1}{\sqrt{d}} \frac{f(s)}{s}.$$

Such a solution,  $l_{12} := t(s)$  exists and is unique, by virtue of the fact that both  $\frac{g(l)}{l}$ , and  $\frac{f(l)}{l}$  are monotonically decreasing and, moreover, assume all positive values as seen in Fig 3.1. In general though,  $l_{12} \neq l_{13} = l_{23}$ . We conclude that relative equilibria are given by isosceles triangles. Note, however that these are not arbitrary isosceles triangles. (Recall that in the planar (one-layer) model as on the sphere, arbitrary equilateral triangles form relative equilibria.) For the two-layer model, given any  $s > 0$  there exists an isosceles triangle relative equilibria, for which  $l_{13} = l_{23} = s$ . The shape of this isosceles, for a given  $s$  is obtained from  $l_{12} := t(s)$ , which is uniquely determined by the solution of

$$\frac{g(l_{12})}{l_{12}} = \frac{g(t)}{t} = \frac{\alpha H_1}{\sqrt{d}} \frac{f(l_{13})}{l_{13}} = \frac{\alpha H_1}{\sqrt{d}} \frac{f(s)}{s}.$$

The solution of these implicit equations depends, in general, on many parameters. It is clear that they define a whole family of isosceles triangles. We illustrate this with the simplified model mentioned earlier, (3.16), where the implicit equations are

$$\tilde{g}(s) = \tilde{f}(t).$$

The only parameter appearing in this equation is the Rossby radius of deformation,  $\lambda$ . Solutions of  $t(s)$  as a function of  $s$  for various  $\lambda$  are shown in Fig. 3.3. Notice that for each fixed  $s$  there is a unique  $t$  as seen from the monotonicity of the function  $t(s)$ . Observe also in Fig. 3.3(b), that for large  $s$ , regardless of  $\lambda$ , there is only one isosceles triangle equilibrium, since for large  $s$  the ratio  $\frac{t}{s}$  is one (an equilateral triangle). It is also seen, in Fig. 3.3 (b), that for every  $\lambda$ , the ratio  $\frac{t(s)}{s}$ , takes all values in the range  $(1, \infty)$ , i.e. for any  $\lambda$ , given any  $\alpha \in (1, \infty)$ , there is an isosceles triangle relative equilibrium with  $\frac{t(s)}{s} = \alpha$ .

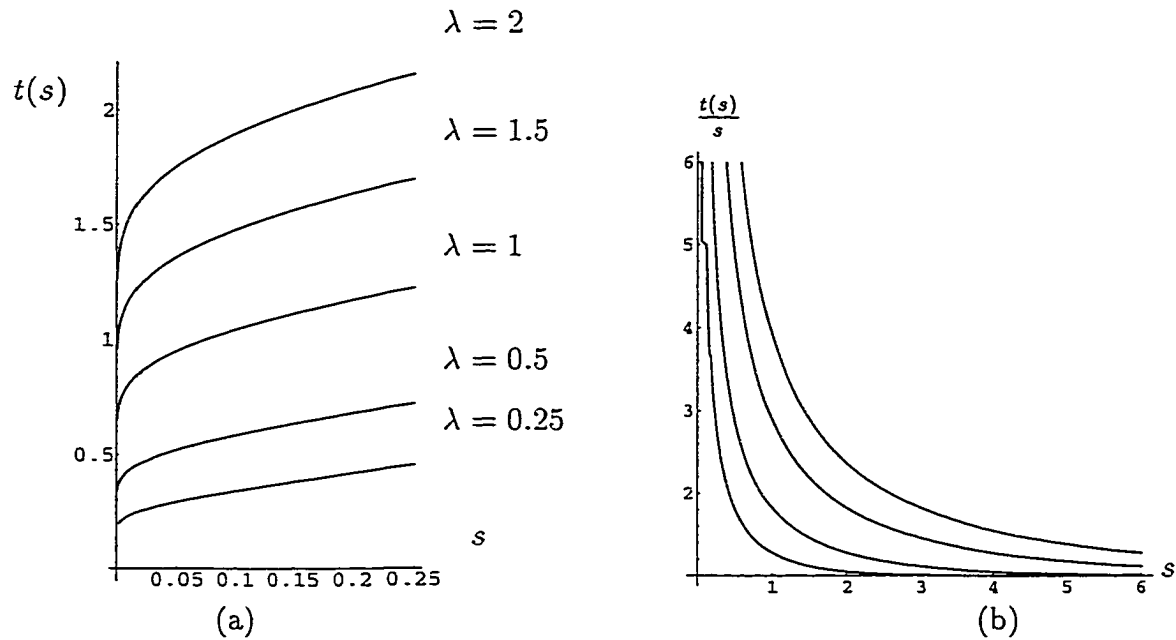


Figure 3.3: Families of relative equilibria for different Rossby radii of deformation,  $\lambda$ . ( $s$  is one length of the isosceles triangle, and  $t(s)$  the other, (a)  $t$  against  $s$ , (b) The ratio  $\frac{t}{s}$  against  $s$ . ( $\lambda = 0.5, 1, 2, 3$ , with  $\lambda = 0.5$ , the bottom curve and  $\lambda = 3$  the topmost curve.)

Assuming  $\rho_1 H_1(\Gamma_1 + \Gamma_2) + \rho_2 H_2 \Gamma_3 \neq 0$ , it is straightforward to show that the vortices rotate around the center of vorticity with rotation frequency

$$\Omega = \frac{f(s)}{2} \pi s \left[ \frac{\alpha H_1}{\sqrt{d}} (\Gamma_1 + \Gamma_2) + \frac{H_2}{\sqrt{d}} \Gamma_3 \right].$$

The analysis for one vortex in the upper layer (labeled 1) and two vortices (labeled 2 and 3) in the lower layer is similar. In that case (case II), the relative equations are

$$\begin{aligned} \frac{dl_{12}^2}{dt} &= \frac{2\sigma A \Gamma_3}{\pi} \left[ \frac{H_2}{\sqrt{d}} \frac{f(l_{13})}{l_{13}} - \frac{h(l_{23})}{l_{23}} \right], \\ \frac{dl_{23}^2}{dt} &= \frac{H_2}{\sqrt{d}} \frac{2\sigma A \Gamma_1}{\pi} \left[ \frac{f(l_{12})}{l_{12}} - \frac{f(l_{13})}{l_{13}} \right], \\ \frac{dl_{13}^2}{dt} &= \frac{2\sigma A \Gamma_2}{\pi} \left[ \frac{h(l_{23})}{l_{23}} - \frac{H_2}{\sqrt{d}} \frac{f(l_{12})}{l_{12}} \right]. \end{aligned}$$

We summarize these results on relative equilibria in the following proposition.

**Theorem 3.4 (Location of relative equilibria: vortices in different layers)** *The relative equilibria for the three-vortex problem, with vortices lying in different layers are:*

1. *Case I: For two vortices in the top layer (labeled 1 and 2), and, vortex 3 in the bottom layer, the relative equilibria are isosceles triangles, with  $l_{13} = l_{23} := s$ , and  $l_{12} = t(s) = t$ , given by the unique solution of*

$$\frac{g(t)}{t} = \frac{\alpha H_1}{\sqrt{d}} \frac{f(s)}{s}. \quad (3.18)$$

*When  $\rho_1 H_1(\Gamma_1 + \Gamma_2) + \rho_2 H_2 \Gamma_3 \neq 0$ , the vortices rotate about the center of vorticity with rotation frequency*

$$\Omega = \frac{f(s)}{2\pi\sqrt{d}s} = [\alpha H_1(\Gamma_1 + \Gamma_2) + \Gamma_3 H_2].$$

If,  $\rho_1 H_1(\Gamma_1 + \Gamma_2) + \rho_2 H_2 \Gamma_3 = 0$ , the triangle translates parallel to itself with speed

$$v = \frac{f(s)}{2\pi\sqrt{3d}} \left[ \alpha^2 H_1^2 \left( 1 + \frac{1}{2} \left( \frac{t}{s} \right)^2 \right) (\Gamma_1^2 + \Gamma_2^2) + H_2^2 \left( 2 - \frac{1}{2} \left( \frac{t}{s} \right)^2 \right) \Gamma_3^2 + 2\alpha^2 H_1^2 \left( 1 - \left( \frac{t}{s} \right)^2 \right) \Gamma_1 \Gamma_2 \right]^{\frac{1}{2}}. \quad (3.19)$$

When  $\frac{g(s)}{s} = \frac{\alpha H_1}{\sqrt{d}} \frac{f(s)}{s}$ , or  $\frac{g(s)}{f(s)} = \frac{\alpha H_1}{\sqrt{d}}$ , so that  $s = t$ , corresponding to equilateral triangle configurations, this formula (3.19), simplifies to

$$v = \frac{f(s)}{2\pi\sqrt{2d}} = [\alpha^2 H_1^2 (\Gamma_1^2 + \Gamma_2^2) + H_2^2 \Gamma_3^2]^{\frac{1}{2}}.$$

Case II: For vortex 1 in the top layer and vortices 2 and 3 in the bottom, the relative equilibria are isosceles triangles with  $l_{13} = l_{12} := s$  and  $l_{23} = t(s) := t$ , given by the unique solution of

$$\frac{H_2}{\sqrt{d}} \frac{f(s)}{s} = \frac{h(t)}{t}.$$

When  $\rho_1 H_1 \Gamma_1 + \rho_2 H_2 (\Gamma_2 \Gamma_3) \neq 0$ , the vortices rotate about the center of vorticity with rotation frequency

$$\Omega = \frac{f(s)}{2\pi\sqrt{d}s} = [H_2(\Gamma_3 + \Gamma_2) + \Gamma_1 \alpha H_1 H_2].$$

If,  $\rho_1 H_1 \Gamma_1 + \rho_2 H_2 (\Gamma_2 + \Gamma_3) = 0$ , the triangle translates parallel to itself with speed

$$v = \frac{f(s)}{2\pi\sqrt{3d}} \left[ \alpha^2 H_1^2 \left( 2 - \frac{1}{2} \left( \frac{t}{s} \right)^2 \right) \Gamma_1^2 + H_2^2 \left( 1 + \frac{1}{2} \left( \frac{t}{s} \right)^2 \right) (\Gamma_2^2 + \Gamma_3^2) + 2H_2^2 \left( 1 - \left( \frac{t}{s} \right)^2 \right) \Gamma_2 \Gamma_3 \right]^{\frac{1}{2}}. \quad (3.20)$$

When  $\frac{h(s)}{s} = \frac{H_2}{\sqrt{d}} \frac{f(s)}{s}$ , or  $\frac{h(s)}{f(s)} = \frac{H_2}{\sqrt{d}}$ , so that  $s = t$ , corresponding to equilateral triangle configurations, this formula (3.20), simplifies to

$$v = \frac{f(s)}{2\pi\sqrt{2d}} = \left[ \alpha^2 H_1^2 \Gamma_1^2 + H_2^2 (\Gamma_2 + \Gamma_3^2) \right]^{\frac{1}{2}}.$$

2. In both cases there are also collinear relative equilibria for which necessary and sufficient conditions are  $A(0) = \dot{A}(0) = 0$ , which explicitly take the form

$$A(0) = [r(r - l_{23})(r - l_{31})(r - l_{12})]^{\frac{1}{2}} = 0,$$

where  $r = \frac{1}{2}(l_{12} + l_{23} + l_{31})$ , and,

$$\begin{aligned} \dot{A}(0) = 0 &= \frac{(r - l_{23})(r - l_{31})(r - l_{12})}{4\pi l_{12} l_{13} l_{23}} \sum' \Gamma_1 \phi_{23} \\ &+ \frac{r}{4\pi l_{12} l_{13} l_{23}} \sum' [\Gamma_1 \bar{\phi}_{23} + \Gamma_2 \bar{\phi}_{13} + \Gamma_3 \bar{\phi}_{12}] (r - l_{31})(r - l_{12}). \end{aligned}$$

Here both summations, denoted by  $\sum'$ , are over cyclic permutations of the indices and where the  $\phi_{kl}$ , are given by

$$\begin{aligned} \phi_{23} &:= g(l_{12})l_{13} - \frac{\alpha H_1}{\sqrt{d}} f(l_{13})l_{12}, & \bar{\phi}_{23} &:= -[g(l_{12})l_{13} + \frac{\alpha H_1}{\sqrt{d}} f(l_{13})l_{12}], \\ \phi_{13} &:= \frac{\alpha H_1}{\sqrt{d}} [f(l_{23})l_{12} - g(l_{12})l_{23}], & \bar{\phi}_{13} &:= -[\frac{\alpha H_1}{\sqrt{d}} f(l_{23})l_{12} + g(l_{12})l_{23}], \\ \phi_{12} &:= \frac{H_2}{\sqrt{d}} [f(l_{13})l_{23} - f(l_{23})l_{13}], & \bar{\phi}_{12} &:= -\frac{H_2}{\sqrt{d}} [f(l_{13})l_{23} + f(l_{23})l_{13}], \end{aligned}$$

for case I, and for case II, by

$$\begin{aligned} \phi_{23} &:= \frac{\alpha H_1}{\sqrt{d}} [f(l_{12})l_{13} - f(l_{13})l_{12}], & \bar{\phi}_{23} &:= -\frac{\alpha H_1}{\sqrt{d}} [f(l_{12})l_{13} + f(l_{13})l_{12}], \\ \phi_{13} &:= h(l_{23})l_{12} - \frac{H_2}{\sqrt{d}} f(l_{12})l_{23}, & \bar{\phi}_{13} &:= -[h(l_{23})l_{12} + \frac{H_2}{\sqrt{d}} f(l_{12})l_{23}], \\ \phi_{12} &:= \frac{H_2}{\sqrt{d}} [f(l_{13})l_{23} - h(l_{23})l_{13}], & \bar{\phi}_{12} &:= -[\frac{H_2}{\sqrt{d}} f(l_{13})l_{23} + h(l_{23})l_{13}]. \end{aligned}$$



### 3.2.1 Relative equilibria and the energy-momentum mapping

It would be interesting to study the nonlinear stability of these relative equilibria. A systematic study would be fairly involved since there are many parameters to consider in the full two-layer model, as well as more possible cases to consider as regards to vortex strength and sign allocations of the three vortices. There is a further complication regarding the isosceles triangle equilibria, which are defined only implicitly as for example in (3.18).

Nevertheless, a nonlinear stability analysis involves the use of the *energy-momentum mapping*. The relative equilibria have an interesting description in terms of the energy-momentum mapping which we now present. We follow Arnold's treatment [5, 6].

In Chapter 2 we saw that the Hamiltonian for the two-layer model is invariant with respect to arbitrary displacements in  $x$  and  $y$  as well as arbitrary rotations. Call  $G$  the connected Lie group of these symmetries acting (as symplectic diffeomorphisms) on the phase space  $(M^{2n}, \omega^2)$  and  $\mathcal{G}$ , its Lie algebra. Then, to every element  $a \in \mathcal{G}$ , there corresponds a one-parameter group of symplectic diffeomorphisms of  $M^{2n}$  with a single-valued Hamiltonian,  $H_a$ . In addition  $G$  is a Poisson action on  $M^{2n}$ ,

$$H_{[a,b]_{\mathcal{G}}} = [H_a, H_b],$$

where the first brackets denote vector multiplication in the Lie algebra  $\mathcal{G}$ , and the second the Poisson bracket in phase space  $(M^{2n}, \omega^2)$ . In other words the Poisson action of the group  $G$  defines a homomorphism from its Lie algebra  $\mathcal{G}$ , to the Lie algebra of hamiltonian functions on  $(M^{2n}, \omega^2)$ . We are now in a position to define the *momentum mapping*. The Poisson action of the group  $G$  on the symplectic manifold  $(M^{2n}, \omega^2)$  defines a mapping of  $M^{2n}$  into the dual space of the Lie algebra  $\mathcal{G}$

$$P : M \rightarrow \mathcal{G}^*,$$

i.e. choose a point  $x$  in  $M$  and consider the function on the Lie algebra which associates to an element  $a \in \mathcal{G}$ , the value of the Hamiltonian  $H_a$  at the chosen point  $x$

$$p_x(a) = H_a(x).$$

It is well known that a phase curve of a system with a  $G$ -invariant hamiltonian function is a relative equilibrium if and only if it is the orbit of a one-parameter subgroup of  $G$  in the original phase space.

Another theorem from mechanics states the the critical points of the momentum and energy mapping

$$P \times H : M \rightarrow \mathcal{G}^* \times \mathbf{R},$$

on a regular momentum level set are exactly the relative equilibria.

### 3.3 Trilinear formulation and location of equilibria in the trilinear plane

In this section we formulate the equations of relative motion in the phase plane and locate the relative equilibria. The dynamical system given by the relative equations (3.12) for example, has a 3D phase space. However this can be reduced to a 2D ‘phase plane’ by making use of the invariant  $C_1$ , (2.15), as a parameter or time-scale in the problem. We follow the methods introduced by Synge [56] for the planar problem. To this end we begin by considering case I for which the invariant  $C_1$  is,

$$C_1 = (\rho_1 H_1)^2 \Gamma_1 \Gamma_2 l_{12}^2 + (\rho_1 H_1)(\rho_2 H_2)(\Gamma_1 \Gamma_3 l_{13}^2 + \Gamma_2 \Gamma_3 l_{23}^2),$$

and the parameter  $C$  is defined by

$$\rho_2 H_2 \Gamma_2 \Gamma_3 l_{23}^2 + \rho_1 H_1 (\Gamma_1 \Gamma_2 l_{12}^2 + \Gamma_1 \Gamma_3 l_{13}^2) = 3 \Gamma_1 \Gamma_2 \Gamma_3 C,$$

with trilinear coordinates (for  $C \neq 0$ ),

$$b_1 := \frac{l_{23}^2}{\Gamma_1 C} \rho_2 H_2, \quad b_2 := \frac{l_{13}^2}{\Gamma_2 C} \rho_1 H_1, \quad b_3 := \frac{l_{12}^2}{\Gamma_3 C} \rho_1 H_1.$$

Similarly, for case II, the invariant  $C_1$  is

$$C_1 = (\rho_2 H_2)^2 \Gamma_2 \Gamma_3 l_{23}^2 + (\rho_1 H_1)(\rho_2 H_2)(\Gamma_1 \Gamma_2 l_{12}^2 + \Gamma_1 \Gamma_3 l_{13}^2),$$

and the parameter  $C$  is defined by

$$\rho_2 H_2 \Gamma_2 \Gamma_3 l_{23}^2 + \rho_1 H_1 (\Gamma_1 \Gamma_2 l_{12}^2 + \Gamma_1 \Gamma_3 l_{13}^2) = 3 \Gamma_1 \Gamma_2 \Gamma_3 C,$$

with trilinear coordinates (for  $C \neq 0$ ),

$$b_1 := \frac{l_{23}^2}{\Gamma_1 C} \rho_2 H_2, \quad b_2 := \frac{l_{13}^2}{\Gamma_2 C} \rho_1 H_1, \quad b_3 := \frac{l_{12}^2}{\Gamma_3 C} \rho_1 H_1.$$

It is then clear that  $b_1 + b_2 + b_3 = 0$ . Using Heron's formula (3.13), it is easy to verify that the physical region is

$$l_{12}^4 + l_{13}^4 + l_{23}^4 \leq 2(l_{12}^2 l_{13}^2 + l_{12}^2 l_{23}^2 + l_{23}^2 l_{13}^2). \quad (3.21)$$

In the trilinear plane, only parts of the phase space correspond to configurations of three vortices. The reason is that the lengths,  $l_{12}$ ,  $l_{23}$ ,  $l_{13}$ , must form sides of a triangle, and therefore satisfy the triangle inequalities,

$$l_{12} \leq l_{23} + l_{13}, \quad l_{23} \leq l_{13} + l_{12}, \quad l_{13} \leq l_{12} + l_{23}. \quad (3.22)$$

The regions of the phase space where these inequalities hold will be called *physical regions*. It is easy to show that (3.22), is equivalent to (3.21). Assuming that  $C_1 \neq 0$ , the physical region becomes

$$\begin{aligned} \left( \frac{\Gamma_3 b_3}{\rho_1 H_1} \right)^2 + \left( \frac{\Gamma_2 b_2}{\rho_2 H_2} \right)^2 + \left( \frac{\Gamma_1 b_1}{\rho_2 H_2} \right)^2 &\leq 2 \left[ \frac{b_3 \Gamma_3}{\rho_1 H_1} \frac{b_2 \Gamma_2}{\rho_2 H_2} + \frac{b_3 \Gamma_3}{\rho_1 H_1} \frac{b_1 \Gamma_1}{\rho_2 H_2} + \frac{b_1 \Gamma_1}{\rho_2 H_2} \frac{b_2 \Gamma_2}{\rho_2 H_2} \right], \\ \left( \frac{\Gamma_3 b_3}{\rho_1 H_1} \right)^2 + \left( \frac{\Gamma_1 b_1}{\rho_2 H_2} \right)^2 + \left( \frac{\Gamma_2 b_2}{\rho_1 H_1} \right)^2 &\leq 2 \left[ \frac{b_3 \Gamma_3}{\rho_1 H_1} \frac{b_2 \Gamma_2}{\rho_1 H_1} + \frac{b_3 \Gamma_3}{\rho_1 H_1} \frac{b_1 \Gamma_1}{\rho_2 H_2} + \frac{b_1 \Gamma_1}{\rho_2 H_2} \frac{b_2 \Gamma_2}{\rho_1 H_1} \right], \end{aligned}$$

for cases I and II respectively. The case where  $C = 0$ , is relevant to vortex collapse and we defer a discussion of it to Chapter 4. The trilinear plane and physical region are shown in Fig 3.4, for three vortices in the same layer, with  $\Gamma_1 = \Gamma_2 = \Gamma_3 = 1$ .

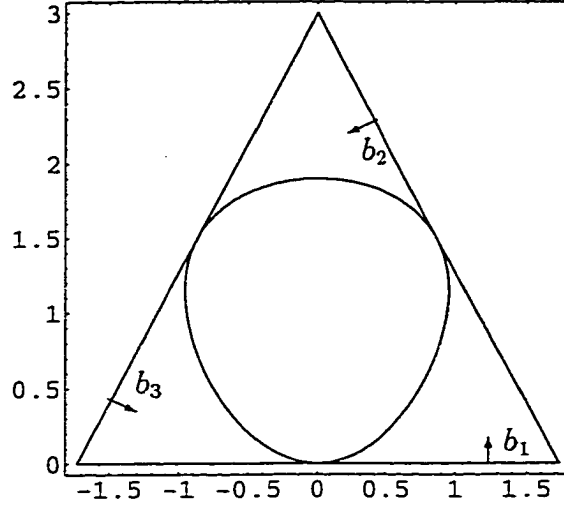


Figure 3.4: The trilinear plane and physical region: three vortices in the same layer with  $\Gamma_1 = \Gamma_2 = \Gamma_3 = 1$ . The arrows indicate the positive directions of  $b_i$ . (Negative values are possible and correspond to vortices not restricted to being positive.)

We make several observations regarding these trilinear coordinates. Firstly, these differ slightly from the one-layer case due to the appearance of the densities and thicknesses of the two layers. Secondly, for three vortices, all in the same layer, or when  $\rho_1 H_1 = \rho_2 H_2$ , the physical region and trilinear coordinates are identical to those of the one-layer model. Finally, observe that the non-homogeneity of the Bessel functions, means that the trilinear plane is not as useful for the two-layer model as on the plane. Indeed, to plot the phase-curves of (3.16), for example, one substitutes  $b_k$  for  $l_{ij}$ . However these are related via the invariant  $C_1$  which cannot be eliminated, as on the plane, due to the homogeneity of the logarithm function. This means that in the two-layer model, the trilinear plane, phase curves are drawn for different energy levels,  $H$ , but for fixed momentum  $C_1$ .

In the  $x$ - $y$  plane these trilinear coordinates are

$$\begin{aligned} b_1 &= y, \\ b_2 &= \frac{1}{2}(3 - y - \sqrt{x}), \\ b_3 &= \frac{1}{2}(3 - y + \sqrt{x}). \end{aligned}$$

One can use these to show that the relative equations assume the following Hamiltonian formulation. In case I,  $C \neq 0$ ,

$$\dot{y} = -\frac{16A\rho_2 H_2}{\sqrt{3}\Gamma_1\Gamma_2\Gamma_3 C^2} \frac{\partial H}{\partial x}, \quad \dot{x} = \frac{16A\rho_2 H_2}{\sqrt{3}\Gamma_1\Gamma_2\Gamma_3 C^2} \frac{\partial H}{\partial y}, \quad (3.23)$$

and in case II,

$$\dot{y} = -\frac{16A\rho_1 H_1}{\sqrt{3}\Gamma_1\Gamma_2\Gamma_3 C^2} \frac{\partial H}{\partial x}, \quad \dot{x} = \frac{16A\rho_1 H_1}{\sqrt{3}\Gamma_1\Gamma_2\Gamma_3 C^2} \frac{\partial H}{\partial y}, \quad (3.24)$$

where  $A(x, y)$  is the area of the triangle formed by the three vortices. Notice that the presence of this term means that (3.23) and (3.24) are in non-canonical Hamiltonian form. It is interesting to note that the Hamiltonian structure of the relative equations (as in (3.17) for example) remains hidden in the original form but becomes transparent when the cartesian variables in the trilinear plane are used, in the manner described above. A general discussion can be found in [41].

Using (3.23) and (3.24), we can conclude that  $\dot{A} = 0$  at points where  $A^2 = \text{constant}$  and the phase curve  $H = \text{constant}$ , are tangent. In particular, in (3.23) for example, we have using the chain-rule,

$$\begin{aligned} \dot{A} &= \frac{\partial A}{\partial x} \dot{x} + \frac{\partial A}{\partial y} \dot{y} = \frac{16A\rho_1 H_1}{\sqrt{3}\Gamma_1\Gamma_2\Gamma_3 C^2} \left[ A \frac{\partial A}{\partial x} \frac{\partial H}{\partial y} - A \frac{\partial A}{\partial y} \frac{\partial H}{\partial x} \right] \\ &= \frac{8\rho_1 H_1}{\sqrt{3}\Gamma_1\Gamma_2\Gamma_3 C^2} \left[ \frac{\partial A^2}{\partial x} \frac{\partial H}{\partial y} - \frac{\partial A^2}{\partial y} \frac{\partial H}{\partial x} \right]. \end{aligned}$$

Using the definitions of the trilinear coordinates and the location of relative equilibria in Proposition 2, it is straightforward to prove the following:

**Theorem 3.5 (Location of relative equilibria in the trilinear plane)** *Relative equilibria are represented by points  $S$  or  $Q$ , where,*

1.  *$S$  are points at which the physical region boundary  $A = 0$  and the phase curve  $H = \text{constant}$  are tangent,*

2.  $Q$  are points representing isosceles triangle configurations with trilinear coordinates given by,

$$Q = \frac{1}{h} \left( \frac{\rho_2 H_2}{\Gamma_1}, \frac{\rho_2 H_2}{\Gamma_2}, \frac{\rho_1 H_1 \beta}{\Gamma_3} \right), \text{ or,}$$

$$Q = \frac{1}{h} \left( \frac{\rho_2 H_2 \beta}{\Gamma_1}, \frac{\rho_1 H_1}{\Gamma_2}, \frac{\rho_1 H_1 \beta}{\Gamma_3} \right),$$

for cases I and II respectively and where  $h$  is the “modified harmonic mean”,

$$h = \frac{3}{\rho_1 H_1 \frac{\beta}{\Gamma_3} + \rho_2 H_2 \left( \frac{1}{\Gamma_1} + \frac{1}{\Gamma_2} \right)}, \text{ or,}$$

$$h = \frac{3}{\rho_1 H_1 \left( \frac{1}{\Gamma_2} + \frac{1}{\Gamma_3} \right) + \rho_2 H_2 \frac{\beta}{\Gamma_1}},$$

for cases I and II respectively, and  $\beta := \left(\frac{s}{t}\right)^2$  is the ratio of the lengths of the sides of the isosceles triangle relative equilibrium, and must belong to the admissible set,

$$\mathcal{A} = \left\{ \beta \mid \beta = \frac{s^2}{t^2}, \text{ where, } \frac{g(t)}{t} = \frac{\alpha H_1 f(s)}{\sqrt{d} s}, \text{ for, case I, and } \right.$$

$$\left. \frac{h(t)}{t} = \frac{H_2 f(s)}{\sqrt{d} s}, \text{ for case II} \right\}.$$

These coordinates simplify when  $t = s$ , corresponding to equilateral triangle configurations, and they become

$$Q = \frac{1}{h} \left( \frac{\rho_2 H_2}{\Gamma_1}, \frac{\rho_2 H_2}{\Gamma_2}, \frac{\rho_1 H_1}{\Gamma_3} \right), \quad h = \frac{3}{\frac{\rho_1 H_1}{\Gamma_3} + \rho_2 H_2 \left( \frac{1}{\Gamma_1} + \frac{1}{\Gamma_2} \right)},$$

$$Q = \frac{1}{h} \left( \frac{\rho_2 H_2}{\Gamma_1}, \frac{\rho_1 H_1}{\Gamma_2}, \frac{\rho_1 H_1}{\Gamma_3} \right), \quad h = \frac{3}{\rho_1 H_1 \left( \frac{1}{\Gamma_2} + \frac{1}{\Gamma_3} \right) + \frac{\rho_2 H_2}{\Gamma_1}},$$

for cases I and II, respectively.

We have not as yet been able to locate the fixed equilibria of Proposition 4 in the trilinear plane. This is a difficult problem because in the two-layer model the lengths  $l_{ij}$  are related only implicitly; for three vortices in the top layer we have for example,

$$\left(\frac{\Gamma_2}{\Gamma_3}\right)^2 = \left(\frac{g(l_{13})}{g(l_{12})}\right)^2, \\ \Gamma_1\Gamma_2g(l_{12})l_{12} + \Gamma_1\Gamma_3g(l_{13})l_{13} + \Gamma_3\Gamma_2g(l_{32})l_{32} = 0,$$

with a similar relationship for  $l_{23}$ . These implicit relations do not allow us to eliminate the lengths  $l_{ij}$ , from both the trilinear coordinates  $b_i$  and the invariant  $C_1$ . This is different from the situation on the plane or the sphere. Indeed, on the plane the fixed equilibria lead to the following explicit relations between the lengths  $l_{ij}$ , [56],

$$l_{12}^2 = \frac{\Gamma_2^2}{\Gamma_3^2}l_{13}^2, \quad l_{23}^2 = \frac{\Gamma_2^2}{\Gamma_1^2}l_{13}^2.$$

On the sphere a necessary and sufficient condition for fixed equilibria is

$$\sum \Gamma_i(\Gamma_j + \Gamma_k)\mathbf{x}_i = 0, \quad i \neq j \neq k,$$

from which one obtains the explicit relations between the lengths  $l_{ij}$ , [31],

$$(\Gamma_1 + \Gamma_2)l_{31}^2 = (\Gamma_1 + \Gamma_3)l_{12}^2, \quad (\Gamma_2 + \Gamma_3)l_{12}^2 = (\Gamma_1 + \Gamma_2)l_{23}^2.$$

## Chapter 4

### Vortex collapse and vortex alignment for the 3-vortex quasi-geostrophic model

In this chapter we study collision of three vortices in the two-layer model. It is seen that although collapse for three vortices in the same layer is possible, the collision process, in general, is not self-similar (homogenous). We also find that if two vortices are in one layer and the third in the other, the two vortices in the same layer cannot collide. Our methods are based on the properties of the invariants, and are in this sense elementary. We also investigate some aspects of a process known as vortex alignment, in which vortices in different layers can merge.

#### 4.1 Vortex collapse in the two-layer model

If we consider simultaneous vortex collapse, it is clear that  $l_{ij} = 0$  at the instance of collapse. Thus using the invariants of Chapter 2 necessary conditions for collapse are:

- i) the vortices are not in equilibrium,
- ii)

$$\begin{aligned} 0 = C_1 &= \left[ \sum_{i=1}^2 \rho_i H_i \left( \sum_{j=1}^{N_i} \Gamma_j^i \right) \right] I - Q^2 - P^2 \\ &= (\rho_1 H_1)^2 \sum_{i < j}^{N_1} \Gamma_i^1 \Gamma_j^1 (l_{ij}^{1,1})^2 + (\rho_2 H_2)^2 \sum_{i < j}^{N_2} \Gamma_i^2 \Gamma_j^2 (l_{ij}^{2,2})^2 \\ &\quad + \frac{(\rho_1 H_1)(\rho_2 H_2)}{2} \sum_{i,j}^{N_1, N_2} \Gamma_i^1 \Gamma_j^2 (l_{ij}^{1,2})^2. \end{aligned} \tag{4.1}$$



It is necessary that  $C_1 = 0$  since  $l_{ij} \rightarrow 0$ , for collapse. We begin by looking at self-similar collapse for three vortices all in the same layer. Recall the definitions of the following functions:

$$\begin{aligned} G(l) &:= A_+ K_0(\lambda_1 l) + A_- K_0(\lambda_2 l), \\ H(l) &:= A_- K_0(\lambda_1 l) + A_+ K_0(\lambda_2 l), \\ F(l) &:= K_0(\lambda_2 l) - K_0(\lambda_1 l). \end{aligned}$$

Without loss of generality we consider three vortices in the upper layer for which the Hamiltonian is:

$$-\frac{H_1 \rho_1}{2\pi} \Gamma_1 \Gamma_2 G(l_{12}) + \Gamma_1 \Gamma_3 G(l_{13}) + \Gamma_3 \Gamma_2 G(l_{23}).$$

(The Hamiltonian for three vortices in the lower layer is the same except that  $H(l)$  replaces  $G(l)$ ). These two functions have the same qualitative behavior. We make use of the fact that  $H$  is invariant to deduce a necessary condition for self-similar collapse to occur. We make the ansatz:

$$l_{ij}(t) = \lambda(t) l_{ij}(0), \quad \lambda(t) \rightarrow 0, \quad \text{as } t \rightarrow t^* < \infty$$

We make use of the property:

$$K_0(z) \sim -\ln z \text{ as } z \rightarrow 0$$

Thus near collapse  $l_{ij} \rightarrow 0$  and,

$$\begin{aligned} H &\sim -\frac{H_1 \rho_1}{2\pi} [\Gamma_1 \Gamma_2 (A_+ \ln \lambda_1 l_{12} + A_- \ln \lambda_2 l_{12}) \\ &\quad + \Gamma_1 \Gamma_3 (A_+ \ln \lambda_1 l_{13} + A_- \ln \lambda_2 l_{13}) \\ &\quad + \Gamma_3 \Gamma_2 (A_+ \ln \lambda_1 l_{23} + A_- \ln \lambda_2 l_{23})] \quad [as \ l_{ij} \rightarrow 0] \\ &\sim [\Gamma_1 \Gamma_2 (A_+ + A_-) \ln \lambda(t) \\ &\quad + \Gamma_1 \Gamma_3 (A_+ + A_-) \ln \lambda(t) \\ &\quad + \Gamma_3 \Gamma_2 (A_+ + A_-) \ln \lambda(t)] \quad [using \ the \ ansatz] \\ &= -\frac{H_1 \rho_1}{2\pi} \ln \lambda(t) [\Gamma_1 \Gamma_2 + \Gamma_2 \Gamma_3 + \Gamma_1 \Gamma_3] \end{aligned}$$

It is now apparent that in order that  $H$  remain invariant as  $\lambda(t) \rightarrow 0$ , that  $\Gamma_1\Gamma_2 + \Gamma_1\Gamma_3 + \Gamma_2\Gamma_3 = 0$ , or,

$$h = \sum \frac{1}{\Gamma_i} = 0. \quad (4.2)$$

We conclude tht although (4.1) is a more general necessary condition for collapse it implies, in particular, (4.2), for self-similar collapse of three vortices in the same layer. Although this is the one-layer case with logarithmic singular vortices, this is not immediate from (4.1) because the two-layer geophysical model contains Bessel function type singular vortices. In addition (4.2) is a relation only on the vortex strengths and unlike (4.1) is independent of the relative distances or coordinates of the vortices themselves. Before we discuss collapse of vortices in different layers there is one other comment we can make regarding the collapse of three vortices in the same layer. Plots of the phase curves in the  $b_1$ - $b_2$  plane for  $h < 0$  reveal them to be closed through the origin  $O$ , but are intercepted by the physical region boundary  $V = 0$  before they can reach  $O$ . Likewise the phase curves for  $h > 0$  are open and do not pass through the origin. These curves are qualitatively similar to those for vortex motion on the sphere, as shown in Fig. 6.1, and are therefore omitted. We shall prove that  $h = 0$  is necessary for any triple-collapse of three-vortices in one layer, regardless of self-similarity. In fact phase plots for  $h = 0$  reveal collapsing configurations which are clearly not self-similar. This is explained by the presence of the Bessel function singularities, Bessel functions, unlike logarithmic functions being non-homogenous. For example if we plot the phase curves for the simplified two-layer model as used by Young [57], and given by equation (1.19), with three vortices in the upper layer the Hamiltonian is:

$$\begin{aligned} H = & -\frac{1}{4\pi}[\Gamma_1\Gamma_2 \left( \ln l_{12} - K_0 \left( \frac{l_{12}}{\lambda} \right) \right) + \Gamma_1\Gamma_3 \left( \ln l_{13} - K_0 \left( \frac{l_{13}}{\lambda} \right) \right) \\ & + \Gamma_3\Gamma_2 \left( \ln l_{23} - K_0 \left( \frac{l_{23}}{\lambda} \right) \right)]. \end{aligned} \quad (4.3)$$

This differs from the usual one-layer case only by the presence of the modified Bessel functions. Phase curves are shown for  $\Gamma_1 = \Gamma_2 = 1$ ,  $\Gamma_3 = -0.5$ ,  $\lambda = 1$  ( $h = 0$ ) in Fig. 4.1, in which the non-self-similar collapsing configurations are clear, since the

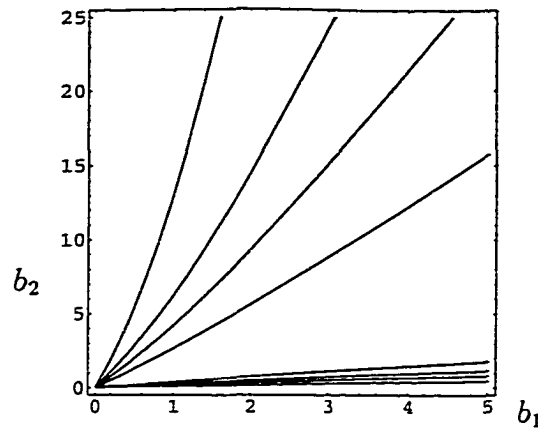


Figure 4.1: Phase diagram for  $C_1 = 0$ : (a)  $\Gamma_1 = \Gamma_2 = 1$ ,  $\Gamma_3 = 0.5$ , for three vortices in the same layer, using the two-layer model, showing non-self-similar collapsing configurations.

phase curves are not straight lines through the origin. We summarize this important observation in the following proposition.

**Proposition 4.1** *The two-layer model admits finite-time, non-self-similar collapse for three vortices in the same layer. Necessary conditions for all collapsing configurations of three vortices in the same layer are  $C_1 = h = 0$ .*

**Proof:** The existence has been demonstrated by the phase curves in Fig. 4.1. In our comments following (4.1), we argued why  $C_1$  must vanish. It is also clear from Fig. 4.1 that the phase curves for collapsing configurations reach the origin with finite non-zero slopes. This means that near collision the collapse is asymptotically self-similar, but our calculations leading to (4.2) show that  $h$  must vanish for self-similar collapse.  $\square$

We conclude by remarking that closed form expressions for these collapsing configurations are difficult to obtain, because the non-homogeneity of the Bessel terms makes the equations difficult to integrate explicitly, unlike the three-vortex problem on the plane or the sphere.

We now consider the case of three vortices lying in different layers. We have the following proposition for three vortices in the 2-layer quasi-geostrophic model:

**Theorem 4.2** *Suppose that vortices 1 and 2 are in layer 1 (or 2) and vortex 3 is in layer 2 (respectively 1), then vortices 1 and 2 cannot collide in finite time.*

**Proof:** Without loss of generality, we consider two vortices in the upper layer and the third in the lower. Now since we are considering vortices and not markers,  $|\Gamma_i| > 0$ . Suppose now that  $l_{12} \rightarrow 0$  so that necessarily,  $l_{13} \rightarrow l_{23}$ . We then have:

$$\begin{aligned} H &= -\frac{\rho_1 H_1}{2\pi} \{ \Gamma_1 \Gamma_2 G(l_{12}) + \frac{H_2}{\sqrt{d}} [\Gamma_1 \Gamma_3 F(l_{13}) + \Gamma_2 \Gamma_3 F(l_{23})] \} \\ &\sim -\frac{\rho_1 H_1}{2\pi} \{ \Gamma_1 \Gamma_2 [(A_+ + A_-) \ln l_{12}] + \frac{H_2}{\sqrt{d}} (\Gamma_1 \Gamma_3 + \Gamma_2 \Gamma_3) F(l_{13}) \}, \end{aligned} \quad (4.4)$$

as

$$l_{12} \rightarrow 0, \text{ and, } l_{13} \rightarrow l_{23}.$$

We consider three cases:

- (a)  $l_{13} \rightarrow 0$  (triple collapse),
  - (b)  $l_{13} \rightarrow \infty$ ,
  - (c)  $l_{13} \rightarrow l$ , where  $0 < l < \infty$ .
- (a) If  $l_{13} \rightarrow 0$  then,

$$\begin{aligned} F(l_{13}) &\sim \ln \lambda_2 l_{13} - \ln \lambda_1 l_{13} \\ &\sim \ln l_{13} - \ln l_{13} + \ln \lambda_2 - \ln \lambda_1. \end{aligned}$$

This gives,

$$\begin{aligned} H &\sim -\frac{\rho_1 H_1}{2\pi} \{ \Gamma_1 \Gamma_2 (A_+ + A_-) \ln l_{12} \\ &\quad + \frac{H_2}{\sqrt{d}} (\Gamma_1 \Gamma_2 + \Gamma_2 \Gamma_3) (\ln \lambda_2 - \ln \lambda_1) \}, \end{aligned} \quad (4.5)$$

as

$$l_{12} \rightarrow 0.$$

The invariance of H implies  $\Gamma_1 \Gamma_2 = 0$ , a contradiction.

- (b) If  $l_{13} \rightarrow \infty$  then:

$$F(l_{13}) = K_0(\lambda_2 l_{13}) - K_0(\lambda_1 l_{13}) \rightarrow 0, \quad (4.6)$$

because  $K_0(x) \rightarrow 0$  as  $x \rightarrow \infty$ .

(c) Finally, if  $0 < l < \infty$  we see that the second term on the RHS of (4.4) is bounded yielding (4.5). This concludes the proof.  $\square$

We remark that the inability of the two vortices in the same layer to collide, indeed, precludes triple collision as seen in the proof. It is also interesting to note that this case, (two vortices in the same layer and the third in the other), is similar in this regard to the two vortex (1-layer) problem on the plane. It is not possible for two vortices to collide, there being a minimum positive distance between the two vortices. In conclusion, given a two vortex configuration in a given layer, introducing a third in the other will not admit the original two vortices to collide. On the other hand, this is very different from the three vortex case on the plane (or on the sphere, see Chapter 6), where for instance three vortices can self-similarly collide.

## 4.2 Vortex alignment in the two-layer model

We have already seen that for the quasi-geostrophic two-layer point vortex model, configurations for which there are two vortices in the same layer (labeled 1 and 2) and a third vortex (vortex 3) in the other, do not admit collision of the two vortices in the same layer. This is due essentially to the nature of the Bessel-type singularity associated with the point vortices. We now demonstrate, however, that the distance in the x-y plane between vortex 3 in the second layer and one of the vortices (either 1 or 2) in the first layer can go to zero. In the literature such an event has been termed vortex alignment, because the vortices align in the x-y plane while remaining in their respective layers. This phenomenon has been studied in detail for vortex patches in the two-layer model by Polvani [52], and numerically by McWilliams [43]. Aspects of this phenomenon have also been mentioned by Polvani et al in [18]. It has been noted that this process, whereby vortices from different layers coalesce, is the fundamental mechanism for the cascade from baroclinic (two-layer) to barotropic (one-layer) modes, in the same way that the well-known collapse process mediates the reverse-energy cascade of two-dimensional turbulence. Before we illustrate this process for the two-layer point vortex model, we mention that a minimum of three-vortices are required, since as shown in Chapter 1 for the two-vortex problem, the distance between any two vortices is invariant. In the three-vortex two-layer problem,

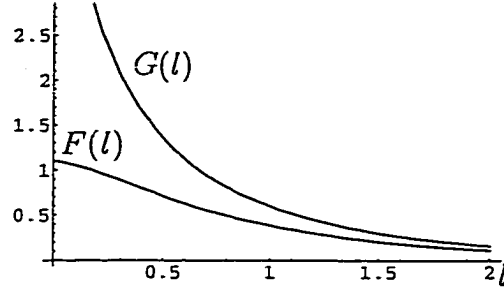


Figure 4.2: Typical graphs of the functions,  $F(l)$  and  $G(l)$ . The function  $H(l)$  is qualitatively similar to  $F(l)$ , and is not shown. In plotting  $F(l)$ , one may take  $\lambda_1 > \lambda_2$ , without loss of generality

two vortices from different layers can merge, while there is a minimum positive distance between the two vortices in the same layer (Proposition 4.2). In the one-layer case (as on the sphere) it is impossible for the three-vortex problem for two vortices to collapse and the third not. This is easily seen by considering the invariants

$$\begin{aligned} H &= \Gamma_1 \Gamma_2 \ln(l_{12}^2) + \Gamma_1 \Gamma_3 \ln(l_{13}^2) + \Gamma_3 \Gamma_2 \ln(l_{32}^2), \\ C_1 &= \Gamma_1 \Gamma_2 l_{12}^2 + \Gamma_1 \Gamma_3 l_{13}^2 + \Gamma_3 \Gamma_2 l_{32}^2. \end{aligned}$$

Now suppose  $l_{12} \rightarrow 0$ , then  $l_{13} \rightarrow l_{23}$  and there is a logarithmic divergence in the Hamiltonian as  $l_{12} \rightarrow 0$ , which means that either  $l_{13} \rightarrow 0$ , which is triple collapse, or  $l_{13}, l_{23} \rightarrow \infty$ , which is inconsistent with the invariance of  $C_1$  for  $l_{12} \rightarrow 0$ . In fact for the three vortex problem on the plane (as on the sphere) the only collisions possible are self-similar triple collisions. We prove these results in Chapter 6.

One can see why vortex alignment solutions may be possible by examining the proof of Proposition 4.2. It was seen there that two vortices in the same layer could not collide due to the unbalanced singular logarithmic term coming from the interaction term  $G(l)$ , for vortices in the same layer. However, the interaction term for vortices in different layers  $F(l)$  does not have a singularity at 0 as seen in Fig. (4.2). This means that the distance between two vortices may go to zero without an unbalanced logarithmic divergence. We now demonstrate the existence of vortex alignment solutions, by considering the case  $\Gamma_1, \Gamma_2 > 0$ ,  $\Gamma_3 < 0$  for a configuration where vortices 1 and 2 are in the upper layer and vortex 3 in the lower. To reduce the problem we will again make extensive use of trilinear phase-plane analysis. Perhaps

the simplest case where vortex alignment occurs is by supposing that the following invariant vanishes

$$C_1 = \rho_1 H_1 \Gamma_1 \Gamma_2 l_{12}^2 + (\rho_1 H_1)(\rho_2 H_2)[\Gamma_1 \Gamma_3 l_{13}^2 + \Gamma_3 \Gamma_2 l_{32}^2] = 0. \quad (4.7)$$

Introducing the trilinear coordinates,

$$b_1 = \frac{l_{23}^2}{\gamma_1}, \quad b_2 = \frac{l_{13}^2}{\gamma_2}, \quad b_3 = \frac{l_{12}^2}{\gamma_3}, \quad \text{where}$$

$$\gamma_1 = \frac{\Gamma_1}{\rho_2 H_2}, \quad \gamma_2 = \frac{\Gamma_2}{\rho_2 H_2}, \quad \gamma_3 = \frac{\Gamma_3}{\rho_1 H_1},$$

obtain

$$b_1 + b_2 + b_3 = 0. \quad (4.8)$$

Now the physical region is

$$(\gamma_1 b_1)^2 + (\gamma_2 b_2)^2 + (\gamma_3 b_3)^2 \leq 2(\gamma_1 \gamma_2 b_1 b_2 + \gamma_1 \gamma_3 b_1 b_3 + \gamma_2 \gamma_3 b_2 b_3) \quad (4.9)$$

Using (4.8) and (4.9), and taking  $\gamma_2 = -\gamma_3$  the physical region boundary is

$$b_1^2(\gamma_1 + \gamma_3)^2 + 4b_1 b_2(\gamma_1 \gamma_3) = b_1[(\gamma_1 + \gamma_3)^2 b_1 + 4b_2 \gamma_1 \gamma_3] = 0$$

Assuming  $\gamma_1 + \gamma_3 \neq 0$ , then the physical region is the wedge bounded by  $b_1 = 0$  and the line

$$b_2 = -\frac{(\gamma_1 + \gamma_3)^2}{4\gamma_1 \gamma_3} b_1, \quad (\gamma_1, \gamma_3 \neq 0).$$

Now assuming  $\Gamma_1$ , and  $\Gamma_3$  have opposite signs, the slope of this line is positive, so that, the physical region is as shown in Figure (4.3). In particular it is a wedge lying in the first quadrant, one of whose boundaries is the line  $b_1 = 0$ . It is interesting to note that the aligning vortices, 2 and 3, in this example have opposite signs. We will now demonstrate the existence of phase curves going through the points  $(b_2, 0)$ , for  $b_2 > 0$ . These phase curves correspond to vortex alignment solutions since they lie locally in the physical region. In order to obtain the phase curves recall the

definition of the functions  $F(l)$  and  $G(l)$ , and notice that for the configuration under consideration the Hamiltonian takes the form

$$\begin{aligned} H &= \frac{1}{4\pi} \left\{ \rho_1 H_1 \Gamma_1 \Gamma_2 G(l_{12}) + 2 \frac{\rho_1 H_1 H_2}{\sqrt{d}} [\Gamma_1 \Gamma_3 F(l_{13}) + \Gamma_2 \Gamma_3 F(l_{23})] \right\} \\ &= \frac{1}{4\pi} \left\{ \rho_1 H_1 \Gamma_1 \Gamma_2 G(\sqrt{\gamma_3 b_3}) + 2 \frac{\rho_1 H_1 H_2}{\sqrt{d}} [\Gamma_1 \Gamma_3 F(\sqrt{\gamma_2 b_2}) + \Gamma_2 \Gamma_3 F(\sqrt{\gamma_1 b_1})] \right\}. \end{aligned}$$

It remains to show phase-curves in the  $b_1$ - $b_2$ , lying in the physical region going through  $b_1 = 0$ , (so that  $b_2 > 0$ ). Begin by observing that as  $b_1 \rightarrow 0$ ,  $l_{23} \rightarrow 0$ , and that  $l_{12} \rightarrow l_{13}$ . Recall further that  $K_0(z) \sim \ln(z)$  as  $z \rightarrow 0$ . When vortices 2 and 3 align, we then have  $l_{12} \approx l_{13}$  so that,

$$\begin{aligned} H &\approx \frac{1}{4\pi} \left\{ \rho_1 H_1 \Gamma_1 \Gamma_2 G(l_{13}) + 2 \frac{\rho_1 H_1 H_2}{\sqrt{d}} [\Gamma_1 \Gamma_3 F(l_{13}) + \Gamma_2 \Gamma_3 F(l_{23})] \right\}, \\ \frac{4\pi H}{\rho_1 H_1} &\approx \left\{ \Gamma_1 \Gamma_2 G(l_{13}) + \frac{2H_2}{\sqrt{d}} [\Gamma_1 \Gamma_3 F(l_{13}) + \Gamma_2 \Gamma_3 F(l_{23})] \right\} \\ &\sim \Gamma_1 \Gamma_2 G(l_{13}) + \frac{2H_2}{\sqrt{d}} \Gamma_1 \Gamma_3 F(l_{13}) + \frac{2H_2}{\sqrt{d}} \Gamma_2 \Gamma_3 \ln \left( \frac{\lambda_2}{\lambda_1} \right), \end{aligned}$$

as

$$l_{23} \rightarrow 0.$$

We, therefore, have

$$\begin{aligned} \frac{4\pi H}{\rho_1 H_1} - \frac{2\Gamma_2 \Gamma_3 H_2}{\sqrt{d}} \ln \left( \frac{\lambda_2}{\lambda_1} \right) &\sim \Gamma_1 \Gamma_2 G(l_{13}) + \frac{2H_2}{\sqrt{d}} \Gamma_1 \Gamma_3 F(l_{13}) \\ &= \Gamma_1 \Gamma_2 G\left(\sqrt{\frac{\Gamma_2 b_2}{\rho_2 H_2}}\right) + \frac{2H_2}{\sqrt{d}} \Gamma_1 \Gamma_3 F\left(\sqrt{\frac{\Gamma_2 b_2}{\rho_2 H_2}}\right). \end{aligned} \quad (4.10)$$

It is now simply a matter of prescribing  $b_2 > 0$ , and then choosing the particular  $H$  to force equality in (4.10). For given  $b_2 > 0$ , there exists an energy level  $H$ , that achieves this, and hence a phase curve passing through  $(b_1, b_2) = (0, b_2)$ , corresponding to a vortex alignment configuration as shown in Fig. (4.3), for which  $\frac{H_2}{\sqrt{d}}$  is regarded as a parameter and taken to be 0.5, and for which  $\rho_1 H_1 = \rho_2 H_2 = 1$ ,  $\lambda_1 > \lambda > 2$ . We have demonstrated vortex alignment solutions for the case  $\Gamma_1, \Gamma_2 > 0, \Gamma_3 < 0$ , and in particular for the case  $C_1 = 0$  and  $\frac{\Gamma_1}{\rho_2 H_2} = -\frac{\Gamma_3}{\rho_1 H_1}$ . It would be interesting to



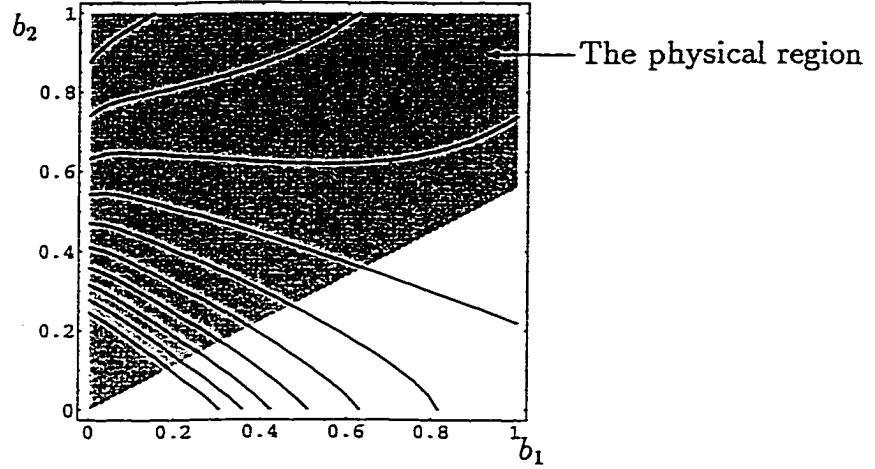


Figure 4.3: Phase curves of vortex alignment.  $C_1 = 0$ ;  $\Gamma_1 = 0.25$ ,  $\Gamma_2 = -\Gamma_3 = 1$ .

classify the regimes that admit vortex alignment solutions, by finding necessary and sufficient conditions for their existence. In our example it was seen that in order for vortex alignment to occur the dynamics had to take place in the physical region, so that the aligning vortices were chosen to have opposite sign. It is easy to show that this is necessary for the case  $C_1 = 0$ . Begin by considering the invariant (4.7) and suppose without loss of generality that vortices 2 and 3 align. This means that  $l_{23} \rightarrow 0$ , so that  $l_{12} \rightarrow l_{13}$ , and at vortex alignment,

$$0 = C_1 \approx (\rho_1 H_1 \Gamma_1 \Gamma_2 + \rho_2 H_2 \Gamma_1 \Gamma_3) l_{12}^2.$$

Now since  $l_{12} \neq 0$  (Proposition 4.2) conclude that  $\rho_1 H_1 \Gamma_2 + \rho_2 H_2 \Gamma_3 = 0$ , so that in particular  $\Gamma_2$ , and  $\Gamma_3$ , the strengths of the aligning vortices, must be of opposite signs. We conclude with a few remarks. Suppose, first, that  $l_{23} \rightarrow 0$ ,  $l_{12}, l_{13} \rightarrow \infty$ , then since  $G(l), F(l) \rightarrow 0$  as  $l \rightarrow \infty$ , we have in (4.10)

$$\frac{4\pi H}{\rho_1 H_1} - \frac{2\Gamma_2 \Gamma_3 H_2}{\sqrt{d}} \ln \left( \frac{\lambda_2}{\lambda_1} \right) = 0,$$

so that such a vortex alignment can occur only with Hamiltonian or energy level,

$$H = \frac{2\Gamma_2 \Gamma_3 \rho_1 H_1 H_2}{\sqrt{d}} \ln \left( \frac{\lambda_1}{\lambda_2} \right).$$

Secondly, we showed that for  $C_1 = 0$ , the aligning vortices had to have opposite signs. Recall in Chapter 2 we showed that we need only consider the cases, (i)  $\Gamma_1, \Gamma_2, \Gamma_3 > 0$ , (ii)  $\Gamma_1, \Gamma_2 > 0, \Gamma_3 < 0$ , and (iii)  $\Gamma_1 > 0, \Gamma_2 < 0, \Gamma_3 > 0$ . So alignment solutions for  $C_1 = 0$  can occur only for the cases (ii) and (iii). Now, since  $C_1$  is invariant, if  $l_{23} \rightarrow 0$ , near vortex alignment

$$C_1 \approx \rho_1 H_1 \Gamma_1 (\rho_1 H_1 \Gamma_2 l_{12}^2 + \rho_2 H_2 \Gamma_3 l_{13}^2).$$

If  $l_{12}, l_{13} \rightarrow \infty$ , it is therefore necessary, by the invariance of  $C_1$ , that  $\Gamma_2$ , and  $\Gamma_3$  be of opposite signs, again ruling out such a vortex alignment for all vortices of the same sign, (case (i)). At this point, we also do not know, for instance, if  $C_1 = 0$  is necessary for vortex alignment, (as it is for the simultaneous collapse of three vortices of three vortices in the same layer).

## Chapter 5

### Numerical investigation of integrable 2-layer quasi-geostrophic vortex dynamics

In this chapter we study some numerical aspects of integrable two-layer vortex dynamics. We focus exclusively on the simplified two-layer given by (1.19). We present a brief study of the streamlines for rotating two-vortex systems. We then perform some simulations of collinear, and therefore integrable, four-vortex dynamics. We conclude with some observations on the advection problem for the two-layer model. Our study is similar to that of Young [57] and Gurzhi et al [27].

#### 5.1 On streamline patterns for rotating two vortex configurations

In [57], Young studied the effect of the Rossby radius of deformation,  $\lambda$ , on the streamlines and the advection problem for two translating vortices in the two-layer model. For translating vortices the vortex strengths must sum to zero so that they are of equal magnitude but of opposite sign. He showed that a pair of translating vortices in the top layer transports no lower layer fluid if the distance between the vortices is less than 1.72 deformation radii. In contrast, the size of the trapped region for translating vortices in different layers (termed a heton) increases without bound as the spacing between the vortices increases. We present a similar analysis for rotating vortices. We focus on the representative case  $\Gamma_1 = \Gamma_2$ . In this section we study the change in the streamline patterns as the ratio of the vortex separation

against deformation radius,  $\frac{d}{\lambda}$ , is varied. We begin with the two vortices in the top layer.

### 5.1.1 Two rotating vortices in the same layer

Suppose that the two vortices are in the upper layer. Then the distance between them,  $d = 2a$ , remains constant. If  $\Gamma_1 = \Gamma_2$ , then  $\Gamma_1 + \Gamma_2 \neq 0$ , and the vortices rotate about the center of vorticity with angular velocity,

$$\omega = \frac{\Gamma}{d^2} G^+\left(\frac{d}{\lambda}\right), \quad G^+(z) := 1 + zK_1(z).$$

To visualize the flow associated with this pair we use a coordinate system translating with the vortices. In this frame the motion is steady and the streamfunctions are:

$$\begin{aligned} \psi_1 &= \frac{1}{2}\omega(x^2 + y^2) + \frac{1}{2}\Gamma \ln(r_1 r_2) - \frac{1}{2}\Gamma \left[ K_0\left(\frac{r_1}{\lambda}\right) + K_0\left(\frac{r_2}{\lambda}\right) \right] \\ \psi_2 &= \frac{1}{2}\omega(x^2 + y^2) + \frac{1}{2}\Gamma \ln(r_1 r_2) + \frac{1}{2}\Gamma \left[ K_0\left(\frac{r_1}{\lambda}\right) + K_0\left(\frac{r_2}{\lambda}\right) \right] \end{aligned}$$

where

$$r_1 := \left[ x^2 + (y - a)^2 \right]^{\frac{1}{2}}, \quad r_2 := \left[ x^2 + (y + a)^2 \right]^{\frac{1}{2}},$$

are the distances from the two vortices at  $(0, \pm a)$  and  $\Gamma_1 = \Gamma_2 = \Gamma$ . The streamline patterns as the ratio,  $\frac{d}{\lambda}$ , is varied are shown in Figure 5.1.

### 5.1.2 Two rotating vortices in different layers

We next examine the interaction of two rotating vortices in different layers. Once again, because of the integral invariants,  $d = 2a$  is constant. If  $\Gamma_1 = \Gamma_2$ , then  $\Gamma_1 + \Gamma_2 \neq 0$ , and the vortices rotate about the center of vorticity with angular velocity,

$$\omega = \frac{\Gamma}{d^2} G^-\left(\frac{d}{\lambda}\right), \quad G^-(z) := 1 - zK_1(z).$$

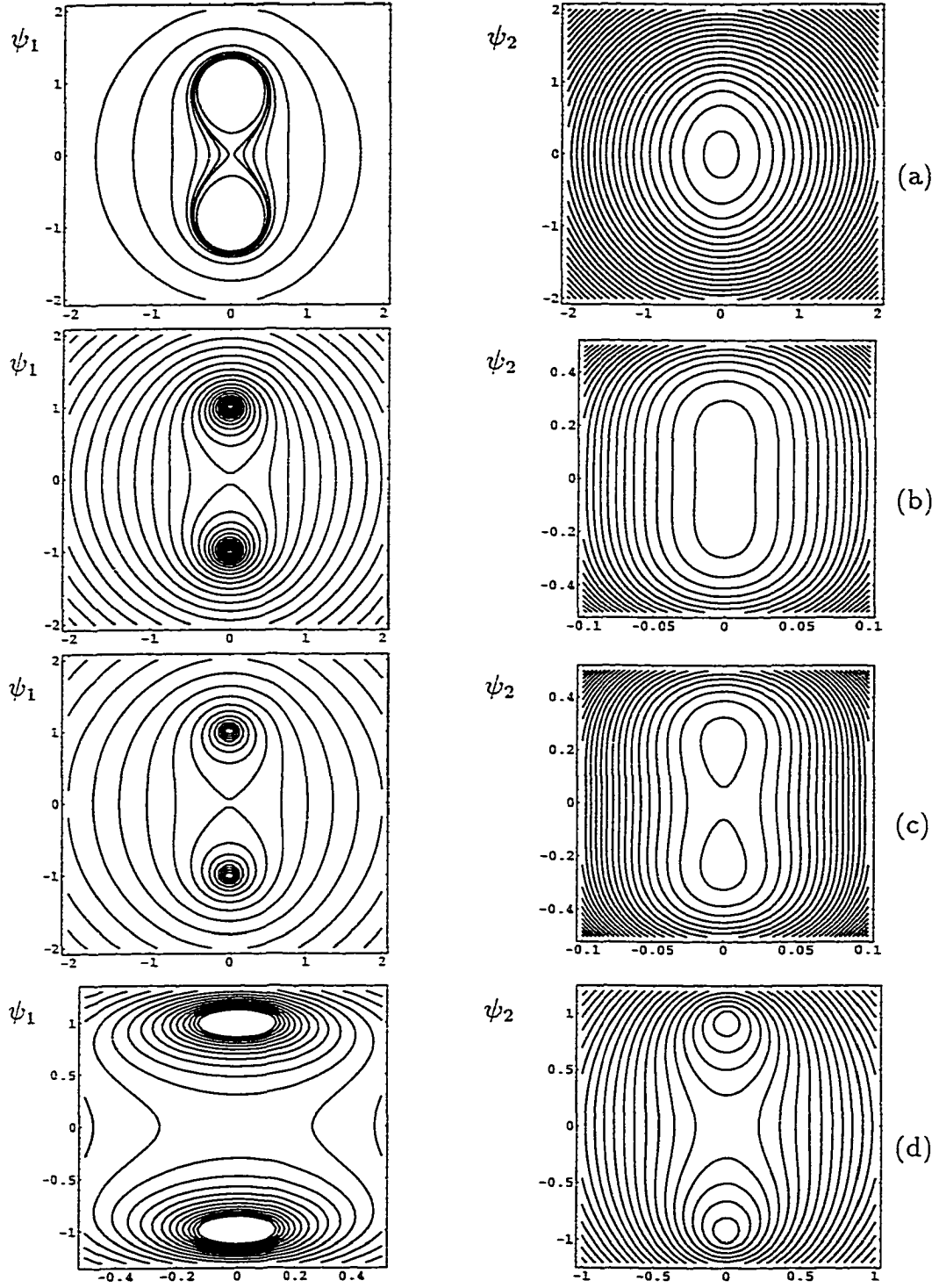


Figure 5.1: Streamline patterns: two rotating vortices in the same layer, (a)  $\frac{d}{\lambda} = 2$ , (b)  $\frac{d}{\lambda} = 4$ , (c)  $\frac{d}{\lambda} = 4.082$ , (d)  $\frac{d}{\lambda} = 8$

In a frame of reference rotating with the pair the motion is steady and the stream-functions are

$$\begin{aligned}\psi_1 &= \frac{1}{2}\omega(x^2 + y^2) + \frac{1}{2}\Gamma \ln(r_1 r_2) + \frac{1}{2}\Gamma \left[ K_0\left(\frac{r_2}{\lambda}\right) - K_0\left(\frac{r_1}{\lambda}\right) \right] \\ \psi_2 &= \frac{1}{2}\omega(x^2 + y^2) + \frac{1}{2}\Gamma \ln(r_1 r_2) - \frac{1}{2}\Gamma \left[ K_0\left(\frac{r_2}{\lambda}\right) - K_0\left(\frac{r_1}{\lambda}\right) \right]\end{aligned}$$

where

$$r_1 := [x^2 + (y - a)^2]^{\frac{1}{2}}, \quad r_2 := [x^2 + (y + a)^2]^{\frac{1}{2}},$$

are the distances from the two vortices at  $(0, \pm a)$  and  $\Gamma_1 = \Gamma_2 = \Gamma$ . The vortex located at  $(0, a)$  is in the upper layer. The streamline patterns as the ratio,  $\frac{d}{\lambda}$ , is varied are shown in Figure 5.2. We observe that in both cases—vortices in the same layer or vortices in different layers—our results are similar to those obtained by Young [57] for rigidly translating vortices (again either in the same layer or different layers). It is noticed that there is a critical value of  $\frac{d}{\lambda}$  at which there is a qualitative change in the streamline patterns. Young found that for a pair of vortices in the top layer, there is no lower layer fluid transport if the distance between the vortices is less than 1.72 deformation radii, and that by contrast the size of the trapped region increases without bound as the spacing between the vortices increases.

## 5.2 Numerical simulation of integrable four-vortex dynamics

### 5.2.1 On integrable four-vortex coaxial configurations

In Chapter 2 we presented four-vortex configurations, for the two-layer model, that are integrable. For the full two-layer model these are systems where  $P = Q = 0$  and  $\sum_{i=1}^2 \rho_i H_i \sum_{j=1}^{N_i} \Gamma_j^i$ . Clearly this holds also for the simplified two-layer model, and examples include the collinear configurations shown in Figure 5.3(b). These are four vortex systems where there is a vortex of strength  $\Gamma_i$  at  $(x_i, y_i)$  and an image vortex of the same strength, (and sign), at  $(-x_i, -y_i)$ . Following the convention of Young [57] if a vortex and its image are in the same layer that pair will be

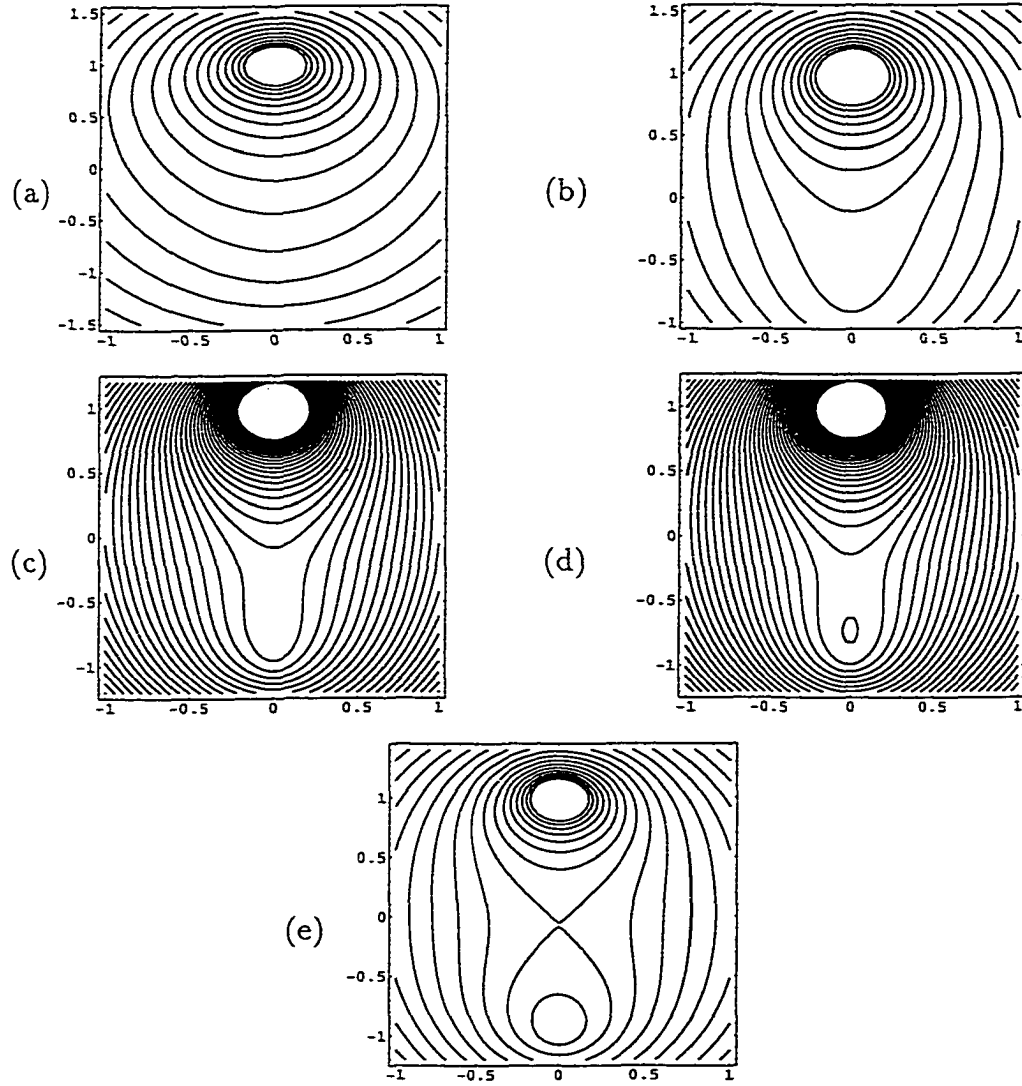


Figure 5.2: Streamline patterns ( $\psi_1$ ): two rotating vortices in different layers, (a)  $\frac{d}{\lambda} = 2$ , (b)  $\frac{d}{\lambda} = 4$ , (c)  $\frac{d}{\lambda} = 5$ , (d)  $\frac{d}{\lambda} = 5.128$ , (e)  $\frac{d}{\lambda} = 8$

called *strongly symmetric*. Image vortices in different layers will be termed *weakly symmetric* pairs. In this chapter we will investigate numerically the dynamics of such integrable configurations.

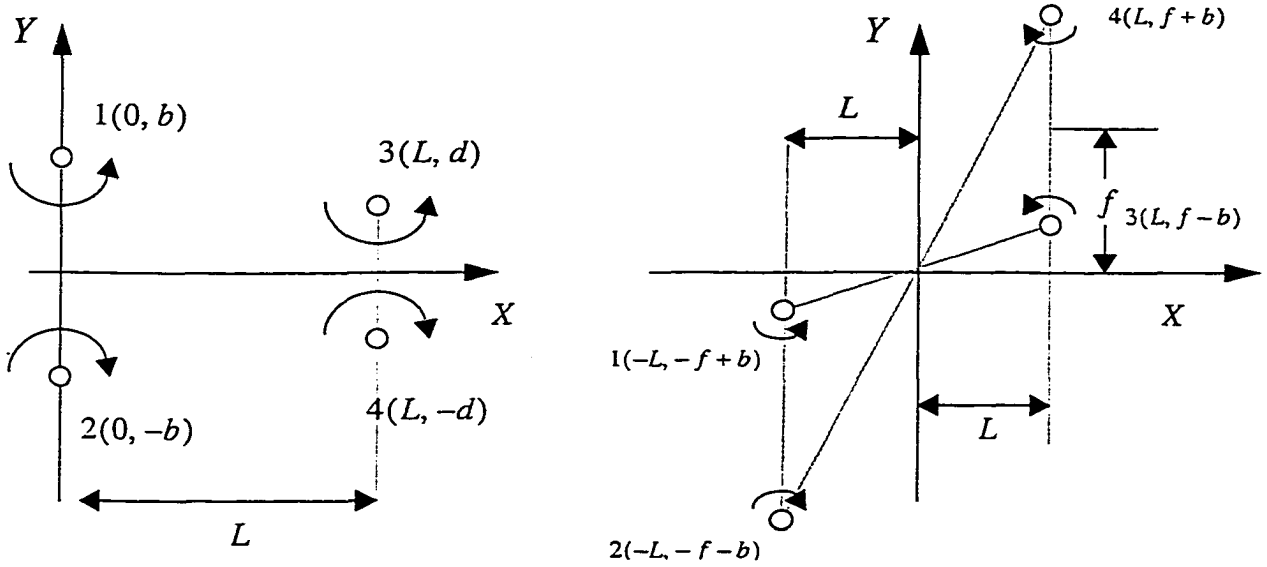


Figure 5.3: Integrable 4 vortex configurations, showing initial positions of vortices. (a) Two coaxial vortex pairs 12 and 34; (b) two collinear vortex pairs.

Other four-vortex systems that are integrable, for the simplified two-layer model, are the coaxial configurations shown in Figure 5.3(a). This was observed by Young [57]. We present a formal proof from a Hamiltonian standpoint. Our purpose is to illustrate that the proof does not carry over to such configurations for the full two-layer model. We conjecture, therefore, that the full two-layer model does not, in general, admit integrable four-vortex coaxial configurations

**Theorem 5.1** *The simplified point vortex two-layer model of (1.19) admits integrable four-vortex coaxial configurations, where image vortices of strengths  $\pm\Gamma_i$  are located at  $(x_i, \pm y_i)$ .*

**Proof:** We prove it for the weakly symmetric configuration of a vortex of strength  $\Gamma_1$  at  $\mathbf{x}_1 = (x_1, y_1)$  in layer one and an image vortex of strength  $-\Gamma_1$  at  $\mathbf{x}_3 = (x_1, -y_1)$ , and a third vortex of strength  $\Gamma_2$ , in the first layer, at  $\mathbf{x}_2 = (x_2, y_2)$ , with image vortex of strength  $\Gamma_2$  at  $\mathbf{x}_4 = (x_2, -y_2)$ . It suffices to show that the line  $y = 0$ , is



an axis of symmetry. (See the proof of Theorem 6.6). The streamfunctions in layer one and two are

$$\begin{aligned} 2\psi_1 = & \Gamma_1(\ln r_1 - K_0(\frac{r_1}{\lambda})) + \Gamma_2(\ln r_2 - K_0(\frac{r_2}{\lambda})) \\ & - \Gamma_1(\ln r_3 + K_0(\frac{r_3}{\lambda})) - \Gamma_2(\ln r_4 + K_0(\frac{r_4}{\lambda})), \end{aligned} \quad (5.1)$$

$$\begin{aligned} 2\psi_2 = & -\Gamma_1(\ln r_3 - K_0(\frac{r_3}{\lambda})) + -\Gamma_2(\ln r_4 - K_0(\frac{r_4}{\lambda})) \\ & + \Gamma_1(\ln r_1 + K_0(\frac{r_1}{\lambda})) + \Gamma_2(\ln r_2 + K_0(\frac{r_2}{\lambda})), \end{aligned} \quad (5.2)$$

where

$$r_k := [(x - x_k)^2 + (y - y_k)^2]^{\frac{1}{2}}.$$

We now show that  $\dot{x}_1 = \dot{x}_3$ . Well,

$$\begin{aligned} 2\dot{x}_1 = 2 \frac{\partial \psi_1}{\partial y} \Big|_{r=r_1} &= \Gamma_2 \frac{y_2 - y_1}{r_{12}^2} + \Gamma_2 K_1(\frac{r_{12}}{\lambda}) \frac{y_2 - y_1}{\lambda r_{12}} \\ &\quad - \Gamma_1 \frac{y_3 - y_1}{r_{13}^2} + \Gamma_1 K_1(\frac{r_{13}}{\lambda}) \frac{y_3 - y_1}{\lambda r_{13}} \\ &\quad - \Gamma_2 \frac{y_4 - y_1}{r_{14}^2} + \Gamma_2 K_1(\frac{r_{14}}{\lambda}) \frac{y_4 - y_1}{\lambda r_{14}}, \\ 2\dot{x}_3 = 2 \frac{\partial \psi_2}{\partial y} \Big|_{r=r_3} &= \Gamma_1 \frac{y_1 - y_3}{r_{13}^2} - \Gamma_1 K_1(\frac{r_{13}}{\lambda}) \frac{y_1 - y_3}{\lambda r_{13}} \\ &\quad - \Gamma_2 \frac{y_4 - y_3}{r_{34}^2} - \Gamma_2 K_1(\frac{r_{34}}{\lambda}) \frac{y_4 - y_3}{\lambda r_{13}} \\ &\quad + \Gamma_2 \frac{y_2 - y_3}{r_{23}^2} - \Gamma_2 K_1(\frac{r_{23}}{\lambda}) \frac{y_2 - y_3}{\lambda r_{23}}. \end{aligned}$$

Now using

$$r_{23} = r_{14}, \quad r_{34} = r_{12}, \quad y_2 = -y_4, \quad \text{and}, \quad y_3 = -y_1,$$

it is clear that  $\dot{x}_1 = \dot{x}_3$ .

Similar calculations show that  $\dot{y}_1 = -\dot{y}_3$ . Again,

$$\begin{aligned} -2\dot{y}_1 = 2 \frac{\partial \psi_1}{\partial x} \Big|_{r=r_1} &= \Gamma_2 \frac{x_2 - x_1}{r_{12}^2} + \Gamma_2 K_1(\frac{r_{12}}{\lambda}) \frac{x_2 - x_1}{\lambda r_{12}} \\ &\quad - \Gamma_1 \frac{x_3 - x_1}{r_{13}^2} + \Gamma_1 K_1(\frac{r_{13}}{\lambda}) \frac{x_3 - x_1}{\lambda r_{13}} \end{aligned}$$

$$\begin{aligned}
-2\dot{y}_3 &= 2 \left. \frac{\partial \psi_2}{\partial x} \right|_{r=r_3} = \Gamma_1 \frac{x_1 - x_3}{r_{13}^2} - \Gamma_1 K_1\left(\frac{r_{13}}{\lambda}\right) \frac{x_1 - x_3}{\lambda r_{13}} \\
&\quad - \Gamma_2 \frac{x_4 - x_3}{r_{34}^2} - \Gamma_2 K_1\left(\frac{r_{34}}{\lambda}\right) \frac{x_4 - x_3}{\lambda r_{13}} \\
&\quad + \Gamma_2 \frac{x_2 - x_3}{r_{23}^2} - \Gamma_2 K_1\left(\frac{r_{23}}{\lambda}\right) \frac{x_2 - x_3}{\lambda r_{23}}.
\end{aligned}$$

Now using

$$r_{23} = r_{14}, \quad r_{34} = r_{12}, \quad x_2 = x_4, \quad \text{and} \quad x_3 = x_1,$$

it is clear that  $\dot{y}_1 = -\dot{y}_3$ . □

To see why this proof does not apply to the full two-layer model, observe, that in the streamfunctions, (5.1-5.2), there are only two types of interaction terms,

$$\ln r - K_0\left(\frac{r}{\lambda}\right),$$

for vortices in the same layer, and

$$\ln r + K_0\left(\frac{r}{\lambda}\right),$$

for vortices in different layers. For the full two-layer model, the interaction terms are given by the functions defined in (1.18). The interaction term for vortices in different layers is given by  $F(l)$ , while there are two interaction terms for vortices in the same layer;  $G(l)$  for vortices in the upper layer, and,  $H(l)$ , for vortices in the lower. It is easy to show that these different interaction terms for the full two-layer model,  $G(l)$ , and  $H(l)$ , together with the nonhomogeneity of the modified Bessel functions do not yield the type of cancellations seen in the proof above for the simplified two-layer model.

A numerical study of integrable coaxial four-vortex two-layer problems was done by Young [57]. We conduct similar work for collinear four-vortex configurations.

## 5.2.2 Numerical simulation of collinear four-vortex configurations

We present some numerical experiments for four-vortex collinear integrable vortex systems. Our study is similar to the coaxial four-vortex integrable work performed by Young [57]. We study strongly symmetric systems where a vortex and its image are in the same layer, but the pairs are in different layers, as well as weakly symmetric systems. We have not studied collinear systems where all vortices are in the same layer. We suspect that such systems share many of the qualitative features of the one-layer four-vortex collinear systems. We remark that the possible motions of four-vortex collinear dynamics has been completely classified. The classification is according to the following parameters [27]:

$$h = \frac{2b}{|f|} \frac{L^2 + f^2}{\sqrt{[L^2 + (f+b)^2][L^2 + (f-b)^2]}},$$

$$\zeta_0 = \frac{\sqrt{[L^2 + (f+b)^2][L^2 + (f-b)^2]}}{2|f|b},$$

where all lengths are as shown in Figure 5.3(b). Such a complete characterization for the two-layer problem is beyond the scope of our work. We present numerical experiments for special initial conditions and compare the strongly and weakly symmetric cases. Throughout our work all four vortices of unit strength  $\Gamma = 1$  and the Rossby radius of deformation is taken to be  $\lambda = 1$ .

### 5.2.2.1 Example 1: coupling and scattering

In this experiment we consider initial conditions of the following type:

- (i) Strongly symmetric configurations with initial positions of the paired vortices in the top layer,  $(\pm a, \pm b)$ , where both  $a$  and  $b$  are positive, and initial positions of the pair in the bottom layer at  $(\pm a, \mp b)$ , for the same  $a$  and  $b$ .
- (ii) Weakly symmetric configurations with one pair with vortex in the top layer at  $(a, b)$ , image vortex in the bottom layer at  $(-a, -b)$ , and second vortex pair with vortex in the top layer at  $(a, -b)$  and image vortex in the bottom layer at  $(-a, b)$ , again for  $a$  and  $b$  positive.

Our results are shown in Figure 5.4. This qualitative behavior was observed for a large set of initial values. However it is seen that although the initial positions of the vortices in case (i) and (ii) are the same, the terminal distances are not. This is an effect due to the different layer allocations of the vortices. One other difference is that if we put one of the vortices at say  $(1, b)$  for  $b > 0$  and a vortex from the other pair at  $(1, -b)$  and let  $b \rightarrow 0$ , the qualitative behavior for case (i) changes at some critical value, (for  $b = b^* = 0.6$  but does not for case (ii)). This is shown in Figure 5.5.

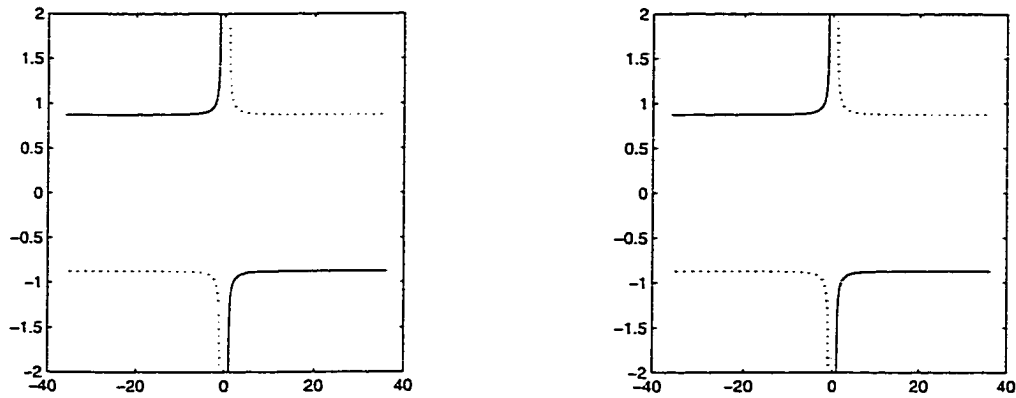


Figure 5.4: Numerical integration of collinear vortices showing a scattering of vortices. (a) Strongly symmetric configuration (b) Weakly symmetric configuration. Initial positions are:(a)Top layer  $(1, 2)$  and  $(-1, -2)$  and bottom layer  $(1, -2)$ , and  $(-1, 2)$ , and for (b)Vortices in top layer at  $(1, 2)$ , and  $(1, -2)$  with image vortices at  $(-1, -2)$ , and  $(-1, 2)$  respectively.

#### 5.2.2.2 Example 2: periodic and quasiperiodic behavior

The second numerical experiment we present is the following:

- (i) For the strongly symmetric case the initial positions of the pair in the top layer are fixed at  $(\pm 0.5, \pm 0.5)$  while the initial positions of the pair in the bottom layer are  $(\pm x, 0)$ , where  $x$  is allowed to vary.
- (ii) For the weakly symmetric case the initial position of one pair is fixed at  $(\pm 0.5, \pm 0.5)$  and the other pair is located at  $(\pm x, 0)$  where  $x$  is allowed to vary.

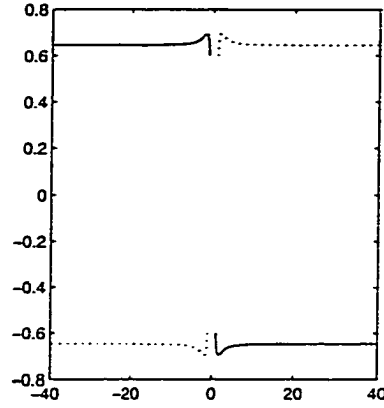


Figure 5.5: Numerical integration of scattering for  $b = b^* = 0.6$  for a strongly symmetric system

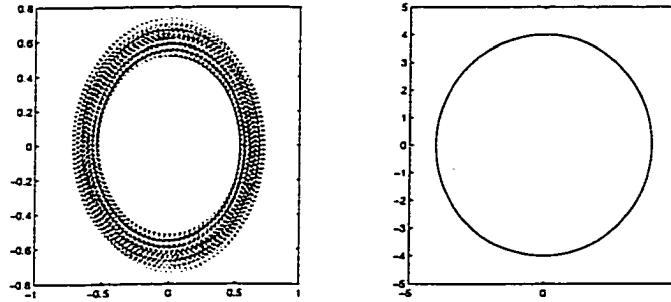


Figure 5.6: Strongly symmetric simulation for Example 2:  $x = 4$ . (Image vortices not shown)

The results for the strongly symmetric simulation are shown in Figures 5.6-5.8. For large  $x$  the motion is quasiperiodic, and is more periodic the larger  $x$  is. There is a critical value of  $x = x^* = 1.03$ , where the behavior changes. This is probably an equilibrium solution.

For the sake of completeness, we present the simulations for  $x < x^*$ . It is seen that the motion is again quasiperiodic except that the time-scale is smaller for both pairs of vortices.

The results for the weakly symmetric simulations are shown in Figures 5.9-5.10. It is seen that for large  $x$  ( $x \geq 4$ ), the motion is quasi-periodic, becoming more periodic the larger  $x$  is. However as  $x$  is decreased below  $x = 4$ , there is a transition in the behavior near a critical  $x^* = 3.48$ . This critical value of  $x$  is larger than that for the strongly symmetric case. This is, again, probably an equilibrium solution.

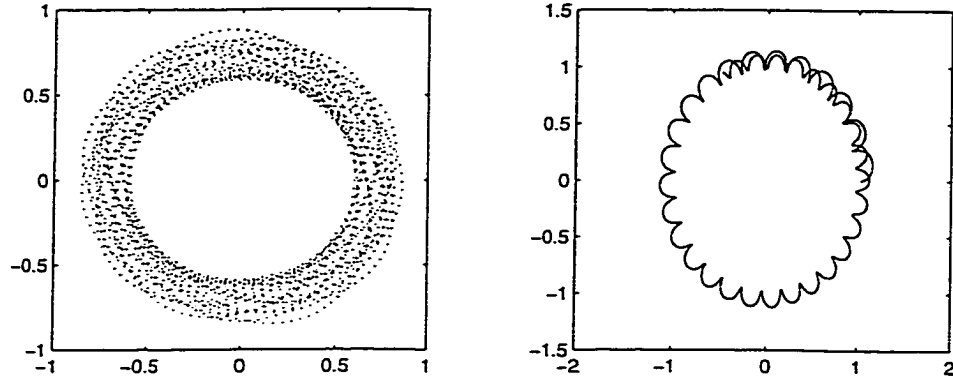


Figure 5.7: Strongly symmetric simulation for Example 2:  $x^* = 1.03$ . (Image vortices not shown)

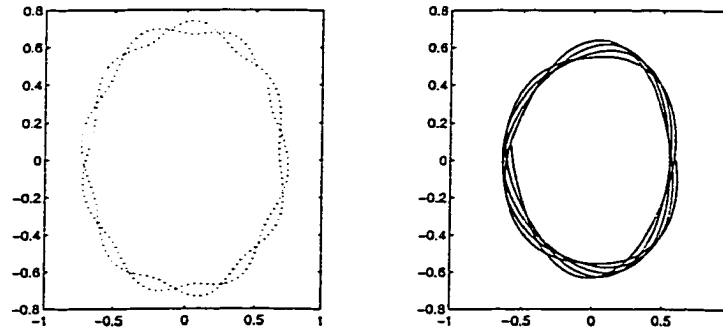


Figure 5.8: Strongly symmetric simulation for Example 2:  $x = 0.5$ . (Image vortices not shown)

### 5.2.2.3 Example 3: From (quasi-)periodic to scattering behavior

The third simulation we performed is the following:

- (i) For the strongly symmetric case the initial positions of the pair in the top layer are fixed at  $(\pm 1, 0)$  while the initial positions of the pair in the bottom layer are  $(\pm x, \pm x)$ , where  $x$  is allowed to vary.
- (ii) For the weakly symmetric case the initial position of one pair is fixed at  $(\pm 1, 0)$  and the other pair is located at  $(\pm x, \pm x_0)$  where  $x$  is allowed to vary.

For the strongly symmetric case for large  $x$  the motion is quasiperiodic as shown in Figure 5.11. However as  $x$  is decreased the motion changes at a critical value of about  $x = x^* = 2.1$  and becomes a scattering as shown in Figure 5.12. The results

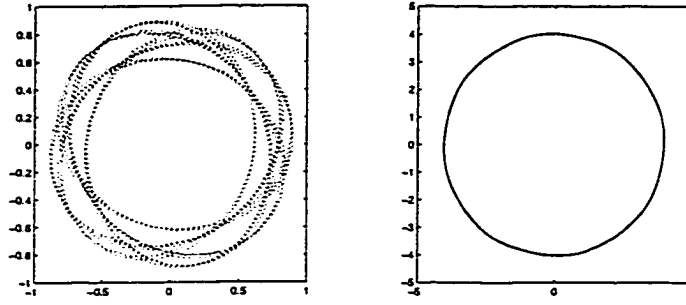


Figure 5.9: Weakly symmetric simulation for Example 2:  $x=4$ . (Image vortices not shown)

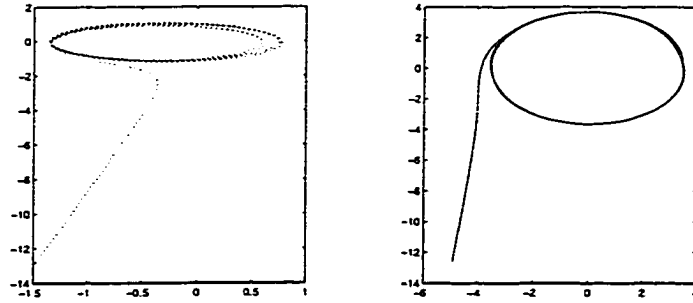


Figure 5.10: Weakly symmetric simulation for Example 2:  $x^* = 3.48$ . (Image vortices not shown)

for the weakly symmetric case are similar and are shown in Figures 5.13-5.14. The only important difference from the strongly symmetric case is that the critical value of  $x$  for which the behavior changes from quasiperiodic to scattering is  $x = x^* = 3$ .

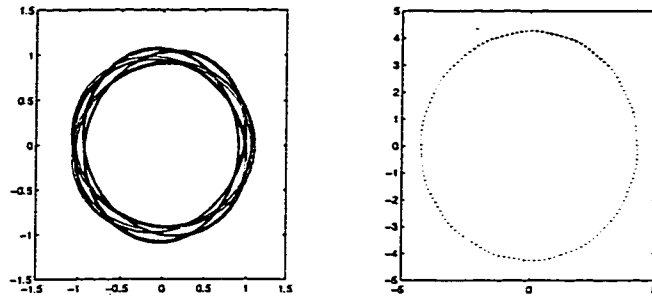


Figure 5.11: Strongly symmetric simulation for Example 3: quasiperiodic behavior,  $x = 3$ . (Image vortices not shown)

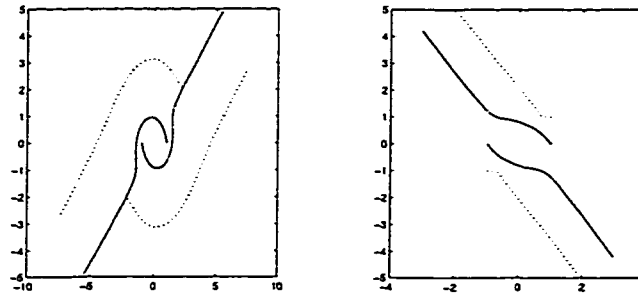


Figure 5.12: Strongly symmetric simulation for Example 3: scattering. (a)  $x = x^* = 2.1$ , (b)  $x = 1 < x^*$ .

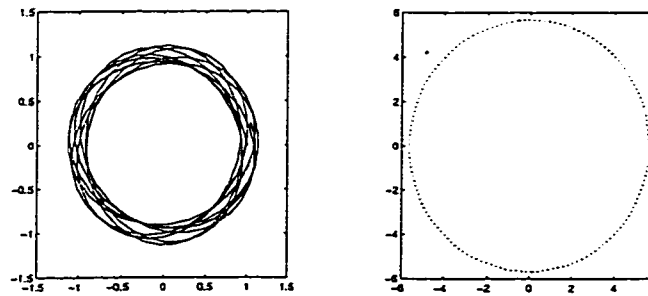


Figure 5.13: Weakly symmetric simulation for Example 3: quasiperiodic behavior,  $x = 4$ . (Image vortices not shown)



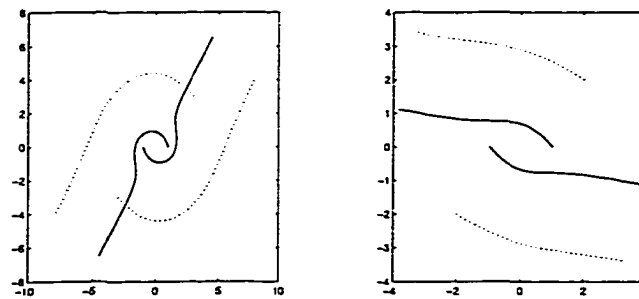


Figure 5.14: Weakly symmetric simulation for Example 3: scattering. (a)  $x = x^* = 3$ , (b)  $x = 2 < x^*$ .

## Chapter 6

### On the motion of point vortices on the sphere

In this chapter we present some results for integrable point-vortex motion on the sphere. Our point of departure is the work of Kidambi and Newton [31], where the Poisson-bracket formalism is carried out and all invariants are computed, as well as the derivation of the relative equations for  $N$  point vortices. In our first result we show that the only collapsing configurations for the three-vortex problem are self-similar or homogenous ones. We also conclude from this that the only self-similar solutions for the three-vortex problem are equilibria, and the collapsing solutions. We also study the simplest and most symmetrical four-vortex problem on the sphere that is analogous to that on the plane (for which self-similar collapse is possible) and show that on the sphere, however, these configurations do not admit self-similar collapse. Our study of the relative equations, also yields non-great-circle four vortex equilibria. We then present the explicit integration of some three-vortex configurations. Finally, we comment on the four-vortex integrable problem by pointing out new symmetrical configurations.

#### 6.1 Equations of motion and geometrical formulation

In vector form the system of  $N$  equations governing the motion of  $N$  vortices on the sphere of radius  $R$  is given by

$$\dot{\mathbf{x}}_i = \frac{1}{4\pi R} \sum_{j=1}^N \frac{\Gamma_j (\mathbf{x}_j \times \mathbf{x}_i)}{l_{ij}^2}. \quad (6.1)$$

$\mathbf{x}_i = (x_i, y_i, z_i)$  represents the vector from the center of the sphere to the  $i$ th vortex, with strength  $\Gamma_i$ , and  $'$  means the summation excludes  $j = i$ .

Although the cartesian representaion of the equations makes the analysis more transparent, one can also write the equations in spherical coordinates. The equation for the  $i$ th vortex is given by

$$\begin{aligned}\dot{\theta}_i &= -\frac{1}{4\pi R^2} \sum_{j=1}^N \frac{\Gamma_j \sin(\theta_j) \sin(\phi_i - \phi_j)}{1 - \cos(\gamma_{ij})}, \\ \sin(\theta_i) \dot{\phi}_i &= \frac{1}{4\pi R^2} \sum_{j=1}^N \frac{\Gamma_j (\sin(\theta_i) \cos(\theta_j) - \cos(\theta_i) \sin(\theta_j) \cos(\phi_i - \phi_j))}{1 - \cos(\gamma_{ij})},\end{aligned}$$

where  $\cos(\gamma_{ij}) := \cos(\theta_i) \cos(\theta_j) + \sin(\theta_i) \sin(\theta_j) \cos(\phi_i - \phi_j)$ . Derivations of these equations can be found in [7, 34].

The equations for the relative dynamics can be derived from the original system (6.1) and is done in [31]:

$$\frac{dl_{ij}^2}{dt} = \frac{1}{\pi R} \sum_{k=1}^N {}''\Gamma_k V_{ijk} \left[ \frac{1}{l_{jk}^2} - \frac{1}{l_{ki}^2} \right],$$

where the  $''$  means the summation excludes  $k = i$  and  $k = j$ .  $V$  is the volume of the parallelopiped formed by the vectors  $\mathbf{x}_i, \mathbf{x}_j, \mathbf{x}_k$ :

$$V = \mathbf{x}_i \cdot (\mathbf{x}_j \times \mathbf{x}_k).$$

Notice that the sign of  $V$  can be positive or negative depending on whether the vectors form a right- or left-handed coordinate. On the plane [2, 56] or in the geostrophic two-layer model, this is addressed by introducing  $\sigma_{ijk}$  which indicates the orientation of the triangle spanned by the three vortices.

## 6.2 On the collapse of three vortices on the sphere

We begin this chapter with a result about self-similar collapse for the three vortex problem on the sphere. In [31] Kidambi and Newton demonstrate self-similar collapsing solutions for the three vortex problem on the sphere, and in [33] they show that these solutions are not self-similar on the projective plane. We show that the

three vortex problem on the sphere as on the plane admits only collapsing states that are self-similar. Recall that on the sphere [31],  $C_1 = \sum_{i<j} \Gamma_i \Gamma_j l_{ij}^2$  is an invariant so that for collapse, since  $l_{ij} \rightarrow 0$ , it is necessary that  $C_1 = 0$ . The proof that only self-similar collapse is possible is based on the other assertion that the harmonic mean of the vortices vanishes,  $h = \sum_i \frac{1}{\Gamma_i} = 0$ .

**Theorem 6.1** *The only finite-time collapsing configurations of the three vortex problem on the sphere are self-similar ones.*

**Proof.** We make use of the following invariants:

$$C_1 = \sum_{i<j} \Gamma_i \Gamma_j l_{ij}^2 = 0, \quad (6.2)$$

$$H = \sum_{i<j} \Gamma_i \Gamma_j \ln l_{ij}^2, \quad (6.3)$$

and the fact that necessarily  $h = \sum_i \frac{1}{\Gamma_i} = 0$ . Note that (6.3) can be written as :

$$(l_{12}^2)^{\Gamma_1 \Gamma_2} (l_{13}^2)^{\Gamma_1 \Gamma_3} (l_{23}^2)^{\Gamma_2 \Gamma_3} = \text{constant}. \quad (6.4)$$

Making the self-similar ansatz, we may, without loss of generality, assume (since  $l_{ij}(t) > 0$ ) that:

$$\begin{aligned} l_{12}(t)^2 &= \alpha(t) l_{13}(t), \\ l_{23}(t)^2 &= \beta(t) l_{13}(t), \end{aligned} \quad (6.5)$$

for  $\alpha(t), \beta(t) > 0$ . Substituting (6.5) into (6.4) yields:

$$[l_{13}(t)^2]^{\Gamma_1 \Gamma_2 + \Gamma_1 \Gamma_3 + \Gamma_2 \Gamma_3} [\alpha(t)^2]^{\Gamma_1 \Gamma_2} [\beta(t)^2]^{\Gamma_2 \Gamma_3} = \text{constant}.$$

Now since  $h = 0$ , conclude that  $[l_{13}(t)^2]^{\Gamma_1 \Gamma_2 + \Gamma_1 \Gamma_3 + \Gamma_2 \Gamma_3} [\alpha(t)^2]^{\Gamma_1 \Gamma_2} = \text{constant}$ . This implies that  $[\alpha(t)^2]^{\Gamma_1 \Gamma_2} [\beta(t)^2]^{\Gamma_2 \Gamma_3} = \text{constant}$ . Hence write:

$$\alpha^2 = \frac{C}{[\beta^2]^{\Gamma_3/\Gamma_1}}. \quad (6.6)$$

Also substituting (6.5) in (6.2) gives

$$l_{13}(t)^2[\Gamma_1\Gamma_3 + \Gamma_1\Gamma_2\alpha^2 + \Gamma_2\Gamma_3\beta^2] = 0.$$

But  $l_{13}(t)^2 > 0$ , on the route to collapse, so that:

$$\Gamma_1\Gamma_3 + \Gamma_1\Gamma_2\alpha^2 + \Gamma_2\Gamma_3\beta^2 = 0. \quad (6.7)$$

Substituting (6.7) in (6.6) yields:

$$\Gamma_1\Gamma_3 + \frac{\Gamma_1\Gamma_2C}{[\beta^2]^{\Gamma_3/\Gamma_1}} + \Gamma_2\Gamma_3\beta^2 = 0.$$

Denoting  $x := \beta^2$ , this is an algebraic equation of the form  $Ax^a + Bx^b = C$ , which has only finitely many solutions in  $x$  for fixed  $A, B, a, b, C \in \mathbf{R}$ . We conclude that since  $x = \beta(t)^2$  is both continuous and assumes only finitely many values, that it must therefore be constant. But  $\alpha(t)$ , and  $\beta(t)$  constant corresponds to the case of self-similar collapse.  $\square$

It now remains to show that  $h = \sum_i \frac{1}{\Gamma_i} = 0$  is necessary for a collapsing configuration of the three vortex problem on the sphere.

**Lemma 6.2** *On the sphere, as on the plane,  $h = \sum_i \frac{1}{\Gamma_i} = 0$  is necessary for any collapsing configuration of the three vortex problem.*

**Proof.** We shall make extensive use of the trilinear plane. Recall that for collapse it is necessary that:

$$C_1 = \Gamma_1\Gamma_2l_{12}^2 + \Gamma_1\Gamma_3l_{13}^2 + \Gamma_2\Gamma_3l_{23}^2 = 0,$$

or  $b_1 + b_2 + b_3 = 0$  where

$$b_1 := \frac{l_{23}^2}{4\Gamma_1R^2} \quad b_2 := \frac{l_{13}^2}{4\Gamma_2R^2} \quad b_3 := \frac{l_{12}^2}{4\Gamma_3R^2},$$

and without loss of generality  $\Gamma_1, \Gamma_2 > 0$  and  $\Gamma_3 < 0$ . The phase curves,  $H = \text{constant}$ , then become

$$b_1^{\frac{1}{\Gamma_1}} b_1^{\frac{1}{\Gamma_2}} (b_1 + b_2)^{\frac{1}{\Gamma_3}} = \text{constant}. \quad (6.8)$$

Now the point of collapse in the  $b_1$ - $b_2$  plane is the origin  $O$ . Notice also that  $b_1 > 0$ ,  $b_2 > 0$  because  $\Gamma_1, \Gamma_2 > 0$ . We consider first the case  $h > 0$ , for which:

$$\frac{1}{\Gamma_1} + \frac{1}{\Gamma_2} > -\frac{1}{\Gamma_3}. \quad (6.9)$$

Let  $b_1 \rightarrow 0$ ,  $b_2 \rightarrow 0$  ( $b_1 > 0, b_2 > 0$ ), then (6.9) implies that  $b_1^{\frac{1}{\Gamma_1}} b_2^{\frac{1}{\Gamma_2}}$  is of smaller order than  $(b_1 + b_2)^{\frac{1}{\Gamma_3}}$ . Hence for  $h > 0$ , it is inconsistent that as  $b_1 \rightarrow 0, b_2 \rightarrow 0$ , that,

$$b_1^{\frac{1}{\Gamma_1}} b_2^{\frac{1}{\Gamma_2}} (b_1 + b_2)^{\frac{1}{\Gamma_3}},$$

remain invariant. We next consider the case  $h < 0$ . To this end we examine the proof for the three-vortex problem on the plane, for  $h < 0$ . We first show that  $h < 0$  on the plane implies that the physical region is a wedge with apex at the origin  $O$ , lying entirely in the first quadrant of the  $b_1$ - $b_2$  plane. Now on the plane, as on the sphere, for collapse,  $C_1 = \sum_{i < j} \Gamma_i \Gamma_j l_{ij}^2 = 0$ , and introducing the trilinear variables:

$$b_1 := \frac{l_{23}^2}{\Gamma_1} \quad b_2 := \frac{l_{13}^2}{\Gamma_2} \quad b_3 := \frac{l_{12}^2}{\Gamma_3},$$

yields  $b_1 + b_2 + b_3 = 0$ .

Now the physical region boundary is given by:

$$(\Gamma_1 b_1)^2 + (\Gamma_2 b_2)^2 + (\Gamma_3 b_3)^2 = 2(\Gamma_1 \Gamma_2 b_1 b_2 + \Gamma_2 \Gamma_3 b_2 b_3 + \Gamma_1 \Gamma_3 b_1 b_3). \quad (6.10)$$

Substituting for  $b_3$  using the invariant  $C_1 = 0$  in (6.10) results in an equation homogenous in  $b_1$  and  $b_2$ , so that the conic section it describes is degenerate. Thus we may substitute  $b_2 = m b_1$  to get the following relation for  $m$ :

$$\Gamma_1^2 + m^2 \Gamma_2^2 + \Gamma_3^2 (1 + m)^2 = 2[\Gamma_1 \Gamma_2 m - \Gamma_2 \Gamma_3 m(1 + m) - \Gamma_1 \Gamma_3 (m + 1)]. \quad (6.11)$$

After a little algebra we obtain:

$$(\Gamma_2 + \Gamma_3)^2 m^2 + 2[\Gamma_3(\Gamma_3 + \Gamma_2) + \Gamma_1(\Gamma_3 - \Gamma_2)]m + (\Gamma_1 + \Gamma_3)^2 = 0. \quad (6.12)$$

Observe that for the case  $h < 0$ , that both,  $(\Gamma_2 + \Gamma_3) > 0$  and  $(\Gamma_1 + \Gamma_3) > 0$ , as follows from the fact that  $\Gamma_1 > 0, \Gamma_2 > 0, \Gamma_3 < 0$  and:

$$h = \frac{1}{\Gamma_1} + \frac{1}{\Gamma_2} + \frac{1}{\Gamma_3} < 0.$$

Rewriting (6.12) gives  $am^2 + bm + c = 0$  where:

$$\begin{aligned} a &= (\Gamma_2 + \Gamma_3)^2 > 0, \\ b &= 2[\Gamma_3(\Gamma_3 + \Gamma_2) + \Gamma_1(\Gamma_3 - \Gamma_2)] < 0, \\ c &= (\Gamma_3 + \Gamma_1)^2 > 0. \end{aligned}$$

Hence

$$m_{1,2} = \frac{-b \pm \sqrt{b^2 - 4ac}}{2a},$$

from which it is clear that  $m_{1,2} > 0$  and that the physical region is a wedge in the first quadrant with apex at the origin,  $O$ . We now consider the physical region for the three-vortex problem on the sphere of radius  $R$ . We will need the formula for the volume of the parallelopiped formed by the three vortices on the sphere:

$$V^2 = \frac{1}{4}(16R^2 A^2 - l_{12}^2 l_{13}^2 l_{23}^2),$$

where  $A$  is the area of the triangle formed by the three vortices and using Heron's formula this is given by:

$$A = \pm \frac{1}{4}(2l_{12}^2 l_{23}^2 + 2l_{31}^2 l_{23}^2 + 2l_{12}^2 l_{13}^2 - l_{12}^4 - l_{23}^4 - l_{13}^4)^{1/2}.$$

Since  $C_1 = \sum_{i < j} \Gamma_i \Gamma_j l_{ij}^2 = 0$  we may introduce the trilinear coordinates:

$$b_1 = \frac{l_{23}^2}{4\Gamma_1 R^2} \quad b_2 = \frac{l_{31}^2}{4\Gamma_2 R^2} \quad b_3 = \frac{l_{12}^2}{4\Gamma_3 R^2}.$$

Using these coordinates the equation for the physical region boundary  $V = 0$  then becomes :

$$2(\Gamma_1 \Gamma_3 b_1 b_3 + \Gamma_1 \Gamma_2 b_1 b_2 + \Gamma_2 \Gamma_3 b_2 b_3) =$$

$$(\Gamma_1 b_1)^2 + (\Gamma_2 b_2)^2 + (\Gamma_3 b_3)^2 + 4\Gamma_1 \Gamma_2 \Gamma_3 b_1 b_2 b_3. \quad (6.13)$$

Note that this differs from (6.10) only in the second term on the right-hand side;  $4\Gamma_1 \Gamma_2 \Gamma_3 b_1 b_2 b_3$ . For  $C_1 = 0$  this term becomes  $-4\Gamma_1 \Gamma_2 \Gamma_3 b_1 b_2 (b_1 + b_2)$ . Consider the physical region boundary (6.13) near the origin,  $O$ , of the  $b_1$ - $b_2$  plane, and realize that the term  $-4\Gamma_1 \Gamma_2 \Gamma_3 b_1 b_2 (b_1 + b_2)$ , is of smaller order than terms of the form  $b_i b_j$  for  $0 < b_1 \ll 1$  and  $0 < b_2 \ll 1$ . In other words the physical region boundary at the origin  $O$ , for the three vortex problem on the plane (for  $h < 0$ ,  $C_1 = 0$ ) is asymptotic to the physical region boundary for the three-vortex problem on the sphere (for  $h < 0$ ,  $C_1 = 0$ ). This completes the case  $h < 0$  and the proof.  $\square$

In summary  $h = \sum \frac{1}{\Gamma_i} = 0$ , is necessary for any collapsing configuration on the sphere, because although the physical region boundary  $V = 0$ , passes through the origin, the phase curves either do not pass the origin ( $h > 0$ ) or they are intercepted by the  $V = 0$  curve before they can reach the origin ( $h < 0$ ). Typical phase curves for these cases are shown in Fig. 6.1(a) ( $\Gamma_1 = \Gamma_2 = -\Gamma_3$  ( $h > 0$ )) and Fig. 6.1(b) ( $\Gamma_1 = \Gamma_2 = 1$   $\Gamma_3 = \frac{1}{4}$  ( $h < 0$ )). Physically, this result can be explained by the fact that the scales near collapse for the three-vortex problem on the sphere are asymptotically those for three-vortex collapse on the plane. This means that the spherical geometry near collapse is asymptotic in some sense to the planar case. A more formal and rigorous discussion can be found in [31].

By making use of the invariants  $C_1$  and

$$C_2 = (l_{12}^2)^{\Gamma_1 \Gamma_2} (l_{13}^2)^{\Gamma_1 \Gamma_3} (l_{23}^2)^{\Gamma_2 \Gamma_3},$$

we arrive at the following simple corollary.

**Corollary 6.3** *The only self-similar solutions of the three-vortex problem on the sphere are equilibrium solutions or collapsing solutions.*

**Proof:** Making the self-similar ansatz (6.5), the invariance of  $C_2$  :

$$C_2 = (l_{13}^2)^{\sum \Gamma_i \Gamma_j} \alpha^{\Gamma_1 \Gamma_2} \beta^{\Gamma_2 \Gamma_3},$$



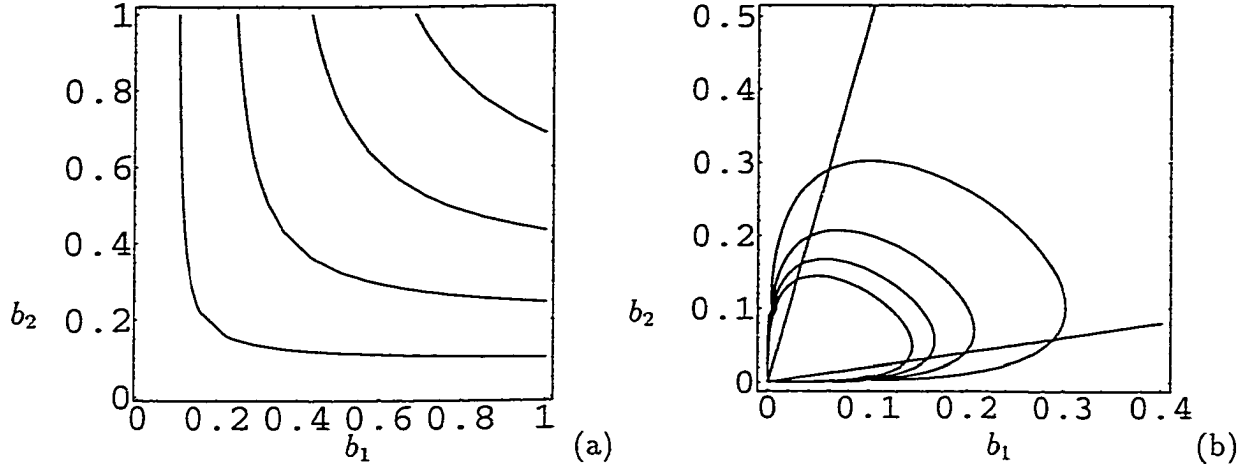


Figure 6.1: Phase diagram for  $C_1 = 0$ : (a)  $\Gamma_1 = \Gamma_2 = -\Gamma_3 = 1$  ( $h > 0$ ), phase curves are open and do not pass through the origin; (b)  $\Gamma_1 = \Gamma_2 = 1$   $\Gamma_3 = -\frac{1}{4}$  ( $h < 0$ ) phase curves are closed through the origin but are intercepted by  $V = 0$  before reaching it.

implies that either  $\sum \Gamma_i \Gamma_j = 0$  or  $l_{13}^2$  is constant. The latter corresponds to an equilibrium solution. For the case  $\sum \Gamma_i \Gamma_j = 0$ , we obtain:

$$C_1 = \sum_{i < j} \Gamma_i \Gamma_j l_{ij}^2 = l_{13}^2 (\Gamma_1 \Gamma_2 \alpha + \Gamma_3 \Gamma_2 \beta + \Gamma_1 \Gamma_3)$$

Now the invariance of  $C_1$  implies that either  $l_{13}^2$  is constant (an equilibrium solution) or  $\Gamma_1 \Gamma_2 \alpha + \Gamma_3 \Gamma_2 \beta + \Gamma_1 \Gamma_3 = 0$ . In summary, assuming a non-equilibrium solution, the self-similar ansatz leads to :

- i)  $h = 0$
- ii)  $C_1 = 0$
- iii) a non-equilibrium solution

Kidambi and Newton [33] show that these are necessary and sufficient conditions for self-similar collapse of three vortices on the sphere. This together with Proposition 6.1 proves the corollary.  $\square$

We continue this section by investigating the existence of self-similar collapsing configurations for four point vortices on the sphere. Novikov [49] demonstrates particular symmetrical four- and five-vortex collapsing configurations on the plane. We investigate the analogs of these on the sphere. Begin with the relative equations.

Self-similar solutions preserve the orientations of the vortex configurations, so that without loss of generality we may consider the relative equations in the following “frozen” form where  $V_{ijk} > 0$ :

$$\frac{dl_{12}^2}{dt} = \Gamma_3 V_{123} \left[ \frac{1}{l_{23}^2} - \frac{1}{l_{13}^2} \right] + \Gamma_4 V_{124} \left[ \frac{1}{l_{24}^2} - \frac{1}{l_{14}^2} \right], \quad (6.14)$$

$$\frac{dl_{23}^2}{dt} = \Gamma_1 V_{123} \left[ \frac{1}{l_{13}^2} - \frac{1}{l_{12}^2} \right] + \Gamma_4 V_{234} \left[ \frac{1}{l_{34}^2} - \frac{1}{l_{24}^2} \right], \quad (6.15)$$

$$\frac{dl_{13}^2}{dt} = \Gamma_2 V_{123} \left[ \frac{1}{l_{12}^2} - \frac{1}{l_{23}^2} \right] + \Gamma_4 V_{134} \left[ \frac{1}{l_{34}^2} - \frac{1}{l_{14}^2} \right], \quad (6.16)$$

$$\frac{dl_{14}^2}{dt} = \Gamma_2 V_{124} \left[ \frac{1}{l_{12}^2} - \frac{1}{l_{24}^2} \right] + \Gamma_3 V_{134} \left[ \frac{1}{l_{13}^2} - \frac{1}{l_{34}^2} \right], \quad (6.17)$$

$$\frac{dl_{24}^2}{dt} = \Gamma_1 V_{124} \left[ \frac{1}{l_{14}^2} - \frac{1}{l_{12}^2} \right] + \Gamma_3 V_{123} \left[ \frac{1}{l_{23}^2} - \frac{1}{l_{34}^2} \right], \quad (6.18)$$

$$\frac{dl_{34}^2}{dt} = \Gamma_2 V_{234} \left[ \frac{1}{l_{24}^2} - \frac{1}{l_{23}^2} \right] + \Gamma_1 V_{134} \left[ \frac{1}{l_{14}^2} - \frac{1}{l_{13}^2} \right]. \quad (6.19)$$

Here the volumes of the parallelopipeds formed by  $\mathbf{x}_i$ ,  $\mathbf{x}_j$ ,  $\mathbf{x}_k$  is given by:

$$V_{ijk} = \pm(16R^2 A_{ijk} - l_{ij}^2 l_{kj}^2 l_{ik}^2),$$

and  $A_{ijk}$  is the area of the triangle formed by  $\mathbf{x}_i$ ,  $\mathbf{x}_j$ ,  $\mathbf{x}_k$  and is given by

$$A_{ijk} = \pm(2l_{ij}^2 l_{ik}^2 + 2l_{ij}^2 l_{kj}^2 + 2l_{ik}^2 l_{jk}^2 - l_{ij}^4 - l_{kj}^4 - l_{ik}^4)^{\frac{1}{2}}.$$

Now, symmetrical configurations which will greatly simplify these equations are those for which  $l_{12} = l_{34}$ , and  $l_{23} = l_{14}$ , so that  $V_{124} = V_{234}$ , and  $V_{123} = V_{134}$ . These are “paralleloid” configurations on the sphere analogous to the parallelogram ones considered on the plane by Novikov [49] and shown in Figure 6.2.

Under these assumptions it is clear by inspection of the relative equations (6.14-6.19) that the most symmetrical configurations ensuring both:

$$\frac{dl_{12}^2}{dt} = \frac{dl_{34}^2}{dt} \quad \frac{dl_{13}^2}{dt} = \frac{dl_{14}^2}{dt},$$

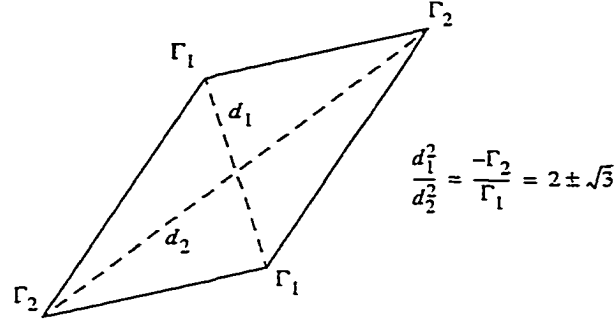


Figure 6.2: Four-vortex collapsing systems on the plane.

are those for which  $\Gamma_1 = \Gamma_3$  and  $\Gamma_2 = \Gamma_4$ , which is exactly the vortex allocation that Novikov makes. We then have the following negative result.

**Theorem 6.4** *On the sphere there are no finite-time collapsing configurations for which  $l_{12} = l_{34}$ ,  $l_{23} = l_{14}$  with  $\Gamma_1 = \Gamma_3$ ,  $\Gamma_2 = \Gamma_4$ .*

**Proof:** Begin by making the self-similar ansatz, namely,

$$\begin{aligned} l_{12}^2 &= \lambda_1 l_{13}^2, \\ l_{23}^2 &= \lambda_2 l_{13}^2, \\ l_{24}^2 &= \lambda_3 l_{13}^2, \end{aligned}$$

where  $\lambda_i > 0$ ,  $i = 1, \dots, 3$ . With these the relative equations simplify to:

$$\frac{dl_{13}^2}{dt} = \frac{2\Gamma_2 V_{123}}{l_{13}^2} \left[ \frac{1}{\lambda_1} - \frac{1}{\lambda_2} \right], \quad (6.20)$$

$$\frac{dl_{24}^2}{dt} = \frac{-2\Gamma_1 V_{124}}{l_{13}^2} \left[ \frac{1}{\lambda_1} - \frac{1}{\lambda_2} \right], \quad (6.21)$$

$$\frac{dl_{12}^2}{dt} = \frac{\Gamma_1 V_{123}}{l_{13}^2} \left[ \frac{1}{\lambda_2} - 1 \right] + \frac{\Gamma_2 V_{124}}{l_{13}^2} \left[ \frac{1}{\lambda_3} - \frac{1}{\lambda_2} \right], \quad (6.22)$$

$$\frac{dl_{23}^2}{dt} = \frac{\Gamma_1 V_{123}}{l_{13}^2} \left[ \frac{1}{1 - \lambda_1} \right] + \frac{\Gamma_2 V_{234}}{l_{13}^2} \left[ \frac{1}{\lambda_1} - \frac{1}{\lambda_3} \right]. \quad (6.23)$$

Comparing (6.20) and (6.21) self-similarity dictates that for all times:

$$\frac{-\Gamma_1 V_{124}}{\lambda_3} = \Gamma_2 V_{123}.$$

Using the formula for the volumes of the parallelopipeds this is equivalent to:

$$\begin{aligned}\lambda_1 \lambda_2 \lambda_3 &= \left(\frac{\Gamma_2}{\Gamma_1}\right)^2 \lambda_3^2 \lambda_1 \lambda_2, \\ \lambda_3(2\lambda_1 \lambda_2 + 2\lambda_1 + 2\lambda_2 - \lambda_1^2 - \lambda_2^2 - 1) &= 2\lambda_1 \lambda_2 + 2\lambda_1 \lambda_3 + 2\lambda_3 \lambda_2 - \lambda_1^2 - \lambda_2^2 - \lambda_3^2.\end{aligned}$$

Henceforth, and, without loss of generality, we assume that the radius of the sphere  $R = 1$ . After some cancelations these last equations become, for  $\lambda_3 \neq 1$ ,

$$\begin{aligned}\lambda_1^2 + \lambda_2^2 - 2\lambda_1 \lambda_2 - \lambda_3 &= 0, \\ V_{124} &= \frac{-\Gamma_1 V_{123}}{\Gamma_2},\end{aligned}$$

from which, incidentally,  $\Gamma_1$  and  $\Gamma_2$  must be of opposite sign. Further simplification leads to:

$$\frac{dl_{12}^2}{dt} = \frac{\Gamma_1 V_{123}}{l_{13}^2} \left[ \frac{2}{\lambda_2} - \left(1 + \frac{1}{\lambda_3}\right) \right].$$

Comparing this with  $\frac{dl_{13}^2}{dt}$  we see that  $2\Gamma_2(\lambda_2 - \lambda_1) = \Gamma_1[2 - \lambda_2(1 + \frac{1}{\lambda_3})]$ . The self-similar assumption together with the invariance of the Hamiltonian (6.3) imply that the harmonic mean of the vortex strengths vanishes, that is  $\sum \Gamma_i \Gamma_j = 0$ . We summarize all of these constraints:

- (i)  $\Gamma_1^2 + 4\Gamma_1 \Gamma_2 + \Gamma_2^2 = 0$  or  $\frac{\Gamma_1}{\Gamma_2} = -2 \pm \sqrt{3}$ ,
- (ii)  $\lambda_3 = \left(\frac{\Gamma_1}{\Gamma_2}\right)^2 = (-2 \pm \sqrt{3})^2$ ,
- (iii)  $\lambda_1^2 + \lambda_2^2 - 2\lambda_1 \lambda_2 - \lambda_3 = 0$  (for  $\lambda_3 \neq 1$ ),
- (iv)  $2\Gamma_2(\lambda_2 - \lambda_1) = \Gamma_1[2 - \lambda_2(1 + \frac{1}{\lambda_3})]$ .

A solution of (i)-(iv) will yield a self-similar collapsing configuration. The case  $\lambda_3 = 1$  is clearly not possible by (ii). For the case  $\lambda_3 \neq 1$  we solve the quadratic, (iii), for  $\lambda_2$  to obtain  $\lambda_2 = \lambda_1 \pm \sqrt{\lambda_3}$ . Substituting in (iv), using  $\frac{\Gamma_1}{\Gamma_2} = -2 \pm \sqrt{3}$  gives

$2\frac{\Gamma_2}{\Gamma_1}(\lambda_2 - \lambda_1) = 2 - \lambda_2(1 + \frac{1}{\lambda_3})$  or  $2(-2 \pm \sqrt{3})(\pm\sqrt{\lambda_3}) = 2 - \lambda_2(1 + \frac{1}{\lambda_3})$ . Rearranging we get:

$$\lambda_2 = \frac{2 - 2(-2 \pm \sqrt{3})(\mp\sqrt{\lambda_3})}{1 + \frac{1}{\lambda_3}}.$$

It is easily verified that for  $\lambda_3 = (-2 \pm \sqrt{3})^2$ , that this last is zero, violating the self-similar assumption that  $\lambda_i > 0$ . We conclude that self-similar solutions for the 4-vortex problem of this kind do not exist on the sphere.  $\square$

**Remark:** This illustrates another difference between vortex dynamics on the sphere and the plane. We remark that obtaining self-similar solutions for more than three vortices on the sphere is particularly difficult in view of the volume terms  $V_{ijk}$  that appear in the relative equations. Observe that on the plane all the terms in the area formula  $A_{ijk}$  are of the same order (namely quadratic) so that under the self-similar ansatz these area terms become, for instance  $A_{ijk} = C(\lambda)l_{13}^2$ , with the  $l_{13}^2$  term cancelling with terms of the form  $[\frac{1}{l_{12}^2} - \frac{1}{l_{13}^2}]$  to give  $\frac{dl_{13}^2}{dt} = \tilde{C}_{13}(\lambda)$ , which is readily integrated. Naturally a system of algebraic equations must be solved to ensure compatibility of these constants. On the sphere however the  $V_{ijk}$  contains a term of the form  $R^2 A_{ijk}$  which involves quadratic terms of the form  $l_{ij}^2 l_{jk}^2$ , as well as the cubic terms  $l_{ij}^2 l_{ik}^2 l_{jk}^2$ . Under the self-similar ansatz we obtain terms of the form  $\omega_i \sqrt{1 - \beta_i l_{13}^2}$  in the vector field for  $l_{13}^2$ . In the case of three vortices the differential equation for  $l_{13}^2$  is:

$$\frac{dl_{13}^2}{dt} = \pm \omega_i(\lambda) \sqrt{1 - \beta l_{13}^2},$$

which again is readily integrated. The system of algebraic equations needed to ensure compatibility of the self-similar assumption involves the  $\omega_i$ . For the four-vortex problem, the vector field becomes:

$$\frac{dl_{13}^2}{dt} = \omega_1^1(\lambda) \sqrt{1 - \beta_1^1(\lambda) l_{13}^2} + \omega_2^1(\lambda) \sqrt{1 - \beta_2^1(\lambda) l_{13}^2},$$

so that the compatibility equations now involve  $\omega_i^j$  and  $\beta_k^j$  which is a more complicated system of algebraic equations and in any case the differential equation for  $l_{13}^2$  is difficult to solve by quadrature.

We conclude our discussion of vortex collapse on the sphere with the following observation. If the center of vorticity of four vortices is  $c=0$ , then the four vortex problem is integrable [31]. This means that this integrable problem does not admit simultaneous collapse, self-similar or otherwise, since necessarily the vortices collapse at the center of vorticity. This is clearly not possible on the sphere if  $c=0$ .

## 6.3 Further solutions of integrable point vortex dynamics on the sphere

### 6.3.1 Non-great-circle four-vortex relative equilibria

From the relative equations (6.14-6.19) it is evident that  $l_{12} = l_{13} = \dots = l_{24}$ , is a relative equilibrium solution (independent of the vortex strengths). Clearly on the plane such a configuration is not possible. On the sphere however it corresponds to a tetrahedron. Observe that for a given sphere of radius  $R$  a tetrahedron of edge length  $\sqrt{3}R$  can be inscribed in it. It is also easy to show that another non-great-circle relative equilibrium admitted on the sphere is the four-vortex configuration shown in Fig. 6.3. It would be interesting to study the non-linear stability properties of these equilibria. Another open problem is the study of relative equilibria for the general  $N$ -vortex problem on the sphere. Such a study would, perhaps, entail the use of a symmetry group analysis.

### 6.3.2 Explicit integration of three-vortex configurations on the sphere

In this section we explicitly perform the quadrature of some symmetrical three-vortex problems on the sphere.

#### 6.3.2.1 Example 1

We begin by considering the case:

$$C_1 = \sum \Gamma_i \Gamma_j l_{ij}^2 = 3R^2, \quad \Gamma_1 = \Gamma_2 = \Gamma_3 = 1.$$

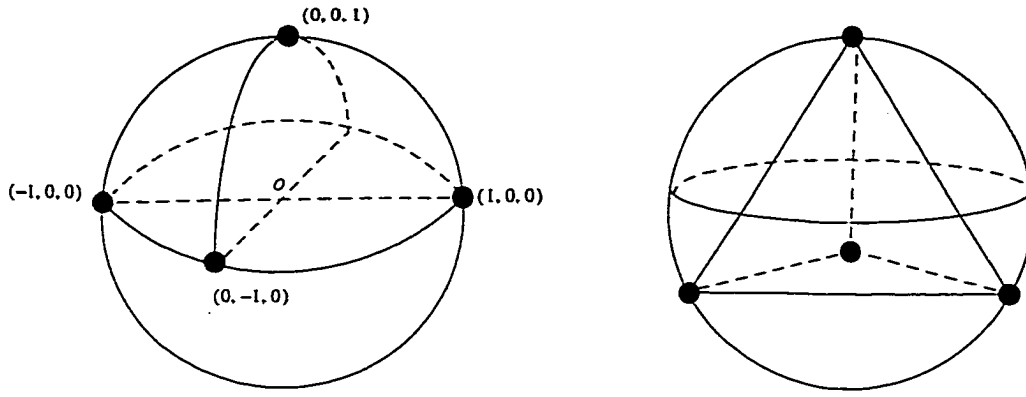


Figure 6.3: Non-great-circle 4-vortex relative equilibria. (a)  $l_{12} = l_{13} = l_{14} = l_{23} = l_{24}$  where  $\Gamma_1$  is at  $(0, 0, 1)$ ,  $\Gamma_2$  is at  $(0, -1, 0)$  and  $\Gamma_3$  and  $\Gamma_4$  are at  $(-1, 0, 0)$  and  $(1, 0, 0)$ , (b) A tetrahedral configuration.

Making use of the trilinear coordinates,

$$l_{12}^2 = b_3 R^2 \quad l_{13}^2 = b_2 R^2 \quad l_{23}^2 = b_1 R^2,$$

the Hamiltonian takes the form,

$$l_{12}^2 l_{13}^2 l_{23}^2 = \mu R^6 \text{ or } b_1 b_2 b_3 = \mu,$$

from which using Cartesian coordinates,

$$\begin{aligned} b_1 &= y, \\ b_2 &= \frac{1}{2}(3 - y - \sqrt{3}x), \\ b_3 &= \frac{1}{2}(3 - y + \sqrt{3}x), \end{aligned}$$

we obtain,

$$x = \pm \sqrt{\frac{(3 - y)^2}{3} - \frac{4\mu}{3y}}.$$

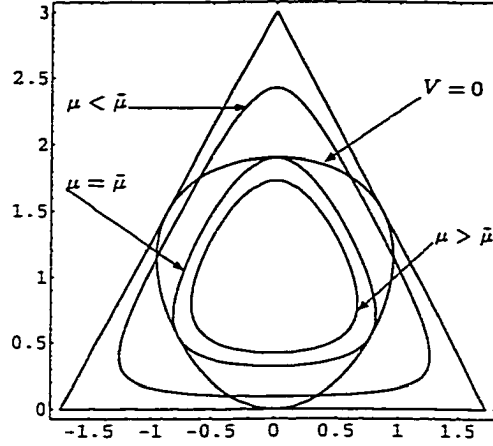


Figure 6.4: Phase curves for  $\Gamma_1 = \Gamma_2 = \Gamma_3 = 1$  and  $C_1 = 3R^2$ , showing a family of periodic solutions ( $\mu < \tilde{\mu}$ ), a saddle connection, where the phase plane and the physical region boundary  $V = 0$  are tangential ( $\mu = \tilde{\mu}$ ), which we explicitly integrate, and a family of solutions where the physical region boundary is reached, ( $\mu > \tilde{\mu}$ ) transversally.

Substituting into the relative equations, and making use of the parameter  $\mu$ , we obtain after further simplification,

$$\begin{aligned} \frac{dy}{dt} = \frac{db_1}{dt} = \frac{1}{R^2} \frac{dl_{23}^2}{dt} &= \frac{V}{\pi R^3} \left[ \frac{1}{l_{13}^2} - \frac{1}{l_{12}^2} \right] \\ &= \pm \frac{V}{\pi R^3} \sqrt{y(y(3-y)^2 - 4\mu)}. \end{aligned}$$

Similarly the volume  $V$  of the parallelopiped can be simplified to,

$$V^2 = \frac{R^6}{4} \left[ 12y - 4y^2 + \frac{4\mu}{y} - \mu - 9 \right].$$

With this the vector field for  $y$  is given by:

$$\frac{dy}{dt} = \pm \frac{1}{2\pi R^2} \sqrt{12y^2 - 4y^3 + 4\mu - \mu y - 9y} \sqrt{y(3-y)^2 - 4\mu}.$$

We integrate this for the saddle connection shown in Fig. (6.4) where  $\tilde{\mu} = 3(-39 + 4\sqrt{96})$ . By solving for  $V = 0$ , (the phase curve for the saddle connection is tangent



to the  $V = 0$  curve), in terms of  $y$ , it can be shown, with a little algebra, that the dynamics on the saddle connection are governed by the differential equation:

$$\frac{dy}{dt} = \pm \frac{1}{\pi R^2} (y - y_1)(y - y_2) \sqrt{-(y - \alpha)(y - \beta)}, \quad (6.24)$$

where

$$\begin{aligned} y_1 &= \frac{-6 + \sqrt{96}}{2}, & y_2 &= \frac{1}{2} \left[ 3 - \frac{-6 + \sqrt{96}}{2} \right], \\ \mu &= 3(-39 + 4\sqrt{96}), \\ \alpha, \beta &= \frac{6 - y_1 \pm \sqrt{15\sqrt{96} - 135}}{2}. \end{aligned}$$

The sign is determined according to which side of the phase plane is under consideration. Eq. (6.24) can be integrated by a separation of variables and several trigonometric substitutions to obtain a parametrization of the saddle connection for different initial conditions. For instance, if we take the positive sign in (6.24) then the orbit is given by:

$$A(t - t_0) = \frac{a_2}{\theta_1 + 1} \ln \left| \frac{\tan(\frac{\theta}{2}) - a_1}{\tan(\frac{\theta}{2}) + a_1} \right| - \frac{a_1}{\theta_2 + 1} \ln \left| \frac{\tan(\frac{\theta}{2}) - a_2}{\tan(\frac{\theta}{2}) + a_2} \right|,$$

or upon rearranging,

$$e^{A(t-t_0)} = \frac{\left| \frac{\tan(\frac{\theta}{2}) - a_1}{\tan(\frac{\theta}{2}) + a_1} \right|^{\frac{a_2}{\theta_1 + 1}}}{\left| \frac{\tan(\frac{\theta}{2}) - a_2}{\tan(\frac{\theta}{2}) + a_2} \right|^{\frac{a_1}{\theta_2 + 1}}},$$

where,

$$\begin{aligned} A &:= \frac{(y_1 - y_2)a_1a_2(\alpha - \beta)}{2\pi R^2}, \\ a_i^2 &:= \frac{1 - \theta_i}{1 + \theta_i}, & \theta_i &:= \frac{y_i - \frac{\alpha + \beta}{2}}{\tilde{\alpha}} \quad i = 1, 2, \\ \cos(\theta) &= \frac{y - \frac{\alpha + \beta}{2}}{\tilde{\alpha}}, & \tilde{\alpha} &:= \frac{\alpha - \beta}{2}. \end{aligned}$$

Castilla et al [13] use the analog of this solution as a starting point for a Melnikov analysis to prove non-integrability of the four-vortex problem on the plane. It is conceivable that the above solution for the relative equations on the plane may serve as the unperturbed configuration for a similar analysis on the sphere. The relative equations on the trilinear plane may be the proper framework on the sphere, since action-angle variables for the sphere have not as yet been identified. This is currently being investigated.

### 6.3.2.2 Example 2

Other explicit solutions of this form can also be found. Our second example is for the case  $\Gamma_1 = \Gamma_2 = -\Gamma_3 = 1$ .

Denoting by  $x = l_{12}^2$ ,  $y = l_{13}^2$ ,  $z = l_{23}^2$  the energy and momentum conservation yield the relations:

$$\begin{aligned} yz &= \alpha x, \\ x - y - z &= \beta R^2, \end{aligned}$$

where,  $\alpha$  and  $\beta$  are the energy and momentum levels respectively (i.e  $C_1 = \beta R^2$ ). Using these. and working with the relative equations again, we obtain:

$$\begin{aligned} \dot{x} &= \pm \frac{V}{\pi R \alpha x} \sqrt{(\beta R^2 - x)^2 - 4\alpha x} \\ &= \pm \frac{1}{2\pi R \alpha x} \sqrt{4\alpha x - \beta^2 - \alpha x^2} \sqrt{(\beta R^2 - x)^2 - 4\alpha x}. \end{aligned} \quad (6.25)$$

We now consider three cases. To this end, recall that the center of vorticity has length:

$$\begin{aligned} ||\mathbf{c}||^2 &= R^2 - \frac{C_1}{\sigma^2} \\ &= R^2 - C_1 = R^2(1 - \beta) \end{aligned}$$

where  $0 \leq \beta \leq 1$  and  $\sigma = \sum \Gamma_i = 1$ . Without loss of generality (by rescaling if necessary) we may take the radius of the sphere to be  $R = 1$ . The three cases that we need to consider are then the following:

(i) If  $\beta = 1$  then  $\mathbf{c} = \mathbf{0}$ . Since,  $\mathbf{c} \cdot \mathbf{n} = \mathbf{x} \cdot \mathbf{n}$ , [31], the vortices lie on a great circle from

we conclude that these are relative equilibria because  $V = 0$ .

(ii) If  $\beta = 0$ ,

$$\dot{x} = \pm \frac{\sqrt{(4\alpha - \alpha x)(x - 4\alpha)}}{2\pi\alpha} = \pm \frac{\sqrt{(4 - x)(x - 4\alpha)}}{2\pi\sqrt{\alpha}}.$$

This is readily integrated (for  $x \neq 4$ ,  $x \neq 4\alpha$ , which correspond to equilibria) to give the special periodic solution computed by Kidambi and Newton [31].

(iii) In general the quadrature of (6.25) for the case  $0 < \beta < 1$  leads to solutions in terms of elliptic integrals. However if the quadratics  $p_1 := 4\alpha x - \beta^2 - \alpha x$  and  $p_2 := (\beta - x)^2 - 4\alpha x$  have a common root the integration is similar to the saddle connection computed previously. Now  $p_1$  and  $p_2$  have roots:

$$\begin{aligned} x_{1,2} &= 2 \pm \sqrt{\frac{4\alpha - \beta^2}{\alpha}}, \\ x_{3,4} &= (\beta + 2\alpha) \pm \sqrt{2\alpha(\beta + 2\alpha)}, \end{aligned}$$

respectively. For example if  $\beta = 0.5$  we calculate, numerically,  $x_1 = x_3 = 0.2957$ ,  $x_2 = 3.7042$ ,  $x_4 = 1.6179$  for  $\alpha = 0.2282$ . Hence for  $x_1 = x_3 > 0$ ,  $x_2, x_4 > 0$ , as in the example above,  $\dot{x}$  is governed by:

$$\dot{x} = \pm \frac{(x - x_1)\sqrt{-(x - x_2)(x - x_4)}}{2\pi\sqrt{\alpha}x}.$$

The integration then becomes:

$$\begin{aligned} \int \frac{dt}{2\pi\sqrt{\alpha}} &= \int \frac{xdx}{(x - x_1)\sqrt{-(x - x_2)(x - x_4)}} \\ &= \int \left[ \frac{1}{\sqrt{-(x - x_2)(x - x_4)}} + \frac{x_1}{(x - x_1)\sqrt{-(x - x_2)(x - x_4)}} \right] dx, \end{aligned}$$

from which we finally obtain a parametrization of the orbit as follows:

$$A(t - t_0) = \sin^{-1} \left( \frac{x - \frac{x_2 + x_4}{2}}{a_1} \right) - \frac{4x_1}{a_2(a_3 - 1)(x_2 - x_4)} \tan^{-1} \left( \frac{\tan \frac{\theta}{2}}{a_2} \right).$$

Here,

$$\begin{aligned} a_1^2 &= \left(\frac{x_2 + x_4}{2}\right)^2 - x_2 x_4, \\ a_2^2 &= \frac{1 + a_3}{a_3 - 1}, & a_3 &= \frac{x_2 + x_4 - 2x_1}{x_2 - x_4}, \\ A &= \frac{1}{2\pi\sqrt{\alpha}}, & \cos \theta &= \frac{2\left[x - \frac{x_2 + x_4}{2}\right]}{x_2 - x_4}. \end{aligned}$$

The closed-form expression for these solutions may, for instance, be used in a numerical study of particle advection on the sphere in the manner done on the plane by Gurzhi et al [27].

We mention in closing the corresponding solution on the plane for case (ii), which as far as we know has not appeared in the literature. On the plane with  $\Gamma_1 = \Gamma_2 = -\gamma_3 = 1$ , with the convention  $x := l_{12}^2$ ,  $y := l_{13}^2$ ,  $z := l_{23}^2$  the energy and momentum satisfy,

$$yz = \alpha x, \quad x - y - z = \beta,$$

so that the dynamical equation for  $x$  is:

$$\begin{aligned} \dot{x} &= \frac{dl_{12}^2}{dt} = \frac{\sigma A_{123}}{\pi} \left[ \frac{1}{l_{23}^2} - \frac{1}{l_{13}^2} \right] \\ &= \frac{\sigma A_{123}}{\alpha\pi} \frac{y - z}{x} = \frac{\sigma A_{123}}{\alpha\pi x} \sqrt{(\beta - x)^2 - 4\alpha x}. \end{aligned}$$

Using Heron's formula for the area this simplifies to:

$$\dot{x} = \frac{\sigma \sqrt{4\alpha x - \beta^2} \sqrt{(\beta - x)^2 - 4\alpha x}}{4\alpha\pi x}.$$

Now taking  $\beta = 0$ , gives  $\dot{x} = \frac{\sigma}{4\sqrt{\alpha\pi}} \sqrt{x - 4\alpha}$ . With positive orientation,  $\sigma = 1$ , this is easily integrated to yield:

$$x(t) = \left( \frac{t}{2\sqrt{\alpha\pi}} + c \right)^2 + 4\alpha,$$

which is an explicit solution of the scattering example discussed in Aref [2]. The difference between the planar case and the situation on the sphere for the case  $\beta = 0$ ,  $\Gamma_1 = \Gamma_2 = -\Gamma_3 = 1$  is clear; while on the plane the solution is a scattering, on the sphere the solution is periodic. This is explained partly by the fact that for this situation the phase space on the plane is unbounded while on the sphere it is evidently compact.

### 6.3.3 Remarks on integrable four-vortex problems on the sphere

It was shown by Kidambi and Newton [31] that on the sphere the following are invariant:

$$\begin{aligned} Q &= \frac{1}{R} \sum_1^N \Gamma_i x_i \equiv \sum_1^N \Gamma_i \sin(\theta_i) \cos(\phi_i), \\ P &= \frac{1}{R} \sum_1^N \Gamma_i y_i \equiv \sum_1^N \Gamma_i \sin(\theta_i) \sin(\phi_i), \\ S &= \frac{1}{R} \sum_1^N \Gamma_i z_i \equiv \sum_1^N \Gamma_i \cos(\theta_i). \end{aligned}$$

There are three integrals in involution

$$[H, P^2 + Q^2] = 0, \quad [H, S] = 0, \quad [P^2 + Q^2, S] = 0,$$

and moreover,

$$[P, Q] = S, \quad [Q, S] = 0, \quad [S, P] = 0.$$

Since  $P$  and  $Q$  are invariant,  $[H, P] = [H, Q] = 0$ , so that if one chooses the values  $(Q, P, W) = (0, 0, 0)$  then there are four integrals in involution, namely  $(H, P, Q, S)$  implying that this four-vortex problem is integrable. This is equivalent to a zero center of vorticity,  $\mathbf{c} = 0$ . On the sphere, however, it is not necessary, as on the plane, that  $\sum_1^4 \Gamma_i = 0$ . We now consider the analogs of the collinear vortices of Fig. 5.3 on the sphere. These are integrable four-vortex configurations for which, indeed,  $\sum_1^4 \Gamma_i = 0$ . Primary vortices of strengths  $+\Gamma$  and  $-\Gamma$  are placed at  $(x, y_0 +$

$b, \sqrt{R^2 - x^2 - (y_0 + b)^2}$  and  $(x, y_0 - b, \sqrt{R^2 - x^2 - (y_0 - b)^2})$ . In the  $x$ - $y$  plane the primary vortices are reflected as on the plane, thereby ensuring that  $P = Q = 0$ . The  $z$ -coordinate has to be chosen in order to obtain  $S = 0$ . To this end it is apparent that the reflected vortices of strengths  $+\Gamma$  and  $-\Gamma$  are located at  $(-x, -y_0 - b_0, -\sqrt{R^2 - x^2 - (y_0 + b)^2})$  and  $(-x, -y_0 + b, -\sqrt{R^2 - x^2 - (y_0 - b)^2})$ . But then this is a planar configuration lying on a great-circle, and hence a relative equilibrium. This illustrates yet again a difference between vortex dynamics on the plane and on the sphere. It seems that to obtain more interesting integrable four-vortex configurations of the type  $P = Q = S = 0$  one really has to consider the case for which  $\sum_1^4 \Gamma_i \neq 0$ .

We now consider the coaxial configurations of Fig. 5.3 on the sphere. On the plane these are integrable four-vortex systems of the kind for which  $P = I = 0$ ,  $Q$  arbitrary, and for which the line  $y = 0$  is an axis of symmetry. One can show that on the sphere, these correspond to, for instance,  $Q = S = I = 0$ ,  $P$  arbitrary, with the line  $y = 0$  an axis of symmetry. Here  $I = \sum_1^4 \Gamma_i |\mathbf{x}_i|^2 = R^2 \sum_1^4 \Gamma_i = 0$ , so that necessarily  $\sum_1^4 \Gamma_i = 0$ , in which case the center of vorticity has magnitude,  $\|\mathbf{c}\| = \infty$ . By inspection it is then clear that coaxial configurations on the sphere are of the form:

$$\begin{aligned} \Gamma_1 \text{ at } (x_1, y_1, \pm\sqrt{R^2 - x_1^2 - y_1^2}), \quad -\Gamma_1 \text{ at } (x_1, -y_1, \pm\sqrt{R^2 - x_1^2 - y_1^2}), \\ \Gamma_2 \text{ at } (x_2, y_2, \pm\sqrt{R^2 - x_2^2 - y_2^2}), \quad -\Gamma_2 \text{ at } (x_2, -y_2, \pm\sqrt{R^2 - x_2^2 - y_2^2}). \end{aligned}$$

Note that either sign can be taken for the  $z$ -coordinate with the proviso that the  $z$ -coordinate of the primary and the image vortices be of the same sign in order to ensure that  $S = 0$ . For instance:

$$\Gamma_1 \text{ at } (x_1, y_1, -\sqrt{R^2 - x_1^2 - y_1^2}), \quad -\Gamma_1 \text{ at } (x_1, -y_1, -\sqrt{R^2 - x_1^2 - y_1^2}),$$

is permissible. It is easy to show, using the equations

$$\dot{\mathbf{x}}_i = \frac{1}{4\pi R} \sum_{j=1}^N \frac{\Gamma_j (\mathbf{x}_j \times \mathbf{x}_i)}{l_{ij}^2}, \quad (6.26)$$

that the symmetry of the configuration is preserved, namely that the vortices remain symmetrical about the plane  $y = 0$ , as seen in Fig. 6.5.

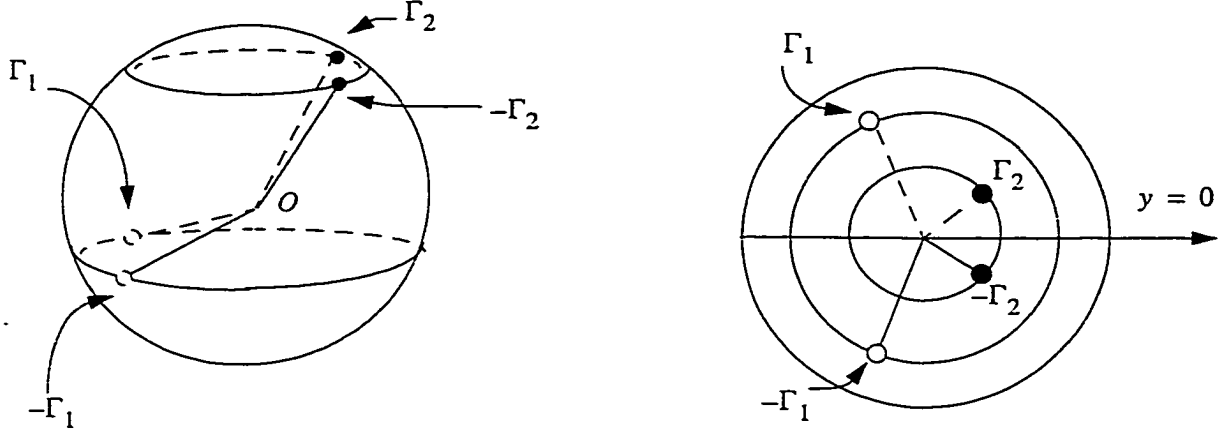


Figure 6.5: Co-axial four-vortex configurations on the sphere

For completeness, we present a rigorous justification of the integrability of this four-vortex problem. For notational convenience we adopt the following definition.

**Definition 6.5** *A vortex configuration on the sphere will be called coaxial if it has an even number of vortices and for which a vortex of strength  $\Gamma_i$ , located at  $(x_i, y_i, z_i)$ , has an image vortex of strength  $-\Gamma_i$ , located at  $(x_i, -y_i, z_i)$ .*

It is clear, then, that  $Q = S = I = 0$ , and  $P$  is arbitrary.

**Theorem 6.6** *Coaxial four-vortex configurations on the sphere are integrable.*

**Proof:** Begin by realizing that the canonical Hamiltonian formulation of the  $N$ -vortex problem on the sphere is given by [31]

$$H = \frac{1}{4\pi R^2} \sum_{i < j} \Gamma_i \Gamma_j \ln(l_{ij}^2)$$

$$\dot{P}_i = \frac{\partial H}{\partial Q_i}, \quad \dot{Q}_i = -\frac{\partial H}{\partial P_i}$$

with canonical coordinates  $P_i := \sqrt{|\Gamma_i|} \cos(\theta_i)$  and  $Q_i := \sqrt{|\Gamma_i|} \phi_i$ . Here  $R^2(1 - \cos(\gamma_{ij})) = l_{ij}^2/2$ , and  $\cos(\gamma_{ij}) := \cos(\theta_i) \cos(\theta_j) + \sin(\theta_i) \sin(\theta_j) \cos(\phi_i - \phi_j)$ . Consider

a coaxial configuration at  $\mathbf{x}_1, \mathbf{x}_2, \mathbf{x}_3, \mathbf{x}_4$ , with coordinates  $(x_i, y_i, z_i)$ , for  $i = 1, \dots, 4$ . Here  $\mathbf{x}_1$ , and  $\mathbf{x}_2$  are image vortices with strenghts  $+\Gamma_1$  and  $-\Gamma_1$  respectively, so that  $(x_1, y_1, z_1) = (x_2, -y_2, z_2)$ , and likewise with  $\mathbf{x}_3$  and  $\mathbf{x}_4$ , which have strengths  $+\Gamma_2$  and  $-\Gamma_2$ . Next, observe that initially  $l_{14}^2 = l_{23}^2$  and  $l_{13}^2 = l_{24}^2$ . Now using (6.26), obtain

$$\begin{aligned}\dot{\mathbf{x}}_1 &= \Gamma_2 \frac{\mathbf{x}_2 \times \mathbf{x}_1}{l_{12}^2} + \Gamma_3 \frac{\mathbf{x}_3 \times \mathbf{x}_1}{l_{13}^2} + \Gamma_4 \frac{\mathbf{x}_4 \times \mathbf{x}_1}{l_{14}^2}, \\ \dot{\mathbf{x}}_2 &= \Gamma_1 \frac{\mathbf{x}_1 \times \mathbf{x}_2}{l_{12}^2} + \Gamma_3 \frac{\mathbf{x}_3 \times \mathbf{x}_2}{l_{23}^2} + \Gamma_4 \frac{\mathbf{x}_4 \times \mathbf{x}_2}{l_{24}^2}, \\ \dot{\mathbf{x}}_3 &= -\Gamma_1 \frac{\mathbf{x}_2 \times \mathbf{x}_1}{l_{12}^2} + \Gamma_2 \frac{\mathbf{x}_3 \times \mathbf{x}_1}{l_{13}^2} - \Gamma_2 \frac{\mathbf{x}_4 \times \mathbf{x}_1}{l_{14}^2}, \\ \dot{\mathbf{x}}_4 &= \Gamma_1 \frac{\mathbf{x}_1 \times \mathbf{x}_2}{l_{12}^2} - \Gamma_2 \frac{\mathbf{x}_4 \times \mathbf{x}_2}{l_{13}^2} + \Gamma_2 \frac{\mathbf{x}_3 \times \mathbf{x}_2}{l_{14}^2}.\end{aligned}$$

Observe that the first terms on the RHS are equal. We now show that  $\dot{\mathbf{x}}_1 = \dot{\mathbf{x}}_2$ . Calling the common first term  $I$ , we obtain using the definition of cross-product

$$\begin{aligned}\frac{\dot{x}_1}{\Gamma_2} &= I_x + \frac{y_2 z_1 - z_2 y_1}{l_{13}^2} - \frac{-y_2 z_1 - z_2 y_1}{l_{14}^2}, \\ \frac{\dot{x}_2}{\Gamma_2} &= I_x - \frac{-y_2 z_1 - z_2(-y_1)}{l_{13}^2} + \frac{y_2 z_1 - z_2(-y_1)}{l_{14}^2},\end{aligned}$$

which are evidently equal. Clearly, by construction, we also have  $\dot{z}_1 = \dot{z}_2$ . It remains to show that  $\dot{y}_1 = -\dot{y}_2$ , and thereby conclude that  $y = 0$  is an axis of symmetry. To do this we first show that the  $y$ -component of  $I$  is zero. The  $y$ -component of  $\mathbf{x}_1 \times \mathbf{x}_2$  is  $z_1 x_2 - x_1 z_2$ , but by construction initially  $z_1 = z_2$  and  $x_1 = x_2$ . This means that,

$$\begin{aligned}\frac{\dot{y}_1}{\Gamma_2} &= \frac{z_2 x_1 - x_2 z_1}{l_{13}^2} - \frac{z_2 x_1 - x_2 z_1}{l_{14}^2}, \\ \frac{\dot{y}_2}{\Gamma_2} &= -\frac{z_2 x_1 - x_2 z_1}{l_{13}^2} + \frac{z_2 x_1 - x_2 z_1}{l_{14}^2},\end{aligned}$$

from which it is clear that  $\dot{y}_1 = -\dot{y}_2$ . In conclusion the Hamiltonian system of this four-vortex problem is completely described by  $\mathbf{x}_1$  and  $\mathbf{x}_3$  which have canonical coordinates  $(P_1, Q_1)$  and  $(P_3, Q_3)$ . This is a two degree of freedom canonical Hamiltonian system with an invariant,  $Q$ , not depending on the Hamiltonian,  $H$ , (recall



$P=S=I=0$ ). It is a simple corollary of the Arnold-Liouville-Jost theorem that this is integrable [5].  $\square$

## Chapter 7

### On the collapse of two vortices in a circular (planar) domain

In this chapter we study aspects of vortex collision for two vortices in a circular (planar) domain. Our methods are similar to those used in Chapter 3. We begin by computing the Hamiltonian for this system by using the method of images. We compare our results with similar results in the literature, obtained by other techniques.

References for vortex problems on the plane include the work of Lin [40] where the existence of the Kirchoff-Routh function is established, and the work of Zannetti and Franchessi [21] where a number of solutions in squares, rectangles and circles are described. They have also worked on aspects of the advection problem in closed domains [20]. Flucher and Gustafsson have studied, in detail, the collapse process, for domains with boundaries [19].

#### 7.1 Derivation of the Hamiltonian for the $N$ -vortex system in a circular domain

We begin by presenting a derivation of the equations of motion for vortices in a circular domain. The starting point is to use the method of images [23] to determine the advection of a point vortex and then use superposition. Consider two points  $\xi$

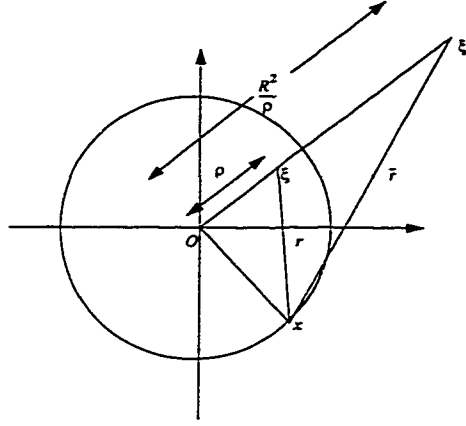


Figure 7.1: Method of Images

and  $\xi^*$  inverse to each other with respect to the circle  $D$  of radius  $R$  centered at the origin  $O$ :

$$\xi^* = \frac{R^2 \xi}{|\xi|^2}.$$

Notice that the point inverse to the origin  $O$  is the point at infinity, and that points on the boundary  $\partial D$  of the circle are their own inverses. To solve:

$$\begin{aligned} \Delta \psi &= -\omega, \text{ in } D, \\ \psi|_{\partial D} &= 0, \end{aligned}$$

use the Green function obtained by the method of images:

$$\psi = -G(x, \xi) = -\frac{1}{2\pi} \ln \frac{\rho \tilde{r}}{Rr} = \frac{1}{2\pi} [\ln |x - \xi| - \ln \frac{|x - \xi^*| |\xi|}{R}],$$

where  $x \in \bar{D}$ ,  $\xi \in D$ ,  $x \neq \xi$  as shown in Figure 7.1. It is easy to verify that  $G(x, \xi) = 0$  for  $x \in \partial D$ ,  $\xi \in D$ . We consider the point vortex decomposition for two vortices,  $\omega = \Gamma_1 \delta(x - \xi_1) + \Gamma_2 \delta(x - \xi_2)$ . The divergence theorem yields,

$$\int_D |\mathbf{v}|^2 d\mathbf{x} = \int_D |\nabla \psi|^2 d\mathbf{x} = - \int_D \psi \Delta \psi^2 d\mathbf{x} + \int_{\partial D} \psi \frac{\partial \psi}{\partial \nu} d\mathbf{x}.$$

But,

$$\begin{aligned}\Delta\psi &= -\omega = -\sum_i \Gamma_i \delta(x - \xi_i), \text{ and,} \\ -\psi &= \frac{1}{2\pi} \sum_i \Gamma_i \ln \frac{\rho_i \tilde{r}_i}{R r_i}.\end{aligned}$$

By superposition  $\psi|_{\partial D} = 0$ , so that

$$H := \int_D |v|^2 d\mathbf{x} = \int_D \psi \omega d\mathbf{x}.$$

Substituting for  $\psi$  and  $\omega$  we finally obtain:

$$\begin{aligned}2H = -\frac{1}{2\pi} \left[ -\Gamma_1^2 \ln \frac{|\xi_1 - \xi_1^*| |\xi_1|}{R} - \Gamma_2^2 \ln \frac{|\xi_2 - \xi_2^*| |\xi_2|}{R} + 2\Gamma_1 \Gamma_2 \ln |\xi_1 - \xi_2| \right. \\ \left. - \Gamma_1 \Gamma_2 \ln \frac{|\xi_1 - \xi_2^*| |\xi_2|}{R} - \Gamma_2 \Gamma_2 \ln \frac{|\xi_2 - \xi_1^*| |\xi_1|}{R} \right]. \quad (7.1)\end{aligned}$$

Observe that the Hamiltonian is not invariant with respect to arbitrary displacements in space. It is however invariant with respect to rotations about the origin. Hence  $H$  and by Noether's theorem, the angular momentum,  $I := \sum_i \Gamma_i |\xi_i|^2$  are the two integrals of motion.

## 7.2 Proof that two vortices in a circular domain cannot collide

We are now in a position to state and prove our main result.

**Theorem 7.1** *The two-vortex problem, in a circular domain, does not admit finite-time collisions.*

**Proof:** For collisions  $\xi_1 \rightarrow \xi_2$ , and  $\xi_1^* \rightarrow \xi_2^*$ , so that near collision we have asymptotically:

$$2H \sim -\frac{1}{2\pi} \left[ -(\Gamma_1^2 + \Gamma_2^2) \ln \frac{|\xi_1 - \xi_1^*| |\xi_1|}{R} + 2\Gamma_1 \Gamma_2 \ln |\xi_1 - \xi_2| - 2\Gamma_1 \Gamma_2 \ln \frac{|\xi_1 - \xi_1^*| |\xi_1|}{R} \right]. \quad (7.2)$$

Suppose first that  $\xi_1$  and  $\xi_2$  collide at some point in the interior not the origin  $O$  (and not on  $\partial D$ ), then  $\xi_1^*$  and  $\xi_2^*$  (being inverse to  $\xi_1$  and  $\xi_2$ ) meet at some finite

point ( $\neq \infty$ ) which does not lie on  $\partial D$  i.e belonging to  $\bar{D}^c$ . This implies that both  $|\xi_1 - \xi_1^*|$  and  $|\xi_1|$  are bounded away from 0 and  $\infty$ . Hence near collision there remains in Eq. 7.2 the unbalanced singular term  $\ln |\xi_1 - \xi_1^*|$  and because  $H$  is invariant this is clearly not possible. Suppose instead that  $\xi_1$  and  $\xi_2$  collide at the origin  $O$ , then near collision:

$$\begin{aligned}
4\pi H &\sim -\Gamma_1^2 \ln \frac{|\xi_1|}{R} - \Gamma_1^2 \ln \frac{|\xi_1^*|}{R} - \Gamma_2^2 \ln \frac{|\xi_2|}{R} - \Gamma_2^2 \ln \frac{|\xi_2^*|}{R} + 2\Gamma_1\Gamma_2 \ln |\xi_1 - \xi_2| \\
&\quad - \Gamma_1\Gamma_2 \ln \frac{|\xi_1|}{R} - \Gamma_1\Gamma_2 \ln \frac{|\xi_1^*|}{R} - \Gamma_1\Gamma_2 \ln \frac{|\xi_2|}{R} - \Gamma_1\Gamma_2 \ln \frac{|\xi_2^*|}{R} \\
&\sim -(\Gamma_1^2 + \Gamma_2^2) \left( \ln \frac{|\xi_1|}{R} + \ln \frac{|\xi_1^*|}{R} \right) + 2\Gamma_1\Gamma_2 \ln |\xi_1 - \xi_2| \\
&= -(\Gamma_1^2 + \Gamma_2^2) \ln \frac{|\xi_1||\xi_1^*|}{R^2} + 2\Gamma_1\Gamma_2 \ln |\xi_1 - \xi_2| \\
&= 2\Gamma_1\Gamma_2 \ln |\xi_1 - \xi_2|.
\end{aligned}$$

The last follows because  $\xi_1$  and  $\xi_1^*$  are inverse points so that  $|\xi_1||\xi_1^*| = R^2$ . Again the unbounded term  $\ln |\xi_1 - \xi_2|$  prevents this collision at the origin. Finally suppose  $\xi_1$  and  $\xi_2$  collide at some point on the boundary, then since  $\xi_1 \rightarrow \xi_1^* \rightarrow \xi_2^* \rightarrow \xi_2$ , and  $|\xi_i|, |\xi_i^*| \rightarrow R$ , near collapse Eq. 7.2 becomes:

$$\begin{aligned}
4\pi H &\sim -[(\Gamma_1^2 + \Gamma_2^2) \ln |\xi_1 - \xi_1^*| + 2\Gamma_1\Gamma_2 \ln |\xi_1 - \xi_2| - \Gamma_1\Gamma_2 \ln |\xi_1 - \xi_2^*| \\
&\quad - \Gamma_1\Gamma_2 \ln |\xi_1 - \xi_2^*|] \\
&\sim -(\Gamma_1^2 + \Gamma_2^2) \ln |\xi_1 - \xi_1^*|,
\end{aligned}$$

leaving the unbounded term  $\ln |\xi_1 - \xi_1^*|$ . □

Observe that the methods are very similar to those used to prove our results for the three-vortex two-layer problem. We remark that these results are proved in more generality for a wider class of closed domains by Flucher and Gustafsson [19] using other techniques. Our method is elementary and might possibly be used to prove similar results for other closed domains through the use of conformal mapping.

## Reference List

- [1] Abramowitz, M., Stegun, I., *Handbook of Mathematical Functions*, Dover, New York, (1965).
- [2] Aref, H., Motion of three vortices, *Phys. Fluids* **22** (3) (1979)393-400.
- [3] Aref, H., Integrable, chaotic and turbulent vortex motion in two-dimensional flows, *Ann. Rev. Fluid Mech.* **15** (1983)345-389.
- [4] Aref, H., Pomphrey, N., Integrable and chaotic motion of four vortices, I. The case of identical vortices, *Proc. Roy. Soc. London A* **380** (1982)359-387.
- [5] Arnol'd, V.I., *Mathematical Methods of Classical Mechanics*, Springer-Verlag, New York, (1978).
- [6] Arnol'd, V.I., *Encyclopedia of Mathematical Science*, Vol. **3**, Springer, 1988. Dynamical Systems III, Springer.
- [7] Bogomolov, V. A., Dynamics of vorticity at a sphere, *Fluid Dynamics* **6** (1977)863-870.
- [8] Bogomolov, V. A., Two-dimensional fluid dynamics on a sphere, *Izv. Atmos. Oc. Phys.* **15** (1)(1979)18-22.
- [9] Bogomolov, V. A., On the motion of a vortex on a rotating sphere, *Izv. Atmos. Oc. Phys.* **21** (4)(1985)298-302.
- [10] Carnevale, G. F., Kloosterziel, R. C., Emergence and evolution of triangular vortices, *J. Fluid Mech.* **259** (1994)305-331.
- [11] Carvalho, S. P., Koiller, J., Chaos and Nonintegrability of Point Vortex Motions, *Manuscript*.

- [12] Carvalho, S. P. Koiller, J., Non-Integrability of the 4-vortex system, Analytical Proof, *Comm. Math. Phys.* **120** (1989)643-652.
- [13] Castilla, M., Moauro, V., Negrini, P., Oliva, W., The four positive vortices problem:regions of chaotic behavior and the non-integrability,*Ann. Inst. Henri Poincaré, Physique Théorique* **59** (1) (1993)99-115.
- [14] Deift, P., Integrable Hamiltonian Systems, *Dynamical Systems and Parabolic Methods in PDE*. Eds. Deift, P., Levermore, C. D., Wayne, C. E., Lectures in Applied Math, **Vol. 31**, AMS (1996).
- [15] Dritschel, D. G., Polvani, L. M., The roll-up of vorticity strips on the surface of a sphere, *J. Fluid Mech.* **234** (1992)47-69.
- [16] Dritschel, D. G., Polvani, L. M., Wave and vortex dynamics on the surface of a sphere, *J. Fluid Mech.* **255** (1993)35-64.
- [17] Dritschel, D. G., Zabusky, N. J., On the nature of vortex interactions and models in unforced nearly-inviscid two-dimensional turbulence, *Phys. Fluids A* **8** (5)(1996)1252-1256.
- [18] Flierl, G.R., Polvani, L.M., Zabusky, N.J., Two-layer geostrophic vortex dynamics. Part 1. Upper-layer V-states and merger, *J. Fluid. Mech.* **205** (1989)215-242.
- [19] Flucher, M., Gustafsson, B., Vortex Motion in two dimensional hydrodynamics, *Preprint*.
- [20] Franzese, P., Zannetti, L., Advection of a point vortex in closed domains, *Europ. J. of Mechanics B Fluids* **12** (1) (1993)43-67.
- [21] Franzese, P., Zannetti, L., The nonintegrability of the restricted problem of 2 vortices in closed domains, *Physica D* **76** (1-3) (1994)99-109.
- [22] Friedlander, S., Interaction of vortices in a fluid on the surface of a sphere, *Tellus* **XXVII** (1975)15-24.
- [23] Garabedian, P. R., Partial differential equations, John Wiley & Sons, Inc, (1964).

- [24] Goldstein, H., Classical Mechanics, 2nd ed., Addison-Wesley, Reading, 1980.
- [25] Griffiths, R. W., Hopfinger, E. J., Experiments with baroclinic vortex pairs in a rotating fluid, *J. Fluid. Mech*, **173** (1986)501-518.
- [26] Gryanik, V. M., Dynamics of singular geostrophic vortices in a two-level model of the atmosphere (or ocean), *Bull. (Izv.), Acad. Sci. USSR, Atmospheric and oceanic physics* **19** (3) (1983)171-179.
- [27] Gurzhi, A. A., Konovaljuk, T. P., Konstantinov, M. Y., Meleshko, V. V., Advection of a vortex pair atmosphere in a velocity field of point vortices, *Phys. Fluids A* **4** (12) (1992).
- [28] Hally, D., Stability of streets of vortices on surfaces of revolution with a reflection symmetry, *J. Math. Phys.* **21** (1980)211-217.
- [29] Hogg, N., Stommel, H., The heton, an elementary interaction between discrete baroclinic geostrophic vortices, and its applications concerning eddy heat-flow, *Proc. Roy. Soc. A* **397** (1985)1-20.
- [30] Hogg, N., Stommel, H., Hetonic explosions: the breakup and spread of warm pools as explained by baroclinic point vortices, *J. Atmos. Sci.* **42** (14)(1985)1465-1476.
- [31] Kidambi, R., Newton, P. K., Motion of three point vortices on a sphere, *Physica D* **116** (1998)143-175.
- [32] Kidambi, R., Newton, P. K., Point vortex motion on a sphere with solid boundaries *Phys. Fluids* **12** (3)(2000)581-588.
- [33] Kidambi, R., Newton, P. K., Collapse of three vortices on a sphere, *Nuovo Cimento* **22 C** (6) (1999)779-791.
- [34] Kimura, H., Okamoto, H., Vortex motion on a sphere, *J. Phys. Soc. Japan* **56** (12)(1987)4203-4206.
- [35] Kimura, Y., Chaos and collapse of a system of point vortices, *Fluid Dynamics Research* **3** (1988)98-104.



- [36] Kirwan, F., The topology of reduced phase spaces of the motion of point vortices on the sphere, *Physica D* **30** (1988)99-123.
- [37] Klyatskin, K.V., Reznik, G.M., Point vortices on a rotating sphere, *Oceanology* **29** (1) (1989)12-16.
- [38] Lewis, D., Ratiu, T., Rotating  $n$ -gon/ $kn$ -gon vortex configurations, *J. Non-linear Sci.* **6** (1996)385-414.
- [39] Lim, C. C., Relative equilibria of symmetric  $n$ -body problems on the sphere:Inverse and direct results, *Comm. Pure Appl. Math.***LI** (1998)341-371.
- [40] Lin, C.C., On the motion of vortices in 2D I. Existence of the Kirchhoff-Routh functions *Proc. Natl. Acad. Sci. USA* **27** (1941)570.
- [41] Marsden, J. E., Ratiu, T. S., *Introduction to Mechanics and Symmetry*, TAM **17**, Springer, Berlin, 1994.
- [42] Marsden, J. E., Pekarsky, S., Point vortices on a sphere: stability of relative equilibria, *J. Math. Phys.* **39** (11)(1998)5894-5907.
- [43] McWilliams, J. C., Statistical properties of decaying geostrophic turbulence, *J. Fluid Mechanics* **146** (1989)21-43.
- [44] McWilliams, J. C., Zabusky, N. J., A modulated point-vortex model for geostrophic,  $\beta$ -plane dynamics, *Phys. Fluids*, **25** (12) (1982)2175-2182.
- [45] Morrison, P. J., Hamiltonian description of the ideal fluid, *Reviews of Modern Physics* **70** (2), (1998)467-520.
- [46] Newton, P. K., *The N-Vortex Problem: Analytical Techniques*, to appear, Springer-Verlag, Applied Math. Sci., 2001.
- [47] Novikov, E. A., Dynamics and statistics of a system of vortices, *Soviet Phys. JETP*, **41** (1975)937-943.
- [48] Novikov, E.A., Stochastization of vortices, *JETP Lett.* **29** (1979)677-679.

- [49] Novikov, E. A., Vortex Collapse, *Soviet Phys. JETP* **50** (1979)297-301.
- [50] Olver, P. J., *Applications of Lie Groups to Differential Equations*, Springer-Verlag, Berlin, (1986).
- [51] Pedlosky, J., *Geophysical Fluid Dynamics*, Springer-Verlag, NY, 1987.
- [52] Polvani, L. M., Geostrophic vortex dynamics, *Ph. D Thesis*, Massachusetts Institute of Technology, 1988.
- [53] Salmon, R., Geostrophic turbulence, *Turbolenza e Predicibilità nella Fluidodinamica Geofisica e la Dinamica del Clima*, Scuola Internazionale di Fisica Enrico Fermi **LXXXVIII** (1982)113-158.
- [54] Salmon, R., *Lectures on Geophysical Fluid Dynamics*, Oxford University Press, New York-Oxford, (1998).
- [55] Shepherd, T. G., Symmetries, conservation laws, and Hamiltonian structure in geophysical fluid dynamics, *Adv. Geophys.* **32** (1990)287-338.
- [56] Synge, J. L., On the motion of three vortices, *Can. J. Math.* **1** (1949)257-270.
- [57] Young, W.R., Some interactions between small numbers of baroclinic geostrophic vortices, *Geophys. Astrophys. Fluid Dynamics* **33** (1985)35-61.
- [58] Ziglin, S. L., Nonintegrability of a problem on the motion of four point vortices, *Sov. Math. Dokl.* **21** (1)(1980)296-299.